INTEGRATION AND OPTIMIZATION OF TRIGENERATION SYSTEMS WITH SOLAR ENERGY, BIOFUELS, PROCESS HEAT, AND FOSSIL FUELS

A Dissertation

by

EMAN ABDEL-HAKIM ALY MOHAMED TORA

Submitted to the Office of Graduate Studies of
Texas A&M University
in partial fulfillment of the requirements for the degree of

DOCTOR OF PHILOSOPHY

December 2010

Major Subject: Chemical Engineering

INTEGRATION AND OPTIMIZATION OF TRIGENERATION SYSTEMS WITH SOLAR ENERGY, BIOFUELS, PROCESS HEAT, AND FOSSIL FUELS

A Dissertation

by

EMAN ABDEL-HAKIM ALY MOHAMED TORA

Submitted to the Office of Graduate Studies of
Texas A&M University
in partial fulfillment of the requirements for the degree of

DOCTOR OF PHILOSOPHY

Approved by:

Chair of Committee,	Mahmoud EL-Halwagi
Committee Members,	Maria Barrufet
	Sergiy Butenko
	Sam Mannan
Head of Department	Michael Pishko

December 2010

Major Subject: Chemical Engineering

ABSTRACT

Integration and Optimization of Trigeneration Systems with Solar Energy, Biofuels, Process Heat and Fossil Fuels. (December 2010)
Eman Abdel-Hakim Aly Mohamed Tora, B.S., Elminia University;
M.S., Cairo University, Egypt; M.S., Texas A&M University
Chair of Advisory Committee: Dr. Mahmoud El-Halwagi

The escalating energy prices and the increasing environmental impact posed by the industrial usage of energy have spurred industry to adopt various approaches to conserving energy and mitigating negative environmental impact. This work aims at developing a systematic approach to integrate solar energy into industrial processes to drive thermal energy transfer systems producing power, cool, and heat. Solar energy is needed to be integrated with other different energy sources (biofuels, fossil fuels, process waste heat) to guarantee providing a stable energy supply, as industrial process energy sources must be a stable and reliable system. The thermal energy transform systems (turbines, refrigerators, heat exchangers) must be selected and designed carefully to provide the energy demand at the different forms (heat, cool, power). This dissertation introduces optimization-based approaches to address the following problems:

- Design of cogeneration systems with solar and fossil systems
- Design and integration of solar-biofuel-fossil cogeneration systems
- Design of solar-assisted absorption refrigeration systems and integration with the processing facility
- Development of thermally-coupled dual absorption refrigeration systems, and
- Design of solar-assisted trigeneration systems

Several optimization formulations are introduced to provide methodical and systematic techniques to solve the aforementioned problems. The approach is also sequenced into interacting steps. First, heat integration is carried out to minimize industrial heating and

cooling utilities. Different forms of external-energy sources (e.g., solar, biofuel, fossil fuel) are screened and selected. To optimize the cost and to overcome the dynamic fluctuation of the solar energy and biofuel production systems, fossil fuel is used to supplement the renewable forms of energy. An optimization approach is adopted to determine the optimal mix of energy forms (fossil, bio fuels, and solar) to be supplied to the process, the system specifications, and the scheduling of the system operation. Several case studies are solved to demonstrate the effectiveness and applicability of the devised procedure.

The results show that solar trigeneration systems have higher overall performance than the solar thermal power plants. Integrating the absorption refrigerators improves the energy usage and it provides the process by its cooling demand. Thermal coupling of the dual absorption refrigerators increases the coefficient of performance up to 33%. Moreover, the process is provided by two cooling levels.

ACKNOWLEDGEMENTS

First and foremost, I would like to express my deepest gratitude to the unique God most merciful, my creator, for providing me knowledge, for guiding me in completing my Ph.D., and for blessing my entire life.

Words cannot express my sincere appreciation and gratitude to Dr. Mahmoud El-Halwagi for his guidance, teaching, caring, following up and supporting me during my graduate studies at Texas A&M University. And special thanks to him for caring and insisting on high quality research. He is more than an advisor and a mentor; he also cares about people whoever they are. He always he has an open door, and more appreciated, he always has an open mind and heart for everyone. Many thanks to Dr. El-Halwagi for making me trust myself so that one day I could be a scholar.

Sincere thanks, gratitude, and appreciation go to the members of my committee, Dr. Sam Mannan, Dr. Maria Barrufet, and Dr. Sergiy Butenko. Many thanks to Dr. Mannan for his support all the time and his sincere help too. The feedback provided by Dr. Barrufet, Dr. Butenko, and Dr. Mannan at my prelim is much appreciated. I am grateful that they always challenged me to think more critically and I thank them for their helpful advice.

Many sincere thanks go to the Egyptian Government, the Ministry of Higher Education and Scientific Research, and the National Research Center for funding me these four years and for following my progress here continuously. Much care has been given by them to assure that my research plan has progressed well. Also, I would like to thank my advisor, Dr. Mahmoud EL-Halwagi, for supplementing the funds of my Ph.D. studies and for allowing me to participate in three conferences.

Many thanks to the Chemical Engineering Departments at the Egyptian National Research Center, Cairo University, and Elminia University in Egypt.

I would like to express my heartfelt thanks to my dear mother for her support and for encouraging me to study and to work hard all the time. Many thanks for her prayers for me. Many thanks for my dear sister Dr. ‘Aml Tora’ for encouraging me to do more, progress always and for her love, support, prayers, and encouragement.

NOMENCLATURE

COP	Coefficient of performance
h_i	Enthalpy of stream i
$\dot{m}$	Flow rate (kg/s)
$Q_{Bs}tr$	Bottom cycle stripper heat rate (kW)
Q_{evap}	Condenser heat rate (kW)
$Q^{Ex\text{-}Pro}$	Extracted heat from the process
$Q^{\mathrm{Re}f}$	Evaporator heat rate (kW)
Q^{Ref1}	Refrigerant rate needed at first cooling level (kW)
Q^{Ref2}	Refrigerant rate needed at second cooling level (kW)
Q^{Refi}	Refrigeration needed at cooling level i (kW)
Q_{str}	Stripper heat rate (kW)
Q_{Cond}	Rate of heat recovered from the top cycle to run the bottom cycle (kW)
$\overset{TC}{Q}_{\mathrm{Re}cv}$	Rate of heat recovered from the top cycle to run the bottom cycle (kW)
Q^{Extr}	Rate of heat used to run the bottom cycle provided from external heat sources (kW)
$T^{DP}_{\mathrm{Re}ctf}$	The dew point of the solution at the rectifier (^{o}C)
T^{s}	Source temperature of the a stream (^{o}C)
T^{t}	Target temperature of a stream (^{o}C)
X	Composition; mass fraction of the refrigerant at the mixture
A_s	Area of the s^{th} solar collector
AFC	Annualized fixed cost
C_f^{Fossil}	Cost of fossil fuel
C_p^{Fuel}	Unit operating cost of the fossil fuel

$C_{p,s}^{Solar\_AR}$	Unit operating cost of the solar energy for the AR system
$C_{p,s}^{Solar\_Cogen}$	Unit operating cost of the solar system for cogeneration
$C_{p,s}^{Solar\_Steam\_Direct}$	Unit operating cost for the solar system for direct steam generation
f	Index of fossil utility
$FC_{P,u}$	Flowrate*specific heat of hot stream u
$H_{p}^{Steam\_Cogen}$	Enthalpy of steam received by the turbine in period p
$H_{p}^{Steam\_Exit\_Turbine}$	Enthalpy of steam discharged by the turbine in period p
$HC_{v,z,p}$	Heat added to cold stream v in interval z during period p
$HH_{u,z,p}$	Heat removed from hot stream u in interval z during period p
$H_{p}^{Steam\_Direct}$	Heat needed for direct steam use during period p
N_{C}	Number of process cold streams
N_{H}	Number of process hot streams
N_p	Number of periods
p	Index for periods
$POWER_p$	Electric power produced during period p
Q_{Abs}	Heat removed from the absorber
$QC_{v,p}$	Cooling load of utility v during period p
$Q_{p}^{External\_AR}$	External heat added to the stripper of the AR cycle through fossil fuel and solar energy in period p
$Q_{p}^{Fossil\_Cogen}$	Heat added by the fossil fuel for cogeneration during period p
$Q_{p}^{Fossil\_Steam\_Direct}$	Heat needed for direct steam usage by fossil fuel during period p
$QH_{u,p}$	Heating load of utility u during period p
$Q_{s,p}^{Solar}$	Solar energy collected during period p
Q_{Solar}^{Annual}	Annual energy collected by the solar system
$Q_{p}^{Solar\_Cogen}$	Heat added by the solar system for cogeneration during period p

$Q_p^{Solar\_Steam\_Direct}$	Heat needed for direct steam usage by solar energy during period p
$Q_{s,p}^{Useful\_Solar}$	Useful power collected (and delivered in a thermal form) per unit area of the s^{th} solar collector in period t and As is the area of the s^{th} solar collector
Q_{Str}	Heat added to the stripper
Q_{Ref}	AR refrigeration duty
$Q_{z,p}^{Str,process}$	Excess process heat added to the water loop
$r_{z,p}$	Residual heat leaving interval z during period p
s	Index for solar collectors
T_{Abs}	Temperature of the absorber
T_f^{Fossil}	Temperature of fossil fuel
T_{Ref}	AR refrigeration temperature
T_{str}^{in}	Minimum acceptable temperature for heating the water loop
T_u^s	Supply temperature of hot stream u
T_u^t	Target temperature of stream u
$t_{z\text{-}1,p}$	The cold-scale temperatures at the top line defining the zth interval
u	Index of hot streams
v	Index of cold streams
z	Index for temperature intervals

Greek:

α_s	Function for the annualized fixed cost of the s^{th} solar power plant
$\Delta T^{\min}$	Minimum approach temperature
ψ_p	Function for steam-turbine power
$\Delta T^{Exch,HR}$	Driving force of the heat exchanger recovering heat between the process and the AR hot water feed tank

Index:

i	Number of stream

TABLE OF CONTENTS

LIST OF FIGURES

FIGURE Page

FIGURE Page

LIST OF TABLES

TABLE Page

CHAPTER I
INTRODUCTION

I.1. SOLAR HYBRID TRIGENERATION

The dwindling fossil energy sources and the increasing concern about the consequences of greenhouse gas emissions on global climatic changes provide much motivation for the use of renewable energy sources. As such, there is a significant need to incorporate renewable energy sources in industrial processes. There is also much need for integrated energy systems that address the combined cooling, heating, and power needs of the process "CCHP" which is referred to as trigeneration. Figures 1.1 and 1.2 describe power generation and cogeneration (combined heat and power) where steam turbines are used to produce power and the discharged steam is used for heating. Figure 1.3 is an absorption refrigeration cycle where two fluids are used: a working fluid and an absorbent. The mixture of the working fluid and the absorbent is pumped then the working fluid is stripped using a heat source (e.g., steam). The stripped working fluid is condensed at higher pressure to discharge heat to a high-temperature sink then let down to an evaporator that extracts heat from a low-temperature heat source and the cycle continues.

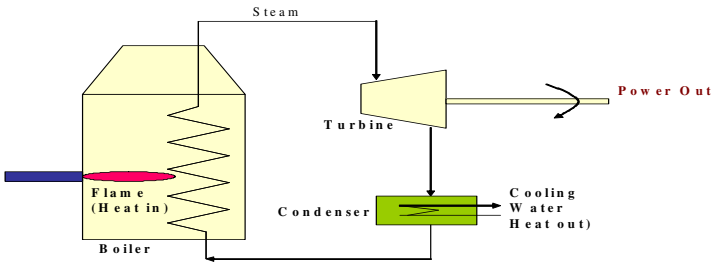

Figure 1.1. Power Generation through a Steam Turbine System [1].

This dissertation follows the style and format of *International Journal of Energy Research.*

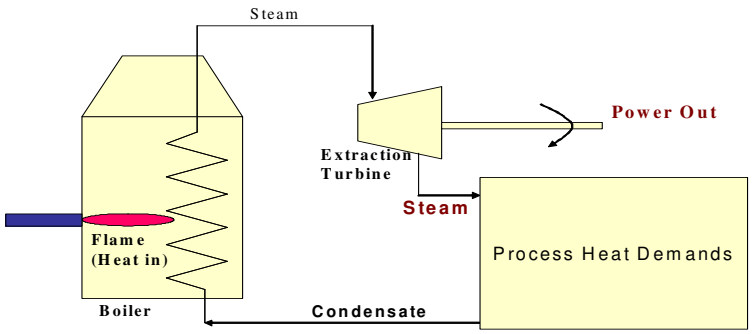

Figure 1.2. Combined Heat and Power (Process Cogeneration).

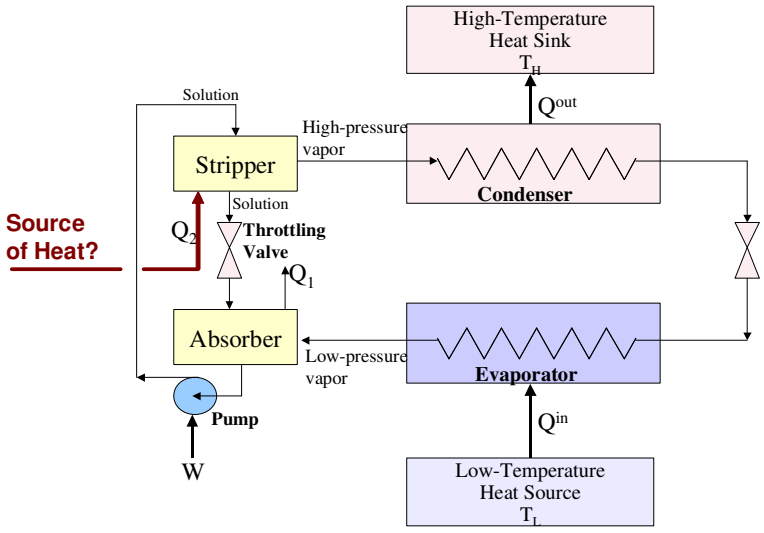

Figure 1.3. An Absorption Refrigeration Cycle [1].

Figure 1.4 represents a trigeneration system which uses a fossil fuel to produce steam which is fed to turbines for power generation and with the discharged steam used for heating and for an absorption refrigeration cycle.

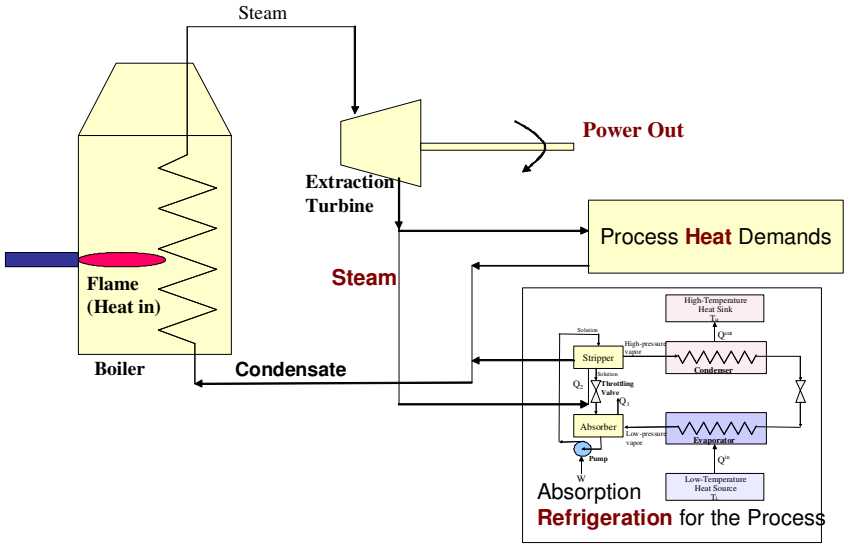

Figure 1.4. A Trigeneration System with Fossil Fuels.

Trigeneration offers several advantages including improving the overall efficiency of the energy system, the reduction of fuel consumption, and the reduction of greenhouse gas "GHG" emissions.

I.2. SOLAR TRIGENERATION SYSTEM AND PROCESS INTEGRATION

In utilizing process integration, it is important to recognize the chemical process as an integrated system and that problem solving strategies must deal with root causes and not just symptoms of the problem. Traditional approaches to process development and improvement have been limited in applicability, can be time and cost intensive, do not guarantee the global solution, and do not reveal solutions that can be non-intuitive. Integration techniques can be used in process synthesis and conserve valuable resources [1].

Cogeneration has been used for a while in industrial sectors. Primary cogeneration has traditionally referred to combined heat and power production. Recently, cogeneration has been used to refer to combined power and useful thermal energy production that includes heating and/or cooling [2]. A cogeneration plant consists mainly of a prime mover, a heat recovery unit, and an electric-power generator. The prime mover can be a steam engine, a gas engine, or a reciprocating engine. The heat recovery unit is heat recovery steam generator for steam or hot water production, and (or) absorption chiller to produce cooling [2].

There are three modes of operation: 1) the base load system: the plant works at a full load for more than 6000 hours per year; 2) the intermediate system: the plant works for average 4000 hours per year; 3) the peak shaving system: the plant operates around 1000 hour per year to provide electricity at the hours of electricity peak [2]. At this work, we propose certain cogeneration plant operation modes to be more suitable for specified industrial processes as given by Table 1.1.

Table 1.1. The Proposed Operation Modes for Cogeneration Plants.

Cogeneration Energy forms	**Cogeneration Operation mode**	**Hours/year**	**System equipment**	**Industry operation mode**
Power + Cool	Peak shaving	≤ 1000	SC - AR - FFB	Heavy continuous processes
Power + Heat	Peak shave	≤1000	SC – TES -FFB	
Power Cool + Heat	Base load	≥ 6000	SC – TES - AR – HRSG FFB	Continuous heavy load
Power Heat or Cool	Intermediate	~ 4000	SC – AR – TES - HRSG - FFB	Batch process Seasonally process Commercial plants Institutional

SC: solar collectors; AR: absorption refrigerator; FFB: fossil fuel boiler; TES: solar thermal energy storage; HRSG: heat recovery steam generation.

These cogeneration systems are available as packages. However these packages have some advantages. They are not customized for certain plants [2]. The design of topping cogeneration systems is usually carried out according to the basics of the Public Utility Regulatory Policies Act (PURPA). Large industrial gas- or oil-fired cogeneration plants can be more efficient than using any combination of power and thermal energy separate systems. To insure the cogeneration plant is well designed, it must have efficiency more than 45% and provide more than 5% thermal energy; or provide thermal energy more than 15% with efficiency more than 42.5 %, where the efficiency is defined as [2]

$$\eta_{top\_cog} = \frac{Power + 0.5 * Thermal}{Fuel} \tag{1.1}$$

For bottoming cycle using oil or gas as supplementary fuel, the efficiency must be more than 45%, but the efficiency is defined as

$$\eta_{Bot\_cog} = \frac{Power}{Fuel} \tag{1.2}$$

PURPA restricts small plants (< 80 MW) to use solar energy, wind energy, wastes, biomass, geothermal, or any combination of them without setting minimum efficiency [2].

The following points should be considered in optimizing solar cogeneration approaches:

1. Process heat integration to determine:
    a) Heating demand
    b) Cooling demand
    c) Power demand
2. Prime-mover selection to choose:
    a) Steam turbine is used if the heat to power ratio (HPR) is high from 4-10; and if the process has big pressure reduction so the valve can be replaced by steam turbine [2].

b) Gas turbine is used if the heat to power ration is in the range of 1-3.
c) Combined gas and steam turbines are used if power is needed and heat as well so the steam turbine produces extra steam.
d) Reciprocating engine if the HTPR is low typically 0.5.

3. Selecting the solar collectors

Each one of the previously mentioned prime movers requires a certain temperature level and heating media. For steam engines, the working fluid is steam. Therefore Fresnel reflector working at temperature typically 285^{o}C [3] and parabolic trough solar collectors working up to 400^{o}C [4] are the suitable solar collectors. The gas turbines use air at high temperature therefore heliostats and central tower is more suitable for temperature typically 500^{o}C. Table 1.2 gives the proposed solar collectors types for each prime mover.

Table 1.2 Proposed Prime Movers and Solar Collector Types for Solar Cogeneration Systems.

Process Heat : Power Ratio	Prime Mover	T (^{o}C)	Solar collectors types
High ≥ 4	Steam turbines "back-pressure"	400 285	Parabolic trough Compact Fresnel
Medium 1:3	Gas turbines	550	Central receiver
Zero	Steam condensing turbines Sterling engine	400 285 Direct Power	Parabolic trough Fresnel Reflector Parabolic dish

4. Selecting the fossil fuel

   Steam turbine: solid fuels like coal are recommended for small steam cogeneration plant [2]. For bigger plants (> 50MW) other fuels (gas, liquid) work too.

   Gas turbines: gas fuels are recommended. Natural gas gives less greenhouse gas emissions (GHGE).

5. Schedule and optimize the integration between the different heat sources of the prime mover based on economic analysis: solar radiation intensity varies continuously; which requires having thermal energy storage and/or fossil fuel as backup system. The fossil fuel is used in addition to the availability of process excess or waste heat to be integrated as well. To get stable power, heat, and cool supply, the different energy sources (solar, process heat, fossil) availability and prices need to be considered simultaneously. Therefore, optimum integration by optimizing design and operation aspects of the entire system should be considered.

6. The environmental aspects (GHGE) are considered as well; solar energy is a clean energy source.

Different industries have different power demands. Therefore, these demands need to be optimized for each industry separately (e.g., petrochemical, pulp and paper, etc.). The location of the power cycle (topping or bottoming) affects the cost and efficiency. Industrial processes that require high temperatures like metal treating can use the bottoming cogeneration; while industries that need medium or low temperatures can use top power cycle. Figure 1.5 shows the differences between the two cases.

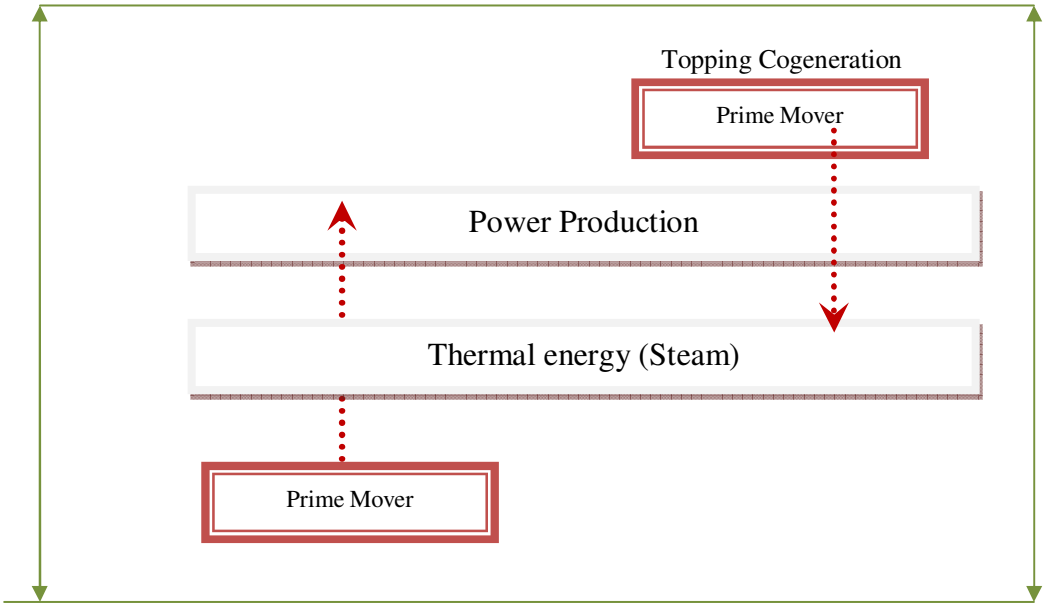

Figure 1.5. Topping and Bottoming Cogeneration Configurations.

7. Design of the heating system: based on the previous six items
8. Selecting and designing the suitable refrigeration cycle: based on the previously mentioned seven items, considering deeply process cooling demand (temperature levels, cooling amount, and profile). Absorption refrigeration (AR) has different kinds, each requiring heat source at certain temperature level, and may produce cooling at different conditions. Therefore, Table 1.3 summarizes the suitable AR for different process cooling requirements.

Table 1.3. Different Types of AR to Be Integrated with a Process Cogeneration Plant.

AR type	Driving heat T(^{o}C)	Cool production T(^{o}C)	working fluid
Single effect	85	1.5-25	H_2O/LiBr
	130	≥ -33.3	NH_3/H_2O
Double effect	>120	1.5-25	H_2O/LiBr
	>150	≥ -33.3	NH_3/H_2O
Thermally coupled dual	≥130	≥1.5 level 1 ≥-33.3 level 2	H_2O/LiBr NH_3/H_2O

I.3. INTEGRATION OF REFRIGERATION CYCLES

Mechanical refrigeration machine (MRM) can be defined as a heat pump that absorbs heat below the ambient temperature and rejects it at the ambient temperature level. This allows integrating the refrigerators into the processes using pinch analysis as the heat pump methodology. Therefore MRM can be integrated across the pinch [1, 4, 5]. The grand composite curve (GCC) can determine how much heat is needed to be removed and at what level. But that requires designing MRM providing different cooling levels if the GCC shows that the cooling demand has different temperature levels [4-6]. MRM has addressed this issue by having different compressors and different expansion valves; each valve corresponds to certain cooling demand level as shown at Fig. 1.6.

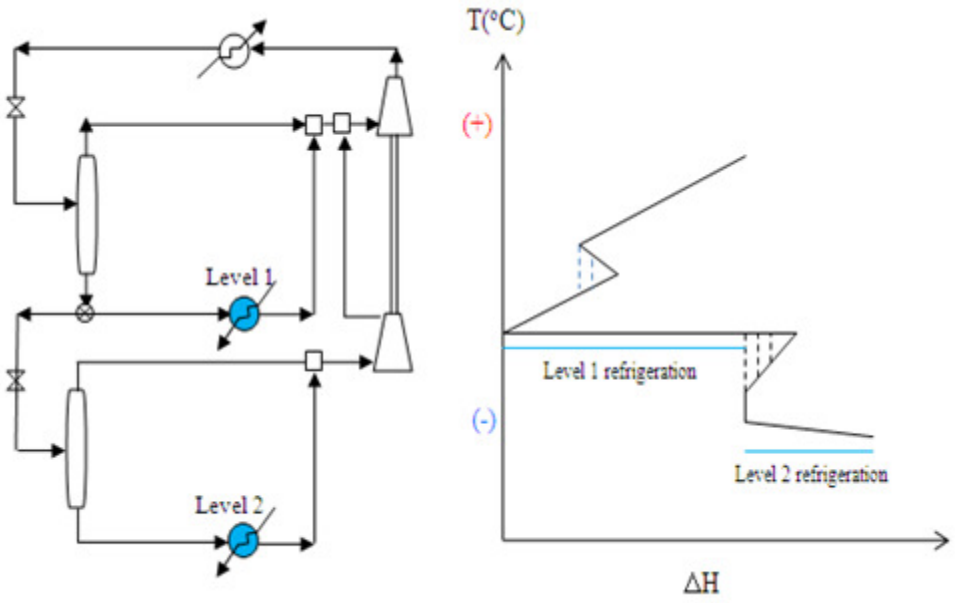

Figure 1.6. Integrating MRM with Two Cooling Levels into Process GCC [5].

On the other hand, integrating absorption refrigerators (AR) has not received the same level of attention as the MRM. Process integration needs to give more attention to AR in two aspects where AR differs from the MRM; these two aspects are:

1. Any single-stage AR is designed to provide one cooling level; which is considered a shortage of the AR in case of a desire to integrate it into industrial processes requiring different cooling levels [4,5,7]. A more expensive double effect AR is needed to provide two cooling levels. Double effect AR is not only expensive, but it also requires a higher temperature heat source (>130^{o}C).
2. AR absorbs heat below the ambient temperature like the MR but AR also absorbs heat at temperatures above 80^{o}C. This heat is the needed to drive AR. Extracting extra heat from the process at this temperature level to drive AR gives the AR potential to compete with MR as this heat is considered waste and is free to be reused by AR.
3. Therefore, this dissertation will address these two issues in details.

I.4. OVERALL OBJECTIVE OF THE DISSERTATION AND RESEARCH CHALLENGES

The problem to be addressed in this work is represented by Fig. 1.7. The overall objective is to develop a systematic procedure for the optimal design and integration of a trigeneration system with energy sources from solar sources and other energy sources including fossil fuels and/or bio fuels. The research challenges include:

- What are the optimum heating and cooling requirements for the process?
- What fractions of energy should be provided by solar energy, fossil fuels, and/or bio fuels?
- How to handle dynamic changes and price fluctuations for the different energy forms while providing a steady-state performance to meet the process requirements for heating, cooling, and power?
- What are the optimum design and operating variables of the system?
- What is the impact of GHG policies (e.g., carbon credits) on the system design?

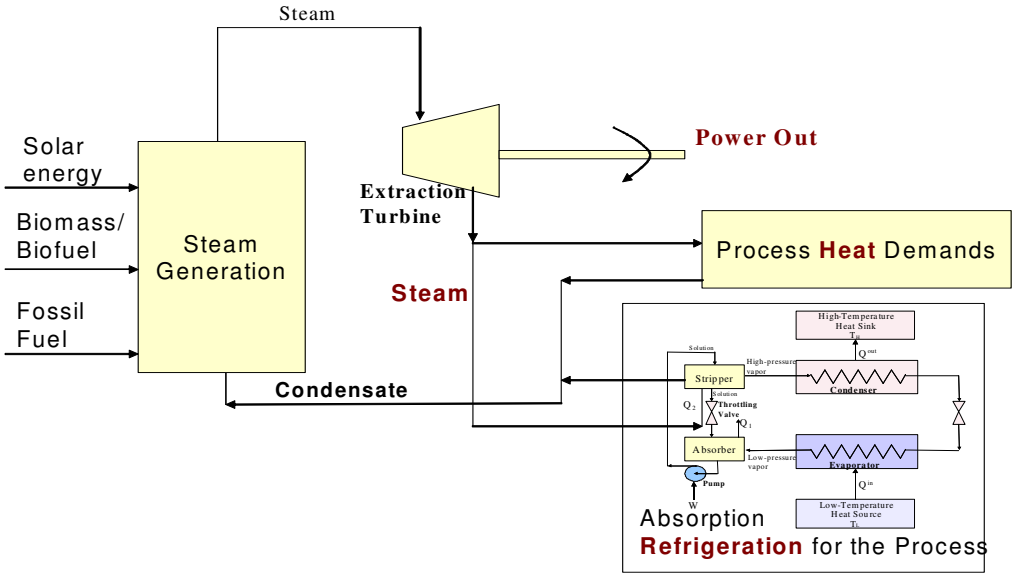

Figure 1.7. Trigeneration Problem with Fossil Fuels, Solar Energy, and Biofuels.

In this work, we consider solar energy and bio fuels in addition to fossil fuels. The objective is to develop a systematic procedure for integrating the three forms of energy to meet the thermal needs of an industrial process. The problem is posed as an optimization program that seeks to minimize the overall cost subject to technical and environmental constraints.

I.5. PROBLEM DECOMPOSITION

Because of the complexity of the problem to be addressed, it has been decomposed into several problems of increasing complexity. These include:

- Solar and fossil for power generation
- Solar, bio, and fossil for cogeneration
- Solar energy, and fossil fuels integration with process extra heat to run absorption refrigeration and produce cool
- AR systems using solar energy, excess process heat, and fossil fuels
- Thermal coupling of dual AR systems
- Solar-assisted trigeneration systems in industrial processes

I.6. DISSERTATION OVERVIEW

- CHAPTER II is a literature survey and background about solar energy industrial basics and applications (heating, cooling, and power), global warming (GW), greenhouse gas emissions, carbon tax, and absorption refrigeration.
- CHAPTER III outlines a systematic approach for the integration, design, and optimization of solar energy into an industrial facility. The dynamic profile of solar radiation through the entire year is adjusted to provide a stable power supply.
- CHAPTER IV covers the first topic “Optimal design and integration of solar systems and fossil fuels for sustainable and stable power outlet”. The option of integration of fossil-fuel with the solar system to provide a compensation effect (power

backup to supplement the power main source from solar energy) that leads to a stable power outlet is considered.

- CHAPTER V considers integrating bio fuels with solar energy as well as fossil fuel. The limited seasonal availability of bio fuels raw material acts as an upper limit of the bio fuel contribution. Also solar energy availability is another variable limited by solar collectors' area. An optimization formulation to determine the optimum mix and schedule under these restrictions has been developed.
- CHAPTER VI deals with the integration of absorption refrigerators into industrial processes with heat extraction from solar energy, fossil fuels, and excess process heat. The problem to be addressed involves the design and integration of an AR system into an industrial facility and the optimal selection of the optimal mix of energy sources which varies dynamically throughout the year.
- CHAPTER VII addresses the topic of thermal coupling of two-level dual absorption refrigeration system with integration with industrial process.
- CHAPTER VIII puts the different problems together to form the trigeneration system. The industrial trigeneration system has its own features. An extended transshipment model is developed to serve as the basis for an optimization approach.
- CHAPTER IX summarizes the major conclusions of this work and offers recommendations for future work.

CHAPTER II
BACKGROUND AND LITERATURE REVIEW

II.1. SOLAR COLLECTORS

Solar collectors (SC) are being used to collect solar radiation, absorb it by a working fluid; which converts the solar radiation energy into hot fluids. SC can be considered a special case of heat exchangers. With some critical differences regarding solar energy has low and variable energy flux. In addition to that the working fluid at the collectors gets heat by radiation. The maximum heat flux without optical concentration is typically 1.1 kW/m^2, and the wave length varies from 0.3 to 3 μm [8]. SC can be divided into concentrating and non-concentrating collectors.

Flat-plate collectors (FPC) are the simplest kind to be manufactured, and require little maintenance. They can provide heat at moderate temperature up to around 100oC. Therefore their applications are limited for low temperature processes, heat water, and simple air conditioners.

FPC can have (a) liquid working fluid, and (b) air working fluid media.
The liquid FPC composed of:

1. Absorber: black metal/plastic sheet absorbs solar radiation and exchange it with the working fluid.
2. Tubes: fluid tubes are the place where the working fluid is circulated
3. Cover: transparent glass cover reduces the convection and radiation loss.
4. Insulation: insulation is used to prevent back and side losses
5. Box: a container for all the four mentioned items

The air FPC is like the liquid FPC with replacing the fluid tubes by a duct for air circulation [8-10]. The steady state useful energy output can be given by:

$$q_{su} = A_c[S - U_L(T_{pm} - T_a) \quad (2.1)$$

S (J/m^2.h) refers to the average energy absorption rate in an hour, and it can be expressed as:

$$S = (I_b + I_d A_i) R_b (\tau\alpha)_b + I_d (1 - A_i)(\alpha\tau)_d \left(\frac{1 + Cos(\beta)}{2}\right)\left(1 + f\, Sin^3\left(\frac{\beta}{2}\right)\right) + I\rho_g (\alpha\tau)_g \left(\frac{1 - Cos(\beta)}{2}\right) \quad (2.2)$$

The last equation is simplified to be expressed as:

$$S = (\tau\alpha)_{av} I_T$$
$$(\tau\alpha)_{av} \cong 0.96 (\tau\alpha)_b \quad (2.3)$$

The efficiency of a collector (thermal efficiency) is the ratio between the useful solar radiations to the incident radiation and can be given by:

$$\eta = \frac{qs}{I_T} \quad (2.4)$$

It is common to re-write equation 1 in the following form [8]:

$$Q_u = A_c[F_R (\tau\alpha)_{av} G_T - F_R U_L (T_i - T_a)] \quad (2.5)$$

The absorber is made of metal sheets with 1-2 mm thickness. The tubes are made of the same metals with diameters of 1-1.5cm. The preferred metal is copper, that followed by aluminum in case of copper unavailability. But aluminum requires special treated water; therefore steel must be used in this case. The covers are made of 3-4 mm glass sheets. And the insulation materials of the bottom and sides are glass wool, and mineral wool. Figure 2.1 shows the FPSC with three possible alternatives to integrate the tubes into the absorber. The tubes can be below, above, or in line with the absorber plate.

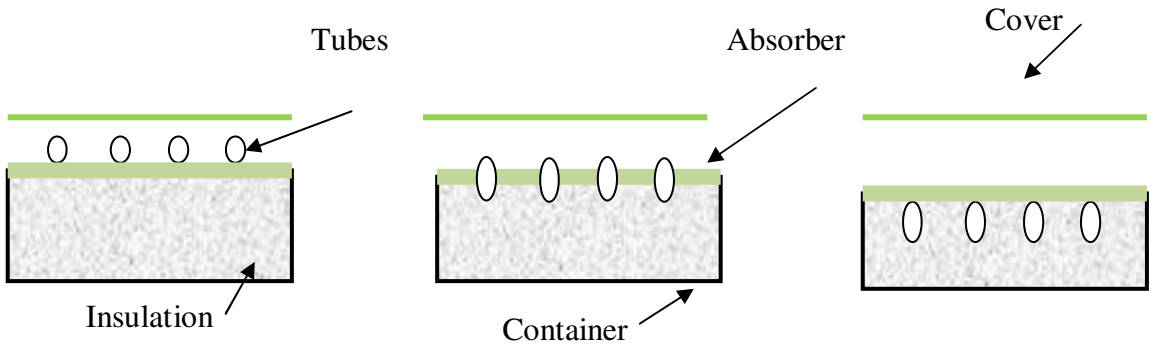

Figure 2.1 Flat-Plate Solar Collectors [8-10].

Plastics are candidates to replace the metals in all previously mentioned FPSC parts in applications requiring temperatures less than 70^{o}C to avoid its decomposition by higher sun temperatures. Plastics production is cheaper and requires less energy than metals production, but its thermal conductivity is lower and its thermal expansion is higher than metals. The life cycle analysis recommend the metals as plastics are produced from fossil fuel derivatives; thus the sustainability design need to consider that in case of producing large amounts of FPSC from plastics.

The metal surface acting as absorber is coated with special coating materials that have high absorptivity of radiation wave length < 4 µm, and low emissivity of radiation wave length more than 4 µm. This is the desired property as solar radiation hits the collectors

with wave length < 4 μm and this radiation comes off the absorber at longer wave length (4-8) μm. This surface layer has thickness of 0.1 μm and almost made of copper oxide on the copper absorber, black chrome on aluminum and steel, or nickel black on galvanized iron; Table 2.1 shows their absorptivity and emissivity values with the maximum temperature that can withstand and work under it [10].

Table 2.1. Absorptivity (A) and Emissivity (ε) of Some Collector Coating Materials [8-10].

	α	ε	T_{max}(^{o}C)
Copper oxide	0.89	0.17	300
Nickel black	0.89	0.12	300
Black chrome	0.868	0.088	400

Table 2.2 shows the effect of the coating on the performance of the galvanized collectors (GC). The comparison is based on a collector with one cover collector.

Table 2.2. Comparison between the GI Collector with and without Selective Coating [8-10].

	Non selective surface	Selective surface
(τε) beam radiation	0.8316	0.7563
(τε) diffuse radiation	0.7567	0.6882
Ut (W/m^2.K)	6.39	3.61
η	40.6	47

The covers made of glass have high transmittance. The covers number is from one to three. Increasing the number decreases the losses but also decrease the transmittance (τ)

and the in turn the absorptivity; therefore there are an optimum number of covers. The effect of the covers on the GI collector's performance is given at Table 2.3. One cover increases the efficiency by around 2% but adding the second cover decreases the efficiency.

Table 2.3. Number of the GI Collectors' Covers on Its Performance [10].

Number of covers	1	2	3
($\tau\varepsilon$) beam radiation	0.8316	0.7305	0.6447
($\tau\varepsilon$) diffuse radiation	0.7567	0.6424	0.5631
Ut ($W/m^2.K$)	6.39	3.87	2.72
η	0.406	0.433	0.418

The calculation of useful solar radiation by any collector is done assuming that the collectors are completely clean; however this is not a practical assumption. Collectors need to be cleaned regularly like once monthly or more frequently.

This collector performance needs to be multiplied by a correction factor to consider that dust cover the cover; which decreases its transmittance. The correction factor changes by location, tilt angle, cover material (glass or plastic). But it is acceptable to have the dust effect correction factor by 0.92-0.99; which means the real useful solar radiation by the collector equals 0.92-0.99 of the estimated values [8-10].

To decrease the convection loss from the top of the FPSC, evacuating the space between the absorber and the cover was proposed. In turn a tubular container and cover were a necessity as only tubular bodies can withstand big pressure difference; that is introduced evacuated tube solar collectors (ETSC). ETSC is an intermediate technology between

the FPSC and the concentrated solar collectors [8-10]. ETSC has two main types; FP-ET and C-ET.

FP-ETSC consists of conventional FPSC with two tubes connected as U surrounded by evacuated tube as shown at Figure 2.2. The modules are stacked together. The vacuum eliminates the convection loss. The second type is the C-ET. Each module has three tubes surrounded each other; the most outer diameter is 6-7 cm diameter. The modules are separate, not stacked together, and below them there is a back diffuser. Therefore the radiation hits the tubes are beam, diffuse, and reflected radiation from the back diffuser as shown at Fig. 2.2. This back diffuser can have two shapes. The first is tubular absorber with diffuse back reflector, and the second with specular cups reflectors as shown at Fig. 2.3.

Figure 2.2 Evacuated Tube Solar Collectors System (Right: FP-ETSC; Left: C-ETSC) [10].

The performance of ETSC is much better than FPSC. The efficiency can increase more than 50% under certain conditions of solar radiation and inlet temperature of the working fluid. And the inlet and out let temperature can be much higher, as the ETSC can work with inlet temperature up to 130^{o}C [10].

Figure 2.3 Evacuated Tube Solar Collectors, Two Concentrating Configurations
(Right: ET with Diffuse Reflector; Left: ET with Cups Reflector) [8-10].

FPSC and ETSC applications are limited to typically 150^{o}C. Higher temperatures require concentrating solar collectors. Concentrating solar collectors (CSC) can provide temperature for intermediate temperature processes (< 300^{o}C), and high temperature applications (>300^{o}C).

CSC have an optical systems (mirrors, lenses) directing the solar radiation for a small size absorber which causes less thermal loss. However there is an optical loss but the total energy collection efficiency is higher than the un-concentrated SC due to have very small absorber. SCSC can be divided into line focusing and point focusing collectors. The line focusing collectors provide intermediate temperatures (<300^{o}C) with efficiency higher than the FPSC and ETSC especially at the range of 150^{o}C, the efficiency can be typically 60% compared to typically 40% respectively. The point focus CSC gives higher temperatures more than 300^{o}C and up to 2000^{o}C [2].

Concentrating collectors compose of two parts; concentrator and receiver. The receiver has an absorber and an evacuated glass tube surrounding it. The concentrator is mirrors or other surfaces with certain optical properties to direct the incident solar radiation to the absorber tube. The opening from where the solar radiation enters the concentrator is called the aperture. The ratio between the apertures of the reflector to the area of the absorber is called the concentration ratio (CR). The energy flux increased on the absorber by a factor equal to this CR. Its value can be up to 100, 1000. The highest CR happens with using the solar furnace. Increasing the CR means higher temperatures; which matches the power and high temperature processes [8-10].

Two parabolas combine together to from the compound parabolic collector (CPC) as shown at Fig. 2.4 CPC has high acceptance angle and concentration ratio typically 3-10 with seasonal adjustment [9].

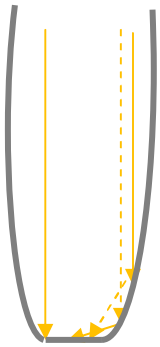

Figure 2.4. Compound Parabolic Collector [5].

Parabolic trough solar concentrators (PTC) composed of three main parts:

1. Absorber: the absorber is 2-4 cm tube made of copper or mild steel. The tube is located at the focal axis of the parabola. The absorber is surrounded by a glass tube as cover to reduce convection loss; the diameter of this cover is more than the diameter of the tube by 1-2 cm.
2. Concentrator: concentrators are reflectors to direct sun rays to the absorber tube with an opening to enter the sun rays called aperture. The aperture width ranges from 1 to 5 m, and the length is more than the width. The concentrators are made of curved back-silvered glass or aluminium sheets (aluminized mylar, aluminized acrylic); but aluminium sheets have lower strength to sun rays than the glass [9].
3. Concentric transparent cover: cover from glass or plastic is used to protect the absorber and the reflecting surface from the weather conditions.

Water is used as the working fluid for applications require temperatures below 100^{o}C.However high pressure water can be used for much higher temperatures. But it

can be work for higher temperatures but under high pressure. Almost these PTC are used for applications require temperatures much higher than that, therefore thermic fluids are used to replace water. The thermic fluids are organic fluids like oil acts as heat transfer agent [10].

Compound parabolic dish (CPD) is one of the imaging and point focusing collectors. Therefore it can concentrate solar radiation from 100 and up to thousand yielding temperature up to 2000^{o}C. But due to mechanical issues there are limits to the CPD size, a dish of 6-7 m diameter is commercialized [11].

PDSC produce the highest temperature that can be obtained by solar energy. Therefore the maximum solar electricity efficiency typically 30% is obtained. Each dish has a sterling engine with a capacity of 1-25 MW [11].

A central receiver is located at the top of a tower where solar radiation is collected and directed to this point by heliostats. Heliostats are independent mirrors with 3-5 m dimensions and there is no limit in the number of mirrors used thus there is no limit on the amount of energy can be obtained at the focus point that is located at top of tower [11]. At the top of this tower there is a receiver. The receiver consists of external type or cavity type.

Central receiver first plant was built in Barstow, CA in 1982 and worked till 1988 with a capacity of 10 MW, the plant was called solar; its electricity capacity was 10MW electricity with using water “steam” as the heating and working media to run the Rankine cycle [11]. Then solar one plant has been retrofitted and molten salt at typically 535^{o}C was used as solar thermal energy storage (TES); with using water as the Rankine cycle working fluid. Solar two worked from 1996 to 1999. Currently in Soville, Spain 2009 is in operation since 2009; the plant capacity is 20 MW [11].

Fresnel lens or mirror is light and thin glass sheet than the conventional convex lenses. It is made of single think glass sheet with separate sections. Its aperture is wide and its focal point is short [12-14].

Fresnel reflectors solar power filed composes of number of thin long mirror sheets reflect the sun rays to a central receiver (absorber). The FR has an advantage more than the PTC that a receiver can be used by more than one reflector (concentrator); which can reduce the cost. Also FR has an advantage over the central tower, FR uses one axis not two tracking axis like the CT [12-14].

Hundred meters Fresnel reflectors have been set in Spain in 2007 with help of Fraunhofer Institute for Solar Energy Systems ISE in Freiburg Germany [13, 14]. Fresnel field composes of long light mirrors that focus the sun rays with the aid of another mirror to a small tube; Fresnel reflectors have potential to reduce solar energy cost, and it is predicted to replace the currently most common PTC in the market soon. The mirrors are made of glass and steel reflecting sun rays on tube acting as an absorber where water under pressure is passing, by concentrated solar radiation the water is heated up to 285^{o}C and forming steam [15]. The Fresnel reflector plant stores solar energy as pressurized hot water so capacity increase and can work day and night.

CLFR has been developed by Austra, CA. Recently Austra assigned a contract with Pacific Gas& Electric to provide it with 177 MW from CLFR; and Ausra is claiming to sell electricity by 10.4 ¢/kWh soon [16].

But the CLFR has a disadvantage makes PTSC and CTR are better in power plants. This shortage that CLFR heat the water to a temperature less than the others concentrated collectors. CLFR heat the water up to 545^{o}F (285^{o}C); which makes its power conversion is less than the solar power plant using PTSC, and CTR. Currently there are two plants

in the land; first one was built as a prototype in 2007 and the second is 177MW in CA [17].

According to thermodynamic, the maximum concentration ratio can be obtained by reaching the maximum collector temperature [18-20]. The maximum temperature happens when the absorber temperature (T_r) becomes equal to the sun temperature (T_S).That happens when the solar energy radiated from the sun to the earth equals the energy radiated from the earth and reached the sun as shown at Fig. 2.5.

$$Q_{S:r} = \sigma_r T_s^4 A_a (r^2 / R^2) \quad (2.6)$$

$$Q_{r:S} = \sigma T_r^4 A_r \Psi \quad (2.7)$$

From equations 6 and 7, the maximum solar concentration occurs when:

$$CR_{\max} = (\frac{A_a}{A_r})_{\max} \quad (2.8)$$

That can be expressed as:

$$CR_{\max} = \frac{D^2}{R^2} = \frac{1}{Sin^2(\theta)} \quad \text{“Circular concentrators”} \quad (2.9)$$

$$CR_{\max} = \frac{1}{Sin(\theta)} \quad \text{“Linear concentrators”} \quad (2.10)$$

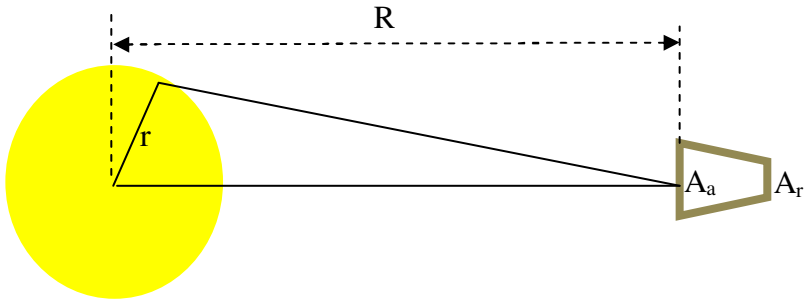

Figure. 2.5. Solar Radiation from Sun to Collector Aperture [8].

II.2. PERFORMANCE OF THE CONCENTRATING COLLECTORS

The useful solar radiation is given by the absorbed solar energy by the absorber of parabolic trough minus the thermal loss as given in next equation [10]:

$$Q_u = F_R\, A_a [S - \frac{A_r}{A_a} U_L (T_i - T_a)] \tag{2.11}$$

$$S = I_b\, \rho\, (\gamma\tau\alpha)\, K_{\gamma\tau\alpha} \tag{2.12}$$

$$A_r = \pi\, D_r\, L_r \tag{2.13}$$

$$A_a = (W_a - D_o)\, L_a \tag{2.14}$$

For a central receiver plant consists of receiver with area A_r located on the top of a tower with H height; and the heliostats filed consist of N mirrors, each with area A_m. The mirrors cover A_g area with spaces; thus the real area is the fraction (ε) occupied of the land times the A_g; that can be expressed as [10]:

$$N.A_m = \varepsilon.A_g \tag{2.15}$$

Therefore the useful solar radiation and the concentration factor are given as [20]:

$$qu = \varepsilon\, A_g\, (I_b\, (r_b)_{av}\, \rho\tau\alpha - U(T_{pm} - T_a)/C) \tag{2.16}$$

$$C = \frac{NA_m}{A_p} = \frac{\varepsilon\, A_g}{A_p} \tag{2.17}$$

II.3. SOLAR SYSTEMS

Solar system composes of the solar collection filed, storage tank, pumps, relief valves, and or controllers. They can be divided into two main systems; which are closed loop and open loop.

The solar collectors' fluid (SCWF) is kept in a closed cycle separate from the load heat transfer media. Figure 2.6 shows the main components of the system. The SCWF is circulated between the solar collectors SC and the storage tank that has variable temperature. The flow rate is constant; therefore different temperatures are expected. The storage tank content passes many times through the SC to be heated (2-5)^{o}C in case of active system, and 10^{o}C in case of thermosyphon system. The storage tank has a coil providing heat to the dispatch tank. The dispatch tank has adjusted temperature by the fossil fuel exchange heat with the load through heat exchanger.

The temperature reached to the desired value by the load by:

1. Using the auxiliary heater if the SC storage tank temperature is less
2. Reducing the temperature if the SC tank temperature is higher by bypass arrangement or pump.

Bypass arrangement: a three-way valve is used to be circulated the part of the load heat transfer media, before be heated through the heat exchanger, to be mixed with the hot fluid and adjust its temperature.

Bang-bang fashion of pump operation can be used; change the flow rate of the pump to take the SCWF out when its temperature reaches the desired value. But this is not recommended as it can cause pump failure [2].

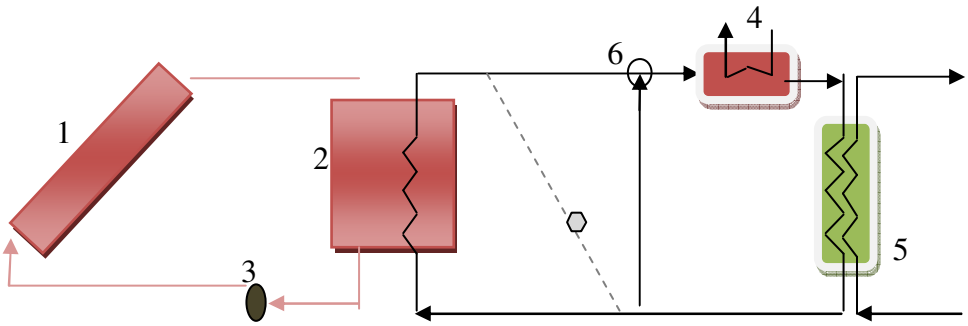

Figure 2.6. Closed Solar System [2].

1: Solar Collector; 2: Storage Tank; 3: Pump; 4: Auxiliary Heater; 5: Process Load Heat Exchanger; 6: Bypass "Three- Way Valve"

The system here has two choices; the SCWF can be re-circulated or exchanged by new WF. The storage tank gets its heat from the SCWF and provides heat to the process load as shown at Fig. 2.7; but it is not allowed to return the process working fluid again to the storage tank [21]. This is useful to keep the storage tank at the temperature of the SC exit all the time.

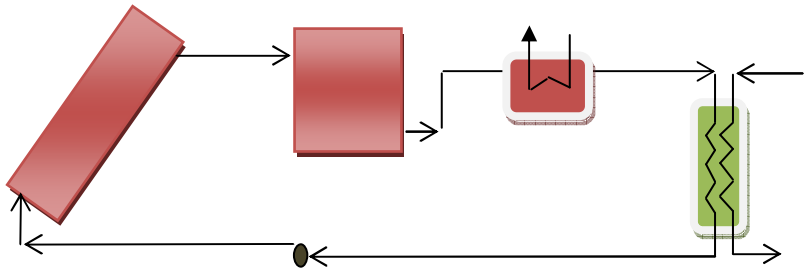

Figure 2.7. Open Solar System [2, 10].

II.4. SOLAR THERMAL PLANTS

Solar energy is used since 1980s in the industrial plants. Eighty four plants are currently in operation worldwide with a capacity of $24MW_{th}$. These are located in different countries including Egypt, Greece, Italy, USA, etc. These industrial processes use solar energy to provide heat at temperatures typically in the range of 60^oC to 250^oC using solar collectors' area of $34{,}000m^2$. The most common plants are textile, food, meat, beverage, and paper industries [2].

Cogeneration has been used for while to refer to simultaneous power and heat production; which includes parallel and series production. Cogeneration term used widely in the period 1980s-1990s, but the term combined heat and power production (CHP) has been used widely recently referring to cogeneration. Now the term "cogeneration, CHP" refers to simultaneous production of power and useful thermal energy; where this useful thermal energy can be heat or cool. Therefore cogeneration mean simultaneous power production and one or more of the useful thermal energy forms (hot water, steam, chilled water) [2].

Cogeneration can save money and fuel; therefore it can be a candidate for any plant needs power and thermal energy (heat or cool) as long as the thermal energy usage covers the cost of the cogeneration system. Therefore cogeneration can be used in industrial sector, and in commercial, and institutional, and district plants as well. The capacity is in the range of 100 kW to 100 MW [2].

Cogeneration widespread at the market depends on the price of the electricity and the natural gas (NG); more specifically it depends on the relative prices between the natural gas and the electricity. Increasing the NG prices motivate the CHP widespread [2].
Therefore the future of CHP is uncertain. It depends on many factors including the NG prices, the electricity prices, grid connection and distribution, etc. [2]. But the increased

overall efficiency of the CHP is predicted to increase the market potential of the CHP [2].

Therefore the overall efficiency of the cogeneration system is given by:

$$\eta_{cog} = \frac{power + thermal\,(heat\ rate)}{Fuel} \tag{2.18}$$

That can be written as

$$\eta_{cog} = \frac{power}{Fuel} + \frac{thermal\,(heat\ rate)}{Fuel} \quad > 65\% \tag{2.19}$$

This efficiency is always higher than 65% and can increase 85% in good design and operated plants. But the conventional power plants has power efficiency is 30% average, and boiler thermal efficiency is typically 80%. Thus the average of the two systems is 55%; which is less than the cogeneration efficiency [2]. Based on that the fuel consumption and saving can be given as:

$$Fuel_{cog} = \frac{Power + Thermal}{\eta_{cog}} \tag{2.20}$$

$$Fuel_{conv} = \frac{Power + Thermal}{\eta_{conv\backslash av}} \tag{2.21}$$

$$Fuel\ saving = (Power + Thermal)\left(\frac{1}{\eta_{cog}} - \frac{1}{\eta_{conv\backslash av}}\right) \tag{2.22}$$

Cogeneration topping cycle means using the heat produced from combusting the fuel first to produce power, then the exhaust hot gases are used to provide thermal energy (heat-cool) by extracting the useful heat by heat recovery boiler (waste heat boiler WHB); this is also called heat recovery steam generator (HRSG) [2]. Most of the

cogeneration plants are top cycle as power generation efficiency increase with increasing the working fluid temperature.

Bottoming cogeneration refers to producing power after providing the heat demand. The fuel burned to produce hot gas or heating media first for the heat demand, then low temperature working fluid is used to drive turbine to produce power. The efficiency of these system is lower, but bottoming cogeneration is still find potential in applications require high heating like metals treatment [2].

In this bottoming cogeneration, the working fluid (water) can be replaced by organic fluids like refrigerants (ammonia, propane...). As these organic fluids have lower boiling point; which makes it more suitable to be used with the available low temperature. But using these fluids requires special equipments from special materials; that increase the cost [2]. The main equipments of the cogeneration plant include:

A. Prime mover: the prime mover is an equipment getting heat from fuel or thermal energy source to produce steam or hot gases. Then this steam or hot gases are used as heat source and to drive electricity generator [2]. The prime mover can be one of three kinds; these are steam turbines (back-pressure turbines), gas turbines, and reciprocating engine (internal combustion).

Steam turbines are very common in industry. It differs from the other two prime movers (gas turbine, reciprocating engine) that is gets its heat demand from an external boiler. The turbines used at the cogeneration plant are the backpressure turbines; which is non-condensing turbines. Where high pressure and high temperature steam is passed through the turbine rotating its blades producing electricity, and the exit steam still can be used as heating media to produce cool or heat [2].

The capacity of back-pressure (non-condensing) turbines has the range of 50 kW to 100 MW and more. It requires steam pressure of 10-135 bars. The heat to power ratio is from

4 to 10 with increasing the efficiency with increasing the size or the power. The efficiency ranges from 8-20% [2].

Gas turbines are used more in the power plants. Air and fuel are fed to the combustion chamber where high temperature air is the product. The heat to power ratio is 1 to 3. The efficiency increase with power from 20 to 45% if it complete at full load (not part load); the size is 100 kW to 100 MW [21]. Liquid fuels (jet fuel, kerosene) and gaseous (natural gas, propane) can be used. The highest efficiency is obtained with liquid fuels, but the lowest GHG emissions are with using natural gas [2].

Reciprocating engine or also called the internal combustion (IC) has its internal combustion unit. It differs from the other two prime movers; as it produces rotated motions; which can be used with cogeneration but not common. The spark-ignited gasoline engine is used in automobiles have been modified to be work continuously to be suitable for cogeneration. The fuels also have been replaced by diesel, and/or diesel fuel [2]. Its size is from 50 kW to 200 MW, also minim cogeneration units of size 6 kW is manufactured now. The average heat to power ratio is 0.5. IC needs to be cooled by liquids; the cooling liquid can be used as a low temperature (71^{o}C) heat source [2].

B. Heat recover units include 1) heat recovery steam generator, and 2) absorber refrigerator. The recovered heat can be used to produce steam for heating purposes. But if the process has a cooling demand, the recovered heat can be used to drive absorption refrigerators to produce the cooling demand.

Heat is recovered in form of hot water, or steam according to the temperature level. The high temperature is used to superheat the working fluids, medium temperature can be used for vaporizing the working fluid, and the low temperature is used to preheat the working fluid at the economizer [2].

The efficiency of the heat recovery increase with decreasing the back pressure; but that also accompanies with the cost increase as well. The known cogeneration plants have back pressure average 0.03 bar; with temperature approach typically of 15^{o}C to 45^{o}C [2]. Absorption chiller is similar to the vapor compressor refrigerators but without the vapor compressor. A pump, absorber, and heat generator replace the compressor. Thus heat is needed to drive the absorption chiller. The heat needed is low quality; thus can be supplied from different sources in different forms (hot water, low pressure steam, hot gases…). Absorption refrigerators (AR) operation is based on absorbing the vapor refrigerant in an absorbent; the yielding mixture is pumped to raise its pressure to a level allow low temperature heat to strip it from the mixture [7].

Absorption refrigeration may be an essential item of the cogeneration plant technically and economically in hot climate areas. In this case, cooling is needed more than heating; so availability of AR is a necessity as the heating unit [18]. There are many advantages of using AR into the cogeneration plant:

1. Eliminate the electricity beak that happens during cooling season if the vapor compressor refrigerators (VCR) are used
2. Power production from the cogeneration becomes stable, as the power demand for VCR is eliminated
3. In case of low heat demand, the thermal energy is used to produce cool instead of venting and losing it; which increase the efficiency.

The AR can use the heat directly or indirectly from the prime mover. The indirect fired AR are the units driven by hot water or steam. The direct fired units are using the hot gases produced from the prime mover directly. With all the heating media (water, steam, gases) of the AR, the higher its temperature the higher is the efficiency. Higher temperature means less heating fluid flow rate and thus less energy. Table 2.4 summarizes the heat demand for some types of AR in case of in direct and direct fired units [2].

Table 2.4. Typical Heat demand for H_2O/LiBr AR to produce 1 ton refrigerant (1 TR) [2].

AR type	Heat demand
Single effect	Steam: 8 kg/h, 121°C
Single effect	Hot water: 100 kg/h, 88°C
Single effect	Hot gases: 35 kg/h, 550°C
	Hot gases: 142kg/h, 290°C
Double effect	Steam: 4.5 kg/h, 185°C

II.5. GREEN HOUSE GAS EMISSIONS AND GLOBAL WARMING

China is the most GHG emitters. Then the USA and India come as reported by the Carbon Tax Center. Countries try to have its own carbon tax and apply it for certain sectors; which in many places met with objections. The objections are based on the relation between economy and industry growth and the emissions, increasing the fuel prices if the tax is implemented. Australia is proposing to apply the cap- and trade based on emissions. The tax has different values based on the emissions source. The tax average in Australian currency is \$23/tCO_2 [19]. New Zealand Emission Trading Scheme set a carbon tax effectively of \$NZ12.5/tonne through the period of July 2010 until December 31, 2012. France proposed a carbon tax of 17 Euros per tonne of carbon dioxide (CO_2), but this proposal is blocked. Canada has a carbon tax in some of its parts since 2007. Beginning of 2008 and ending in 2012, the tax has been set by \$10/tCO_2e with an annual increase to reach \$30/tCO_2e. That corresponds to ¢2.41/liter gasoline and ending by ¢7.2/liter gasoline in the gas stations. The US has the same tiers in different states. For example ¢4.4/tCO_2 has been implemented on business sector since 2008 in San Francisco Bay Area.

Cap and Trade (CT) is another policy to reduce GWGE; cap on greenhouse gas emissions with a market-based scheme and trade as financial instruments the “permits”

to produce those emissions [20]. It differs from the tax. CT set an upper limit of CO_2 emissions that a company can't exceed. But the carbon tax is superior for it for several reasons including CT not encouraging in investment in renewable energy sector, carbon tax is easy and can be applied soon but CT need more time for negotiation, carbon tax address emissions from different sectors but the CT is not yet.

CHAPTER III
OPTIMAL DESIGN AND INTEGRATION OF SOLAR ENERGY, FOSSIL FUELS, AND/OR BIOFUELS FOR SUSTAINABLE AND STABLE POWER OUTLET, AND HEAT SUPPLY*

III.1. INTRODUCTION

Solar energy is one of the most attractive sources of sustainable energies. Much attention of research work has been paid to the design of solar energy systems for providing thermal energy (e.g., solar collectors) or electric power (e.g., photovoltaic systems). However, much less attention has been directed to the use of solar energy for process cogeneration in industrial processes. Process cogeneration involves the utilization of combined heat and power from certain sources. For instance, high pressure steam may be generated in process boilers and fed to steam turbines that generate electric power and deliver exhaust steam that is hot enough (usually low pressure steam) to be used for process heating purposes. The dual usage of steam lends the name "cogeneration" and typically leads to reduction in energy cost and reduction in greenhouse gas emissions. In this regard, it is possible to conceive of promising cogeneration systems that involve the partial usage of solar energy supplemented with the use of fossil fuels. Thus, the collected solar heat may be converted to electric energy using power cycles that use external heat source such as Rankine cycle. The solar-based Rankine power cycle consists of a series of heat exchangers (that work as a solar boiler to produce steam), a reheat turbine, generator, pumps and cooler "condenser", and a steam turbine. Water is used as the working fluid due to its low price and to match the need to steam in the industrial processes. Rankine reheat cycles is designed to run a high pressure steam up to

---

* Part of this chapter is reprinted with permission from "Optimal design and integration of solar systems and fossil fuels for sustainable and stable power outlet" by Tora EA, El-Halwagi MM., 2009. Clean Technology and Environmental Policy, Vol. 11 (4), 401-407, Copyright (2010), Springer.

100 bars to produce electricity with possibility to draw steam at middle stage or hot mixture water at the last stage. The steam produced at 100 bars is suitable to generate power also at temperature of 371^{o}C to assure achieving cycle efficiency not less than the efficiency of the Rankine Organic cycle [22].

Solar power plants have been typically driven by the need for small-scale (200kW - 10MW) power systems in rural areas. There are several factors that motivate the move to more and bigger solar systems. These factors include the dwindling fossil resources and their increasing prices, the need for clean and sustainable energy resources, the global warming problem, and the need for the privatization of the electricity sector in some countries [23]. Another potential usage of solar systems in industrial facilities is intended to shave off peak demands. The basic idea is to provide power supply at the peak demand (peaking power system) that is needed primarily through the peaks load time. It may be operated during all the sunshine time alone or with a back-up fossil fuel system. Furthermore, its power yield can be extended beyond sundown by using solar energy storage.

The solar heat may be collected using various collection systems that include:

a. Flat plat collector (FPC) that are simple in design and operation
b. Parabolic dish collectors (PDC) that are commonly used to produce electricity directly in rural/ isolated locations
c. Central receiver towers that heat air to ~1000^{o}C to run a gas turbine producing electricity
d. Parabolic trough collectors (PTC) that produce high pressure superheated steam

PTC are among the most commonly used collectors used in power plants and has a proven track-record of providing high efficiency and ability to operate at high temperature [24-26]. As an illustration of a proven track-record, the Solar Electric Generating Systems (SEGS) which usually use PTC and produce a power range of 20 –

200 MW have been operational since the mid 1980's. For example, SEGS VI located in Kramer Junction, California is operational since 1989 and produces 30 MW using PTC over a 188,000 m^2 field area. The PTC reflectors reflect the sunlight onto a central tube receiver which passes the heat to a heat transfer fluid which subsequently flows through heat exchangers that produce superheated steam at temperatures as high as 400^oC and pressures as high as 100 atm. The power plant is supplemented by the use of natural gas. This natural gas contribution cannot exceed 25 percent of total energy contribution so as to comply with federal laws providing incentives for solar power plants.

The objective of this chapter can be divided into two main parts:-

1. Development of a systematic approach to the integration of solar and fossil systems to provide stable power outlet:- The approach involves the combination of heat and power aspects of the process, the sizing of the solar system, the distribution of energy input from the fossil, and the scheduling of the operation of the integrated system.
2. Development of a systematic procedure for energy conservation and incorporation of tow renewable sources of energy into industrial usage: biofuels and solar energy.

III.2. PROBLEM STATEMENT

Given a continuous process with:

- A number N_H of process hot streams (to be cooled) and a number N_C of process cold streams (to be heated). Given also are the heat capacity (flowrate x specific heat) of each process hot stream, $FC_{P,u}$; its supply (inlet) temperature, T_u^s; and its target (outlet) temperature, T_u^t, where u = 1,2,...,N_H. In addition, the heat capacity, $fc_{P,v}$, supply and target temperatures, t_v^s and t_v^t, are given for each process cold stream, where v = 1,2,.,N_C.
- Available for service are the following:

- A set C_UTILIITY = {clc = 1,2, …, N_{CU}}of cooling utilities whose supply and target temperatures (but not flow rates) are known.
- A set FOSSIL_UTILITY = {flf = 1,2, …, N_{FHU}}of fossil-based heating utilities. For each fossil-based heating utility, the temperature (T_f^{Fossil}) and the cost (C_f^{Fossil}) are known.
- A candidate solar energy plant. The size and cost of the solar plant are unknown and its delivery of thermal energy and temperature of the heating utility provided by the solar plant will vary over time depending on the variations of solar intensity.
- Power is generated via extraction turbines that use the steam to produce electric power and discharges steam for process heating purposes.

It is desired to develop a systematic approach to the integration of solar energy, fossil fuel, and/or biofuels so as to produce a stable power outlet, or steam supply that can be used for heating, and cooling purposes. The procedure should also determine the dynamic performance of the system, the optimal sizing of the solar and power plants, and the optimal mix of solar energy, fossil fuels, and biofuels throughout the year. Figure 3.1 is a schematic representation of the problem.

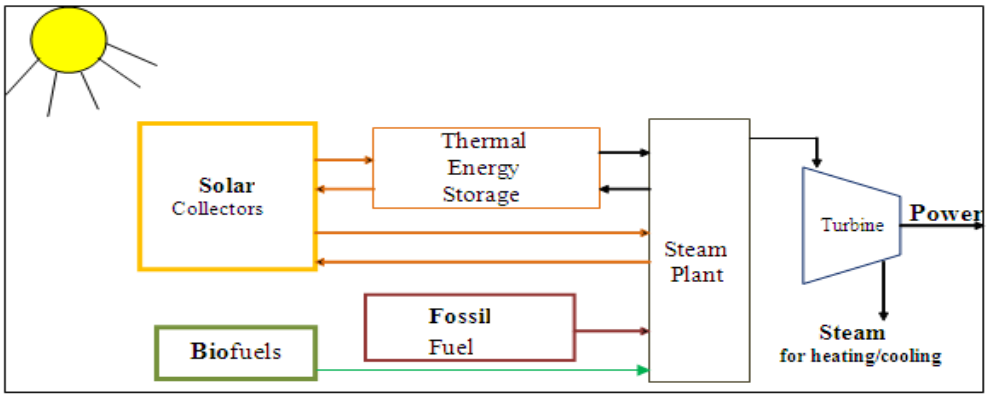

Figure 3.1. Schematic Representation of the Problem Statement.

III.3. APPROACH

To streamline the development of the design procedure, the following assumptions are used:

- The decision-making time horizon (e.g., a year) is discretized into N_t periods leading to a set of operating periods: PERIODS = {t|t= 1,2, …,N_t}. Within each time period, the values of energy usage are averaged and the analysis within that period is carried out for the averaged energy values of each energy type.
- It is only allowed to have intra-period integration (i.e., no energy is stored, integrated, or exchanged over more than one period). In selecting the number and duration of the periods, it is important to reconcile the accuracy of fluctuations (e.g., in solar energy) versus the computation efforts.

The first step in the approach is to perform heat integration to determine minimum heating and cooling utilities and optimal level of utility usage and the extent of process cogeneration via combined heat and power [1, 5]. The cogeneration analysis [27, 28] also provides an optimum distribution of steam balances around the headers. Figure 3.2 shows a representation of the obtained information for the d^{th} steam header. Steam enters headers from two key sources: the process boilers and heat recovery/steam generating units ($Q_d^{Header\_Process}$) as well as from other sources that include let downs from higher-pressure headers, outlets of extraction turbines, etc. ($Q_d^{in\_other}$). The inlet steam is distributed to satisfy process demands at that level for heating ($Q_d^{Heating}$), non-heating ($Q_d^{non-heating}$) such as stripping and blanketing, power generation by feeding to an extraction turbine ($Q_d^{Turbine}$), and letting it down to other headers, venting, and losses (Q_d^{Down}). The heat balance around the header is expressed as:

$$Q_d^{External} + Q_d^{in\_other} = Q_d^{Heating} + Q_d^{non-heating} + Q_d^{Down} + Q_d^{Turbine} \qquad \forall d \qquad (3.1)$$

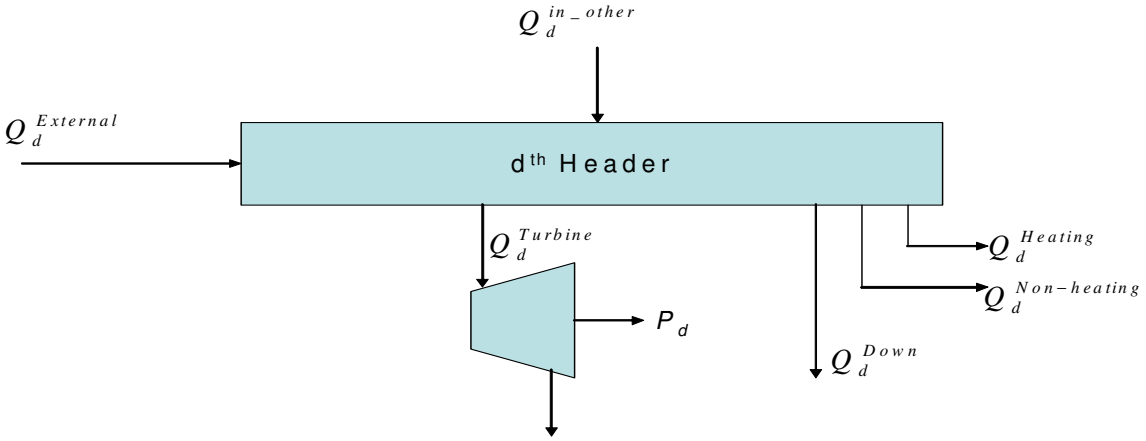

Figure 3.2. Header Balance Resulting from Cogeneration Analysis.

Once the process utilities, the extent of power production through process cogeneration, and the header balances are determined, the approach is carried out through a sequence of steps. These steps include assessment and optimization as follows:

1. Modeling level: In this stage, the performance of the solar system and the power plant is modeled. Specifically, the dynamic fluctuations of the solar-energy collection and dispatch are modeled.
2. Integration level: should solar energy be used alone or in conjunction with fossil fuel? To what extent? Should the solar energy be used directly or partially stored via TES?
3. Operation mode: should the solar system be operated at full or partial load? During which periods of the year?
4. Optimization objectives: there are several factors to be considered in optimization such as fixed and operating costs, collector type and area, extent of CO_2 reduction (solar versus fuel which becomes important if there is a carbon credit), etc. Figure 3.3 is a schematic representation of the elements addressed in the approach.

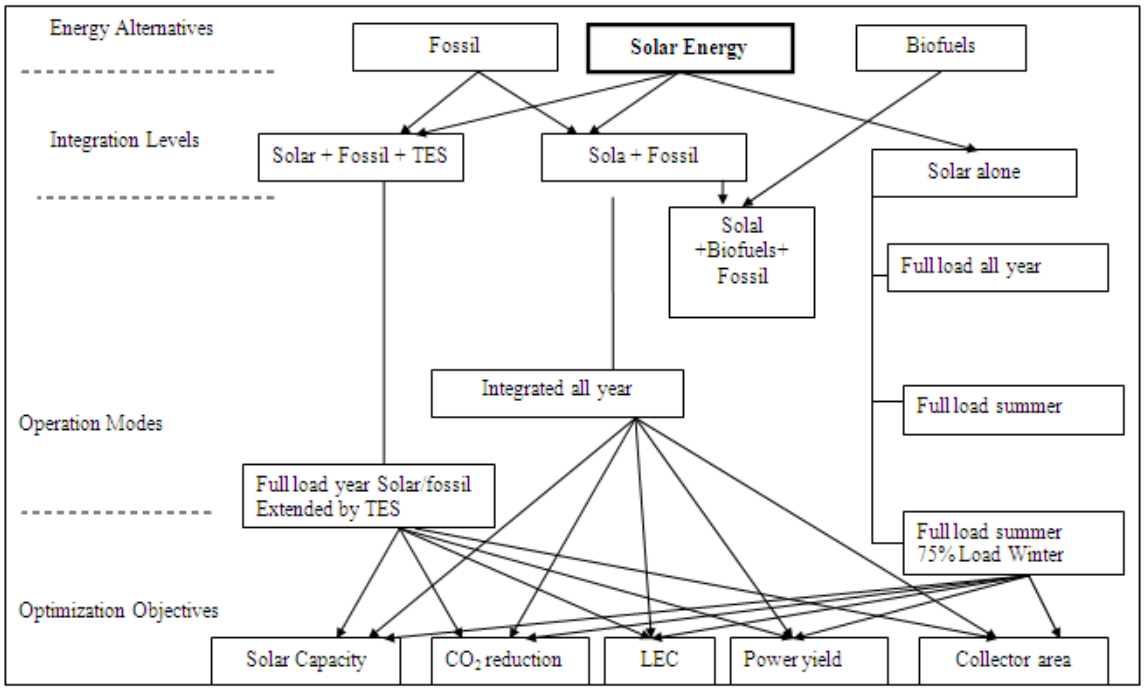

Figure 3.3. Key Aspects Addressed by the Approach.

III.4. MODELING OF THE SOLAR COLLECTION SYSTEM

The following are the steps followed in solving the problem modeling the solar collection system along with the associated equations and sources of information:

1. Determine the longitude and the latitude of the industrial location. The following are good sources to determine this information:

- NASA maps "Or pick a location graphically"

http://eosweb.larc.nasa.gov

- Other web sites that has electronic Atlas, such as:

http://nationalatlas.gov/natlas/Natlasstart.asp

2. Get the weather data of the selected location; the direct normal radiation (kWh/m^2/day); these data are available for a large number of towns in:

- NASA website

http://eosweb.larc.nasa.gov/cgi-bin/sse/sse.cg

- Department of energy (DOE): EnergyPlus Energy Simulation Software- weather data

http://www.eere.energy.gov/buildings/energyplus/cfm/weather_data.cfm

3. The weather data needed in these calculations include:

- average hourly statistical for dry bulb temperature
- average monthly statistical for dry bulb temperature
- monthly statistics for solar radiation (direct normal, diffuse, global horizontal)Wh/m^2
- average hourly statistics for direct normal solar radiation
- monthly statistics of wind speed

1. Determine the performance characteristics of the solar collector
   Performance characteristics are available for many solar collectors through manufacturers resources, professional organizations such as the American Society of Heating, Refrigerating, and Air-Conditioning Engineers (ASHRAE), or through engineering calculations. These characteristics include the optical efficiency of the collector, the length, the aperture width, the inner and outer tube diameters and the concentration ratio.

2. Calculate the portion of the incident solar radiation that will actually reach the collectors.

3. Calculate the absorbed solar intensity; (actual available solar intensity minus the losses due to the optical efficiency of the receiver of the collector).

4. Calculate the thermal losses from the absorber of the collectors.

8. Determine the net solar beam radiation "the useful radiation" (the absorbed radiation less the thermal losses of the absorber tube of the collector).

9. Determine the efficiency of the Rankine cycle; which refers to how much useful work "electricity" can be obtained from the solar net useful radiation.

10. Calculate the power per unit area of the collector receiver surface area. This is equal to the useful net solar radiation times the efficiency of the Rankine cycle.

11. Now, we have the dynamic profile of solar radiation. This profile is used as input data for the optimization formulation which is described in the next section.

III.5. OPTIMIZATION FORMULATION

The optimization formulation has been developed to address the integration of solar energy with fossil fuel. Then it has been modified to consider integrating the biofuels in addition to the fossil fuel with solar energy. In all cases, process heat has been considered available for free.

III.5.1. INTEGRATION OF SOLAR ENERGY AND FOSSIL FUEL

The following optimization formulation is developed to address the design challenges.

Objective function: Minimize total annualized cost =

$$\sum_{f}\sum_{d} C_{f,d}^{Fossil} \sum_{t} Q_{f,d,t}^{Fossil} * D_t + \sum_{s} AFC_{s}^{Solar} + \sum_{s}\sum_{d} \sum_{t} C_{s,d,t}^{Solar} * Q_{s,d,t}^{Solar} * D_t \qquad (3.2)$$

where $C_{f,d}^{Fossil}$ is the cost of the f[th] fossil fuel providing steam to the d[th] header, $Q_{f,d,t}^{Fossil}$ is the rate of heating in the form of steam resulting from the f[th] fossil-based utility and entering the d[th] header during period t, D_t is the duration of period t, AFC_s^{Solar} is the annualized fixed cost of the s[th] solar plant, $C_{s,d,t}^{Solar}$ is the operating cost of the s[th] solar plant feeding the d[th] header in period t, and $Q_{s,d,t}^{Solar}$ is the rate of heating in the form of steam resulting from the s[th] solar plant and entering the d[th] header during period t.

Since the generated steam is provided from fossil and solar sources, Figure 3.3 can be re-drawn to account for these sources as shown in Figure 3.4.

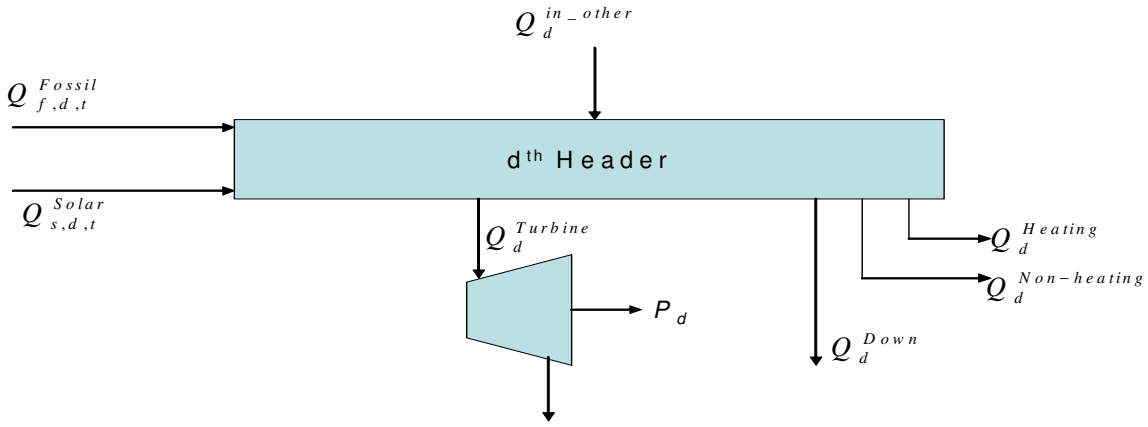

Figure 3.4. Balance around the d[th] Header.

The heat balance around the inlet of the d[th] steam header in period t is given by:

$$\sum_f Q_{f,d,t}^{Fossil} + \sum_s Q_{s,d,t}^{Solar} = Q_d^{External} \qquad \forall d, \forall t \qquad (3.3)$$

Depending on the pressure of generated steam, it is fed to the steam header which has the same or lower pressure.

Next, heat balances are carried out for the total rate of a given fuel is calculated by summing the splits over the headers:

$$Q_{f,t}^{Fossil} = \sum_{d} Q_{f,d,t}^{Fossil} \qquad \forall f\ ,\ \forall t \qquad (3.4)$$

$$Q_{s,t}^{Solar} = \sum_{d} Q_{s,d,t}^{Solar} \qquad \forall s\ ,\ \forall t \qquad (3.5)$$

The collected solar energy in period t is typically given by:

$$Q_{s,t}^{Solar} = Q_{s,t}^{Useful\_Solar} * A_s \qquad \forall s\ ,\ \forall t \qquad (3.6)$$

where $Q_{s,t}^{Useful\_Solar}$ is the useful power collected (and delivered in a thermal form) per unit area of the s^{th} solar collector in period t and As is the area of the s^{th} solar collector.

The annualized fixed cost of the s^{th} solar power plant is given as a function (α_s) of the size:

$$AFC_s^{Solar} = \alpha_s(A_S) \qquad \forall s \qquad (3.7)$$

The power generated from the turbine during period t from the turbine connected to the d^{th} header is calculated through the turbine performance model, $\psi_{d,t}$, as follows:

$$P_{d,t} = \psi_{d,t}(Q_{d,t}^{Turbine}) \qquad \forall d\ ,\forall t \qquad (3.8)$$

where $P_{d,t}$ is the electric power produced during period t from the steam turbine(s) connected to the d^{th} steam header and $Q_{d,t}^{Turbine}$ is the heat rate provided to that turbine in the form of steam during period t.

III.5.2. INTEGRATION OF SOLAR ENERGY, FOSSIL FUEL, AND BIOFUELS

Integrating biofuels makes the optimization more complex. As biofuels has a dynamic profile considering both the price and availability. Biofuels as a fuel differs from solar energy; biofuels have an upper limit that can't be overcome.

Therefore, to simplify the problem, the following assumptions are introduced:

- The decision-making time horizon (e.g., a year) is discretized into N_t periods leading to a set of operating periods: PERIODS = {t|t= 1,2, …,N_t}. Within each time period, the values of energy usage are averaged and the analysis within that period is carried out for the averaged energy values of each energy type.
- It is only allowed to have intra-period integration (i.e., no energy is stored, integrated, or exchanged over more than one period). In selecting the number and duration of the periods, it is important to reconcile the accuracy of fluctuations (e.g., in solar energy) versus the computation efforts.

The approach decomposes the solution into two stages: heat integration followed by energy assignment, design, and scheduling. In the first stage, heat integration is carried out (graphically using thermal pinch analysis or mathematically using linear programming) to determine minimum heating and cooling utilities and optimal level of utility usage [1,5]. This includes the identification of heat to be provided to each steam header characterized by heat and temperature (Q_d^{Header} and T_d^{Header}). In the second stage, the optimal quantity of each type of energy is determined for each operating period and the overall design of the system is synthesized. For each period t, a utility-header-process structural representation (Figure. 3.5) is developed to embed potential configurations of interest. Outputs from each energy type is split into fractions and assigned to different steam headers which subsequently feed the process to satisfy the optimal requirements from the heat integration analysis.

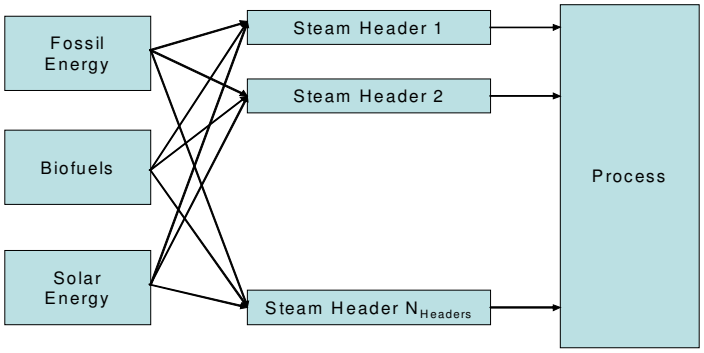

Figure 3.5. Structural Representation of the Problem.

The objective function is given by:

Minimize total annualized cost =

$$\sum_f C_f^{Fossil} \sum_t Q_{f,t}^{Fossil} * D_t + \sum_b \sum_t C_{b,t}^{Biofuel} * Q_{b,t}^{Biofuel} * D_t +$$
$$+ \sum_s AFC_s^{Solar} + \sum_s \sum_t C_{s,t}^{Solar} * Q_{s,t}^{Solar} * D_t -$$
$$- \sum_b \sum_t R_b^{Biofuel} * Q_{b,t}^{Biofuel} * D_t - \sum_s \sum_t R_s^{Solar} * Q_{s,t}^{Solar} * D_t \qquad (3.9)$$

where C_f^{Fossil} is the cost of the fth fossil fuel, $Q_{f,t}^{Fossil}$ is the rate of heating of the fth fossil-based utility during period t, D_t is the duration of period t, $C_{b,t}^{Biofuel}$ is the cost of the bth biofuel, $Q_{b,t}^{Biofuel}$ is the rate of heating of the bth biofuel-based utility during period t, AFC_s^{Solar} is the annualized fixed cost of the sth solar plant, $C_{s,t}^{Solar}$ is the operating cost of the sth solar heating utility, $Q_{s,t}^{Solar}$ is the rate of heating of the sth solar-based utility during period t, $R_b^{Biofuel}$ is the carbon credit of the bth biofuel, and R_s^{Solar} is the carbon credit of the sth solar utility.

The heat balance around the dth steam header in period t is given by:

$$Q_{f,d,t}^{Fossil} + Q_{b,d,t}^{Biofuel} + Q_{s,d,t}^{Solar} = Q_d^{Header} \qquad \forall d, \forall t \quad (12)$$

$Q_{f,d,t}^{Fossil}, Q_{b,d,t}^{Biofuel}, and\ Q_{s,d,t}^{Solar}$ are the heat rates provided from the fossil, the biofeul, and the solar sources, respectively, to the d[th] header. In assigning the heat flows from sources to headers, attention is given to allowing only allocations with the temperature of the source greater than or equal to the temperature of the header.

The total rate of a given fuel is calculated by summing the splits over the headers:

$$Q_{f,t}^{Fossil} = \sum_{d} Q_{f,d,t}^{Fossil} \qquad \forall f,\ \forall t \tag{3.10}$$

$$Q_{b,t}^{Biofuel} = \sum_{d} Q_{b,d,t}^{Biofuel} \qquad \forall b,\ \forall t \tag{3.11}$$

$$Q_{s,t}^{Solar} = \sum_{d} Q_{s,d,t}^{Solar} \qquad \forall s,\ \forall t \tag{3.12}$$

Although the heat collected and delivered by the solar plant will vary from one period to another, for sizing the solar power plant, it should be large enough to accommodate the largest solar heat provided to the headers (which is still unknown to be optimized), i.e.:

$$Q_{s}^{Design\_Solar} = \arg\max\{Q_{s,t}^{Solar} \mid t = 1,2,...,N_t\} \qquad \forall s \tag{3.13}$$

Constraint (4.4) may be equivalently expressed as:

$$Q_{s}^{Design\_Solar} \le Q_{s,t}^{Solar} \quad \forall s,\ \forall t \tag{3.14}$$

The annualized fixed cost of the s[th] solar power plant is given as a function (ψ_s) of the size:

$$AFC_{s}^{Solar} = \psi_s(Q_{s}^{Design\_Solar}) \quad \forall s \tag{3.15}$$

The foregoing expressions constitute the mathematical program for the problem. In general, it is a nonlinear program (NLP) and becomes a linear program when the function ψ_s is linear (which may be a very good approximation in many solar applications). The solution of the optimization program provides the optimal values for

each form of energy over each period, the distribution to the steam headers, and the design of the solar power plant.

III.6. CASE STUDY

Two case studies have been solved. The first one treats integrating solar energy, process heat, and fossil fuel to produce a stable power supply for the industrial facility. The second case study illustrates the integration of biofuels with process heat, fossil fuels, and solar energy to produce a stable heat supply to the process. This heat supply can be used for heating and non heating purposes.

III.6.1. OPTIMUM INTEGRATION OF SOLAR ENERGY, PROCESS HEAT, AND FOSSIL FUELS TO PRODUCE A STABLE POWER SUPPLY

An industrial facility is located at the city of Daggett which is located in San Bernardino County in California with the following coordinates {N 34° 52'} {W 116° 46'}. Heat integration and cogeneration analysis is first carried out for the process. The result is that steam (at 14 atm and 310 ^{o}C) is fed to an extraction turbine that provides power and heating to the process. The rate of heating of the steam entering the turbine is determined to be 5,000 kW. The produced power is 2,000 kW. To provide this heating, both natural gas and solar energy are considered. On an annual basis, it is desired to fulfill at least 65% of the heating load through solar energy to reduce greenhouse gas emissions and to receive subsidy for the use of a renewable energy.

Solar energy is collected using the parabolic trough collectors that produce high pressure superheated steam. The parabolic trough collectors are among the most commonly used collectors and are recognized with a proven track-record of providing high efficiency and ability to operate at high temperature. The data for the collected solar energy are

reported as monthly averages in Table 3.1. The total annualized cost ($/yr) of the solar thermal system is given by:

$$TAC_{Solar} = 15.3A_s + 1{,}085A_s^{0.6} + 0.012Q_{Solar}^{Annual} \quad (3.16)$$

where A_s is the area of the solar collector (m^2) and Q_{Solar}^{Annual} is the annual useful energy collected and delivered by the solar system (kWhr/yr) in a thermal form. The cost of power generation using the steam turbine is $0.012/kWhr. The cost of steam produced from natural gas is $5.0/$10^9$ J.

Table 3.1. Monthly Average of Useful Collected Solar Energy.

Month	Monthly average of collected solar energy kWhr/(m^2.month)
January	60.6
February	69.5
March	115.8
April	162.3
May	186.2
June	169.5
July	159.1
August	159.0
September	138.9
October	104.6
November	67.5
December	51.1

Using the aforementioned approach and coding the optimization formulation using the software LINGO, the minimum cost of the system (solar thermal, fossil, and power production, excluding revenue from power or heat) was found to be $1.539 MM/yr. The optimal area of the solar collectors was found to be 19,715 m^2. Figure 3.6 summarizes the optimization results of the monthly distribution of both forms of energy.

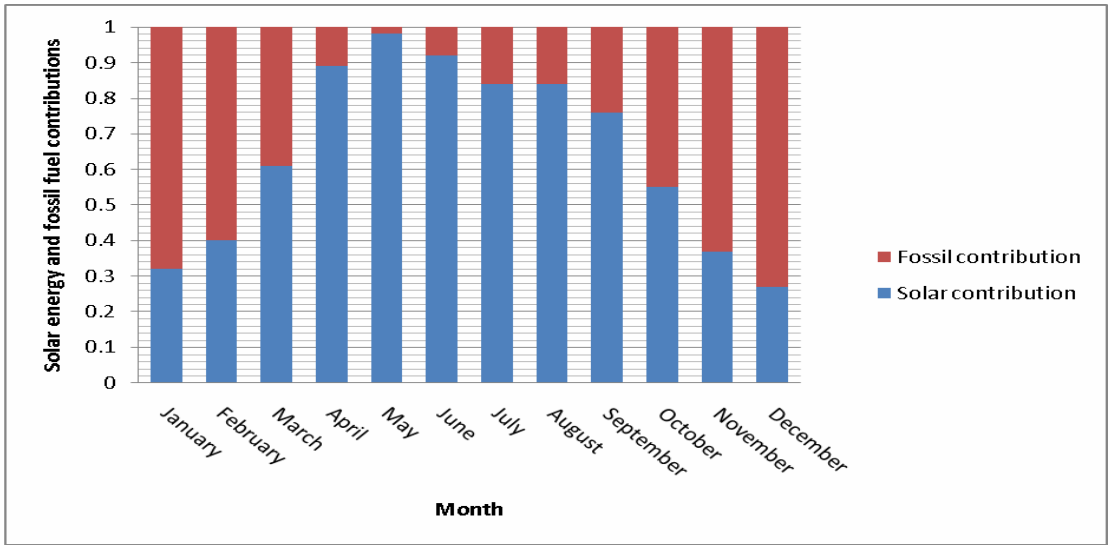

Figure 3.6. Monthly Solar and Fossil Contribution.

III.6.2. OPTIMUM DESIGN AND INTEGRATION OF SOLAR ENERGY, BIOFUELS, PROCESS HEAT, AND FOSSIL FUELS TO PRODUCE A STABLE HEAT SUPPLY

An industrial facility is located at the city of Daggett which is located in San Bernardino County in California with the following coordinates {N 34° 52'} {W 116° 46'}. Upon heat integration, the minimum heating utility of the process is determined to be 5,600 kW. On an annual basis, it is desired to fulfill at least 75% of the process heating utility requirement using renewable sources (solar and biofuel). The biofuel is in the form of biodiesel which is produced from a feedstock of waste cooking oil. The biodiesel process is owned by the company and is based on the oil transestrification technology [30]. The cost and availability of the biofuel are listed in Table 3.2.

Solar energy is collected using the parabolic trough collectors that produce high pressure superheated steam. The parabolic trough collectors are among the most commonly used

collectors and are recognized with a proven track-record of providing high efficiency and ability to operate at high temperature [25, 29]. The data for the collected solar energy are reported as monthly averages in Table 3.3 The total annualized cost ($/yr) of the solar system is given by:

$$TAC_{Solar} = 15.3A_C + 1{,}085A_C^{0.6} + 0.012Q_{Solar}^{Annual} \quad (3.17)$$

A_C is the area of the solar collector (m^2) and Q_{Solar}^{Annual} is the annual energy collected by the solar system (kWhr/yr). The cost of the fossil fuel is $\$5.0/10^9$ J.

Table 3.2. Cost and Availability of Biofuel.

Month	Cost of biofuel $/$10^9$ J	Maximum available heat rate kW
January	3.5	2,970
February	3.8	2,850
March	3.8	2,850
April	3.4	2,490
May	4.8	2,160
June	5.8	1,920
July	5.8	1,920
August	5.8	1,920
September	5.3	2,120
October	4.9	1,990
November	4.3	2,280
December	3.9	2,610

Table 3.3. Monthly Average of Collected Solar Energy.

Month	Monthly average of collected solar energy kWhr/(m^2.month)
January	60.6
February	69.5
March	115.8
April	162.3
May	186.2
June	169.5
July	159.1
August	159.0
September	138.9
October	104.6
November	67.5
December	51.1

Using the aforementioned approach and coding the optimization formulation using the software LINGO, the minimum cost of the heating utility was found to be $1,211,875/yr. The optimal area of the solar collectors was found to be 11,300 m^2. Table 3.4 summarizes the optimization results of the monthly distribution of the three forms of energy.

Table 3.4 Fractional Contribution of Each Form of Energy to the Monthly Heating Utility Requirement of the Process.

Month	Solar	Biofuel	Fossil
January	0.16	0.53	0.31
February	0.21	0.51	0.28
March	0.31	0.51	0.18
April	0.45	0.45	0.10
May	0.50	0.39	0.11
June	0.48	0.34	0.18
July	0.43	0.34	0.23
August	0.43	0.34	0.23
September	0.39	0.38	0.23
October	0.28	0.36	0.36
November	0.19	0.41	0.40
December	0.14	0.47	0.39

CHAPTER IV
INTEGRATION OF ABSORPTION REFRIGERATORS INTO INDUSTRIAL PROCESSES WITH HEAT EXTRACTION FROM SOLAR ENERGY, FOSSIL FUELS, AND EXCESS PROCESS HEAT*

Absorption refrigeration (AR) is gaining an increasing attention in industrial facilities to utilize process heat to partially or completely drive a cooling cycle. We consider three sources of energy to provide the necessary heat for AR. First, excess process heat is effectively utilized instead of using coolants to remove such heat. Fossil fuels are considered as needed. Furthermore, it is desirable to consider the inclusion of solar energy as a sustainable source of heat. There are design and operational challenges in integrating these energy sources and in incorporating AR into industrial facilities. The design and efficiency of the entire system depend on numerous factors including the quantity and quality of the collected solar energy, excess process heat, and fossil fuel. Additionally, the dynamic nature of solar energy poses a complicating factor in design and operation. A systematic approach is proposed for the design of AR systems with hot water loops that are integrated with industrial facilities and employ a combination of excess process heat, fossil fuels, and solar energy. First a graphical procedure is developed to use process insights in determining key design factors. Thermal pinch analysis is performed to determine how much excess heat is available and at what temperature levels as well as the needed refrigeration and the associated temperature levels. Process integration insights are used to determine the placement of the AR system and the sources of heat. Next, a multi-period mathematical model and optimization formulation is developed for the entire system.

---

*Part of this chapter is reprinted with permission from "Integration of solar energy into absorption refrigerators and industrial processes" by Tora EA, El-Halwagi MM., 2010. Chemical Engineering & Technology, Vol. 33 (9), 1495-1505, Copyright (2010), Wiley-VCH, GmbH & CoGaA, Weinhein..

The procedure determines the optimal mix of energy forms (solar versus fossil) to be supplied to the process, the system specifications, and the dynamic operation of the system. A case study is solved to demonstrate the effectiveness and applicability of the devised procedure.

IV.1. INTRODUCTION

Industrial facilities are characterized by the use of significant amounts of cooling. There are various technologies used for industrial refrigeration. Absorption refrigerators (chillers) are among those technologies although they are less common than mechanical refrigeration. The primary source of energy needed to drive the AR cycle is heat [6, 31]. Heat may be provided from different sources. A sustainable source of heat is solar energy. Therefore, solar AR is one of the various types of solar-based cooling systems which also include mechanical-vapor compression refrigeration, absorption, adsorption, desiccant, and photovoltaic-operated refrigeration systems [32]. The energy supplied by the solar system can be in the form of electrical energy from photovoltaic devices to run vapor-compression units and also the thermal energy to drive the mechanical compression systems or absorption units. Solar-powered AR units are gaining increasing utilization in commercial facilities around the world with reviews available in literature [33, 34]. LiBr-H_2O and NH_3-H_2O are the most commonly used commercial AR systems. Flat plate solar collectors and evacuated tube solar collectors are typically used [35-36] although parabolic trough collectors have also been used [37]. Various models have been developed for the characterization, assessment, and optimization of solar AR systems [38-41]. Since solar energy cannot be collected continuously throughout the day, it is usually supplemented with other forms of energy or with an energy storage system. The storage of solar thermal energy may be carried out by storing the heat through a medium (e.g., water in storage tanks) to be used later to run the solar cooling system. Alternatively, the solar energy can be used directly to produce the cooling and then this produced cooling can be stored. Typically, the former option is the common

storage method in industry. When water is used as the storage medium of the solar thermal energy to run solar cooling system, its temperature should be optimized so as to maximize the overall efficiency of the cooling system [42-43].

Since heat is the major contributor to the operating cost of AR systems, it is important to endeavor to reduce this cost item. Process integration provides many effective methods for the conservation and optimization of thermal energy [1, 4, 5]. It can also be used to optimize the various forms of energy including combined heat and power [27- 28] and refrigeration systems [44- 45].

While significant advances have been made in the areas of AR, solar systems, and process integration, there is need to consider these three components simultaneously. Indeed, there is significant potential for the optimization of process heat and its integration with solar energy and fossil fuels to drive AR. The purpose is to introduce an integrated approach to the design of AR systems that are coupled with the industrial process while optimizing the use of excess process heat, fossil fuels, and solar energy. Process integration techniques as well as a systems-based formulation are used to pose the problem as an optimization problem. Targeting techniques are first used to determine the optimal heat integration among process hot and cold streams, the availability of excess process heat, and the amount and quality of the needed refrigeration. Next, a mathematical program is developed to identify the optimal mix of energy forms and their dynamic distribution throughout the year. Additionally, the impact of carbon tax/credit is included in the mathematical formulation and the case study.

Many industrial processes require substantial amounts of low-temperature refrigeration. When excess process heat is available, absorption refrigeration “AR” becomes a promising candidate by utilizing the heat to drive the system. In order to integrate the process heating and cooling duties with an absorption refrigeration systems, there are several design challenges. These include the need to optimize process heating and

cooling demands and the performance of heat integration. There is also the need to determine proper placement of the absorption refrigeration system and the quantity and quality of process heat to be used. A systematic approach is introduced to optimizing absorption refrigeration systems in processing plants. A process integration approach is adopted to modify and optimize the dual AR system and to integrate it with the process. First, thermal pinch analysis is carried out to determine the desired levels if process heat integration, the quantities of heating and cooling utilities, and the temperature levels of the required utilities. Special emphasis is given absorption refrigeration providing cooling at two different levels. A dual cascade double effect NH_3/H_2O-H_2O/LiBr absorption refrigeration system is considered. The NH_3/H_2O cycle is the "top cycle" using heat sources at temperature typically 130^oC. The top generator is cascaded with the bottom generator by recovering the heat from desorbing the refrigerant of the top cycle to run the bottom generator. A case study is solved to illustrate the developed procedure.

Industrial refrigeration is typically required in large quantities for numerous processing facilities. Several technologies are used to provide the required cooling. While mechanical refrigeration is the leading technology, absorption refrigerators "AR" have distinct advantages in industrial plants possessing excess process heat since the primary source of energy needed to drive the AR cycle is heat [46-47]. The LiBr/H_2O and the H_2O/NH_3 systems are still the most commonly used cycles used in absorption refrigerators. Single-, double, and triple-effect H_2O/LiBr cycles have a coefficient of performance "COP" typically around 0.7, 1.2, and 1.7, respectively. The single-effect NH_3/H_2O cycle has COP typically around 0.5 and it is cable of providing cooling at low temperature down to -77.7^oC. On the other hand, H_2O/LiBr cycle typically provides cooling above 0^oC. The principles of designing and modeling AR systems are covered in literature [6, 46].

IV.2. PROBLEM STATEMENT

Industrial facilities may have excess process heat which can be used to drive absorption refrigerators to produce the process refrigeration demand. In many cases, this heat may not be enough. Therefore, it is desired to integrate solar energy and fossil fuel to provide the necessary heat. The problem is divided into the following two topics:-

1. Integration of absorption refrigerators into industrial processes with heat extraction from solar energy, fossil fuels, and excess process heat.
2. Thermal Coupling of two-level dual absorption refrigeration system with integration in industrial process.

IV.2.1. INTEGRATION OF ABSORPTION REFRIGERATORS INTO INDUSTRIAL PROCESSES WITH HEAT EXTRACTION FROM SOLAR ENERGY, FOSSIL FUELS, AND EXCESS PROCESS HEAT

The design and integration of an AR system into an industrial facility and the optimal selection of the optimal mix of energy sources which varies dynamically throughout the year has been addressed. The problem is formally stated as follows:

Given a continuous process with:

- A number N_H of process hot streams (to be cooled) and a number N_C of process cold streams (to be heated) with known heat duties and supply and target temperatures. Available for service are two sets of cooling and heating utilities whose operating temperatures are known but not their heat duties.
- Solar energy is a candidate as a source of heat. The size and cost of the solar energy collection system are unknown and are to be determined through optimization. An economic incentive (e.g., a carbon tax credit) may be available for the use of solar energy to reduce the emission of greenhouse gases GHGs.
- Process refrigeration demand is to be fulfilled using AR. These refrigerators can obtain the needed heat from process excess heat, solar energy, and fossil fuel. Hot

water loops are used to pick up the heat from the three energy sources and deliver the heat to the AR System.

It is desired to develop a systematic approach to integrate AR into industrial facilities with the consideration of solar energy and fossil fuel as supplemental sources of heat so as to produce a stable refrigeration outlet.

The procedure should address the following design challenges:

- How to determine the optimal size, placement, and specifications of the AR system?
- Where and how much should the excess process heat be extracted?
- How to account for the dynamic performance of the solar system and how to size it?
- What is the optimal mix of solar and fossil fuels throughout the year?

Figure 4.1 is a schematic representation of the problem. It shows the three sources of energy as excess process heat, solar energy, and fossil fuels which are used to provide heat to the water tanks that are employed to drive the AR system. The extent contribution of each energy source is unknown and is to be determined via optimization so as to minimize the cost of the system.

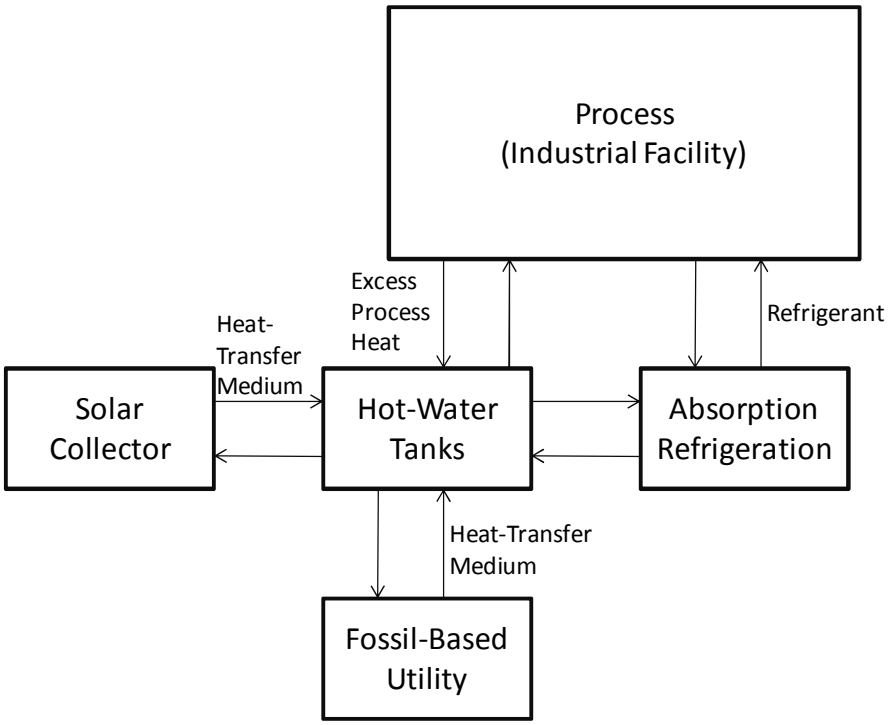

Figure 4.1. Schematic Representation of the Problem Statement.

IV.2.1.1. APPROACH

First, let us consider a typical AR system (Figure 4.2). The system is driven primarily by thermal energy. Two fluids are used in the cycle: an absorbent (water or LiBr) and a working fluid (e.g., ammonia or water, respectively). Different working fluids lead to different refrigeration temperatures. Later, the use of the LiBr-water system is illustrated in the case studies. A low-pressure vapor from the evaporator is absorbed in the absorbent. Heat is released as a result of absorption. The working fluid-absorbent solution is pressurized using a pump. Then, the working fluid is desorbed in a stripper (or generator) where heat is added to the solution. The absorbent is returned to the absorber, the high-pressure vapor is fed to the condenser to condense at a moderate

temperature (e.g. ambient). The high-pressure working fluid is let down and passed through an evaporator which extracts the refrigeration duty at a low temperature.

Because the pumping energy is relatively small compared to the heat input, the coefficient of performance (COP) for the AR system is defined as:

$$COP = \frac{Q_{Ref}}{Q_{Str}} \tag{4.1}$$

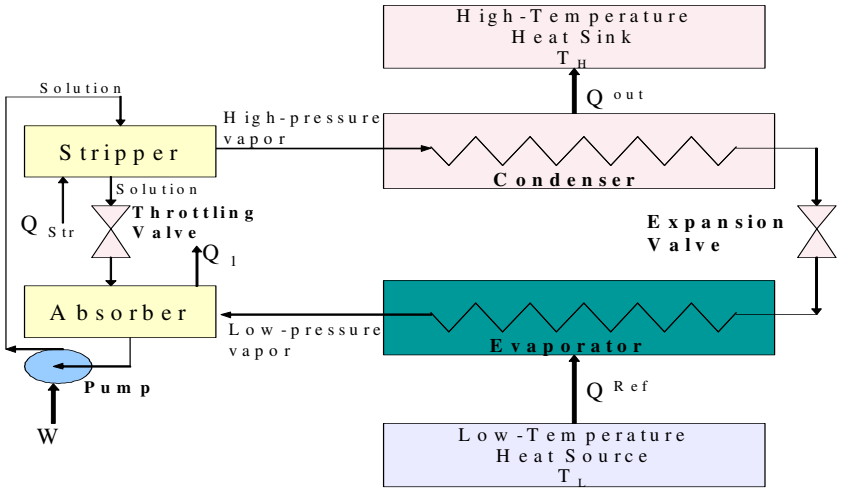

Figure 4.2. A Typical AR System [1].

The heat added to the stripper can be delivered via a heat transfer medium. In this chapter, we consider hot-water loops. Recirculating water is passed via heat exchangers to pick up heat from the three considered sources of energy (excess process heat, fossil, and solar). The heat needed to drive the AR is delivered to the stripper through the hot water then returned back to the heat recovery system. Heat recovered beyond that needed to immediately drive the AR system is stored in well-insulated tanks for later usage. This is particularly important for the solar energy because of its dynamic performance. Energy during daylight hours may be used instantaneously and/or stored in

water tanks to be utilized. The temperature of the hot water is an important optimization variable. In many cases, this temperature has to be at least 80 ^{o}C. Concentrating solar collectors are particularly useful in this regard since they can reach high-enough temperature levels. Figure 4.3 is a schematic representation of the AR system coupled with a hot water loop that extracts heat from a heat recovery and storage-tank network. The hot water is used to provide the heat necessary to strip the high-pressure vapor then the water is returned to be heated again through the heat recovery and storage tank network.

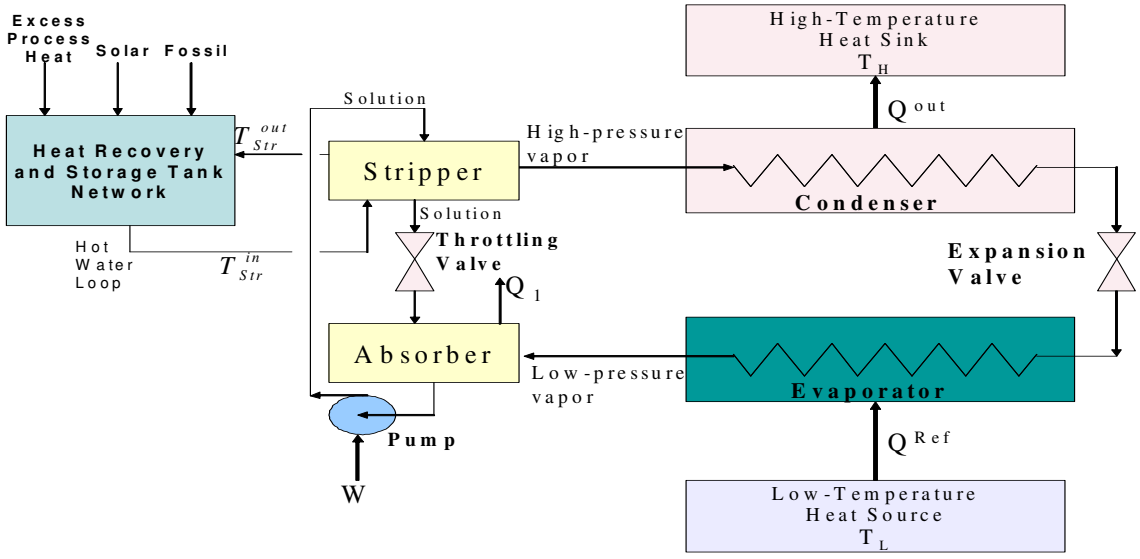

Figure 4.3. Heat Supply to AR via a Heat Recovery Network and a Hot Water Loop.

Before utilizing external energy sources (fossil and solar), it is beneficiary to maximize the use of excess process heat. Therefore, thermal-pinch and heat-integration analyses [1, 4, 5, 44] should be implemented first to transfer heat between process hot and cold streams, to determine minimum heating and cooling utilities, and to determine minimum refrigeration load. The grand-composite curve (GCC) is developed for the process by

plotting temperature (arithmetic average of hot and cold temperatures) versus residual enthalpy (Figure 4.4). The pinch point corresponds to the zero-residual point. Additionally, the top and bottom residuals represent the minimum heating and cooling utilities. Next, it is important to use the GCC to derive additional insights specifically for the AR system. Noting that the hot water leaving the stripper enters the heat recovery network at a temperature (T_{Str}^{out}). This temperature is represented on the GCC by adding half of the minimum approach temperature between the hot and the cold stream ($T_{Str}^{out} + \Delta T^{\min}/2$). Therefore, the excess process heat must be higher than this temperature at least with a minimum heat-transfer driving force, i.e., $T_{Str}^{out} + \Delta T^{\min}/2 + \Delta T^{Exch,HR}$. From the GCC, one can determine the excess heat to be recovered for usage in AR. This is shown on Fig. 4.4 as $Q^{Ex,\Pr o}$. This heat recovery offers two benefits: reduction of the required cooling lead for the process and contribution to the heat needed to drive the AR system. In order to reduce the cooling cost of the process, cooling water is used to remove the maximum feasible load which corresponds to the temperature of the cooling water. This load is referred to as Q^{CW}. Finally, the remaining heat load defines the minimum refrigeration demand for the process to be provided by the AR system (Q^{Ref}).

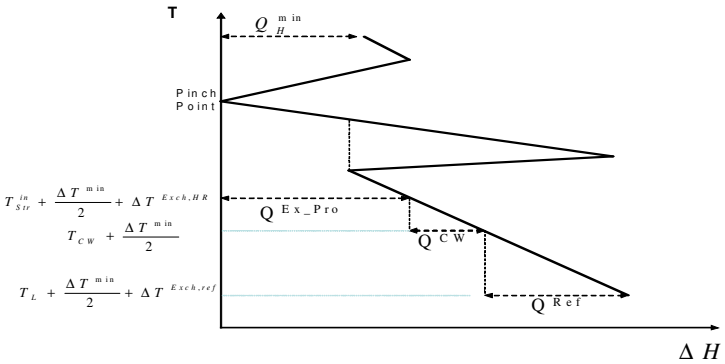

Figure 4.4. Target Identification and Integration of the GCC Representation with the Hot Water Loop.

The graphical approach identifies the values of Q^{Ref} and Q^{Ex_Pro}. For a given COP, the total heating rate needed for AR is determined via Eq. 1.

Next, a dynamic model is developed to represent the temporal variation of the collected solar energy at the plant location throughout the year. It is worth noting that for targeting purposes, the daily average values of useful collected solar energy are sufficient to determine the area of the solar collector. Two sets of hot-water tanks are used for recovery and dispatch. The temperature of the water fluctuates in the recovery tank during heat collection until it reaches a final desirable state. Then, it is switched to become the dispatch tank delivering water at the desired temperature. Once the targets are identified, the details of recovery and dispatch can be determined using hourly rates. In designing the solar system, it is common to use the data of a Typical Meteorological Year (TMY). The TMY statistically-averaged data set of solar radiation intensity derived from the data saved in the archives of the National Solar Radiation Data Base (NSRD) archives. As such the TMY accounts for the uncertainty in solar data and is aimed at developing a nominal design value for the area of the solar collector. Once the design is established, then the uncertainty will impact the operation of the system leading to collected solar energy that may be somewhat higher or lower than that anticipated by TMY. Depending on the actual amount of the collected solar energy, the fossil fuel usage is adjusted so as to close the balance for the needed energy. The procedure described by Tora and El-Halwagi [40] is used to extract the pertinent solar data and represent them in a form ready to be used in an optimization formulation [47]. In order to develop an algebraic formulation of the optimization program, the decision-making time horizon (e.g., a year) is discretized into N_t periods leading to a set of operating periods: PERIODS = $\{t|t= 1,2, \ldots,N_t\}$. Within each time period, the values of energy usage are averaged and the analysis within that period is carried out for the averaged energy values of each energy type.

IV.2.1.2. OBJECTIVE FUNCTION

The objective function for the optimization program is given by:
Minimize total annualized cost =

$$\sum_f C_f^{Fossil} \sum_t Q_{f,t}^{Fossil} * D_t + AFC^{Solar} + \sum_t C_t^{Solar} * Q_t^{Solar} * D_t - \sum_t R^{Solar} * Q_t^{Solar} * D_t + Cost^{Tanks} \tag{4.2}$$

where C_f^{Fossil} is the cost of the fth fossil fuel, $Q_{f,t}^{Fossil}$ is the rate of heating of the fth fossil-based utility during period t, D_t is the duration of period t, AFC^{Solar} is the annualized fixed cost of the solar plant, C_t^{Solar} is the operating cost of the solar heating utility, Q_t^{Solar} is the rate of heating of the solar-based utility during period t, and R^{Solar} is the carbon credit of the solar utility. $Cost^{Tanks}$ is the annualized cost of the storage tanks. These are usually much smaller than the overall investment in the AR system, the solar collectors, and the fossil-based utility units. The following are the necessary constraints for the optimization formulation:

Rate of heat demand for the heat recovery network during any period t:

$$Q^{Ex\_Pro} + \sum_f Q_{f,t}^{Fossil} + Q_t^{Solar} = \frac{Q^{Ref}}{COP} \tag{4.3}$$

While the supplies of the solar and the fossil forms of energy are allowed to vary dynamically, the excess process heat and the refrigeration duty of the process are taken as their steady-state values.

In assigning the heat flows from sources to the hot water loop, attention is given to allowing only allocations with the temperature of the source greater than or equal to the temperature minimum acceptable temperature for heating the water.

The area of the solar collector needed in each time period is related to the needed heating rate from the solar source through the design equation:

$$Q_t^{Solar} = \zeta(A_t^{Solar}) \tag{4.4}$$

Although the heat collected and delivered by the solar plant will vary from one period to another, for sizing the solar power plant, it should be large enough to accommodate the largest needed collector area (which is still unknown to be optimized), i.e.:

$$A^{Design\_Solar} = \arg\max\{A_t^{Solar} \mid t = 1,2,...,N_t\} \tag{4.5}$$

which may be expressed as:

$$A^{Design\_Solar} \geq A_t^{Solar} \qquad \forall t \tag{4.6}$$

The annualized fixed cost of the solar power plant is given as a function (ψ) of the size:

$$AFC^{Solar} = \psi\ (A^{Design\_Solar}) \tag{4.7}$$

The foregoing expressions constitute the mathematical program for the problem. In general, it is a nonlinear program (NLP) and becomes a linear program when the functions ζ and ψ are linear (which may be a very good approximation in many solar applications). The solution of the optimization program provides the optimal values for each form of energy over each period, the distribution to the water heating loop, and the design of the solar plant.

IV.2.1.3. CASE STUDY

CASE STUDY I: A PHMARMCEUTICAL PLANT

A pharmaceutical processing facility is located at the city of Daggett in San Bernardino County in California with the following coordinates {N 34° 52'} {W 116° 46'}. The process flowsheet [48] is given by Figure 4.5. The feed mixture (C_1) is first heated to 513 K, then fed to an adiabatic reactor where an endothermic reaction takes place. The off-gases

leaving the reactor (H_1) at 398 K are cooled to 338 K before it is sent to the recovery unit. The mixture exiting from the bottom of the reactor is separated into a vapor and slurry streams. The vapor stream (H_2) leaves the separation unit at 358 K and is to be cooled to 298 before storage. The slurry stream is washed with a hot immiscible liquid at 328 K. The wash liquid is purified and recycled to the washing unit. During purification, the temperature drops to 308 K. Therefore, the recycled liquid (C_2) is heated to 328 K. The top stream from the purification unit is cooled from 318 to 298 K to condense a solvent which is recycled back to the separation system. The data for the process hot and cold streams are given in Table 4.1. Cooling water may be used as an external utility to cool the hot streams down to 314 K below which an LiBr-water AR system is used to provide chilling water at 283 K. A minimum driving force (ΔT^{min}) value of 10 K is used.

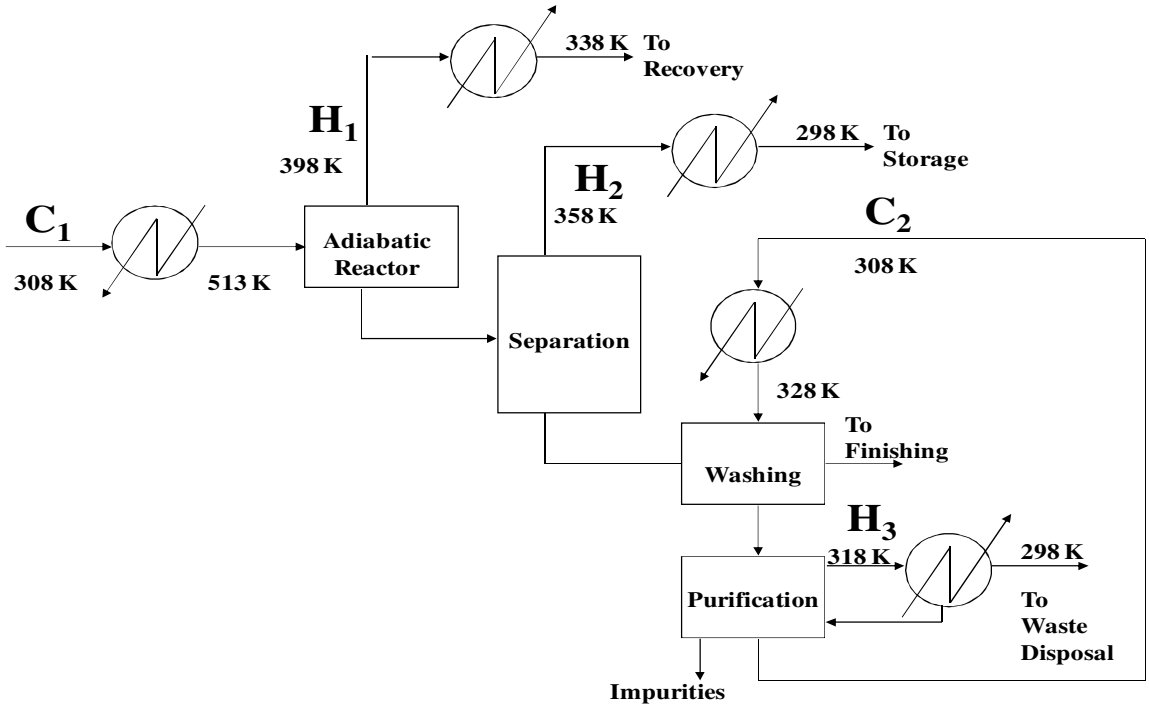

Figure 4.5. A Simplified Flowsheet of the Pharmaceutical Process of Case Study I [48].

Table 4.1. Data for the Process Hot and Cold Streams for Case Study I.

Stream	Supply temperature, K	Target temperature, K	Rate of Enthalpy Change kW
H_1	398	338	-2,325
H_2	358	298	-1,125
H_3	318	298	-875
C_1	308	513	4,100
C_2	308	328	725

By carrying out a thermal-pinch heat integration analysis, the GCC for the process is developed as shown by Figure 4.6. The data extracted from the GCC indicate that the process has refrigeration need of 1 MW and that the process can offer 0.75 MW of excess process heating at 358 K that can be used as part of the energy supply to drive the AR system. Hot water is used as the heat transfer medium in the LiBr-Water AR system whose COP is 0.7.

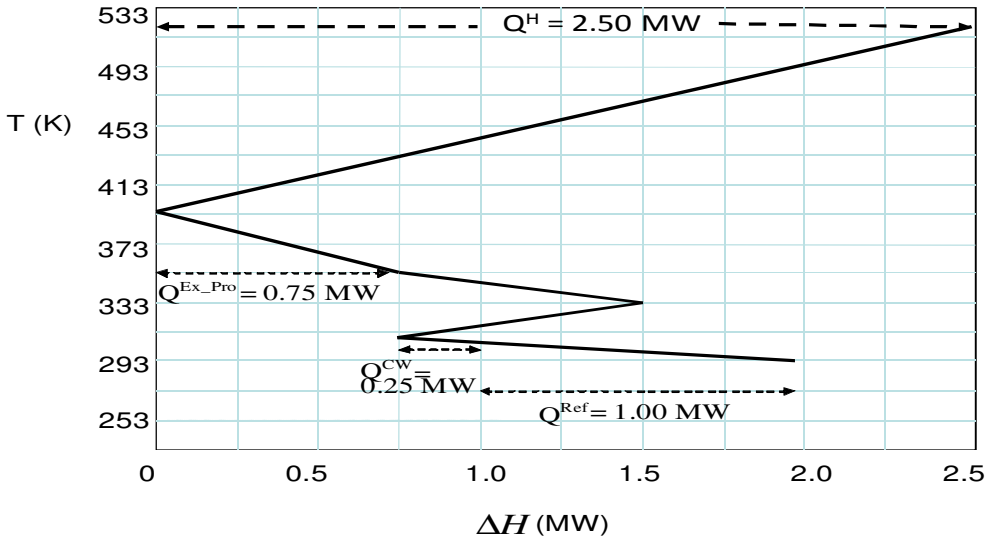

Figure 4.6. The GCC of the Pharmaceutical Process.

Solar energy is collected using parabolic trough collectors that produce hot water that can be used directly or stored in insulated water tanks for later use to drive the AR system. A parabolic trough solar collector is used with the following specifications:

- Aperture width =5.7m
- Aperture length = 99 m
- Receiver diameter = 0.07 m
- Optical efficiency= 0.80
- Receiver absorptivity = 0.96
- Mirror reflectivity = 0.96
- Receiver emittance = 0.19

The procedure reported by Tora [40] is used to evaluate the hourly useful collected solar energy and is shown in Figure 4.7. The hourly data are integrated over the month to calculate the monthly average collected energy as reported in Table 4.2. The total annualized cost ($/yr) of the solar system is given by:

$$TAC_{Solar} = 20A_C + 1{,}085A_C^{0.6} + 0.012Q_{Solar}^{Annual} \qquad (4.8)$$

where A_C is the area of the solar collector (m^2) and Q_{Solar}^{Annual} is the annual energy collected by the solar system (kWhr/yr). The cost of the fossil fuel is $\$6.0/10^9$ J.

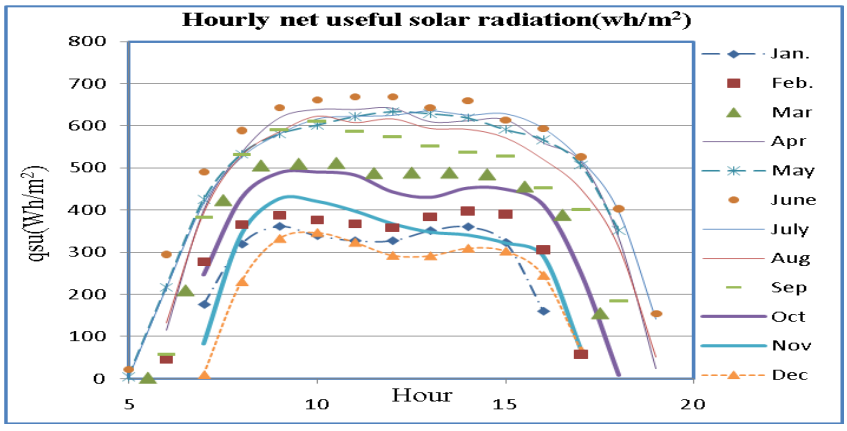

Figure 4.7. Hourly Useful Collected Solar Energy.

Table 4.2. Monthly Average of Usefully Collected Solar Energy.

Month	Useful Collected Energy Per Unit Area of Solar Collector ($kWh/m^2.month$)
January	94.24
February	103.88
March	158.72
April	205.50
May	213.28
June	228.90
July	221.34
August	203.98
September	179.70
October	142.29
November	102.30
December	85.25

The use of solar energy earns the company a GHG credit of \$0.008/kWh is the avoided CO_2 is worth \$1/ton CO_2 equivalent [49]. A sensitivity analysis is carried out for GHG credits ranging from no credit up to \$20/ ton CO_2 equivalent.

The aforementioned optimization formulation has been applied to the case study and coded using LINGO (which is a software that can solve linear, nonlinear, and mixed-integer programming problems. For more details on LINGO, the reader is referred to (www.LINDO.com). The objective function taken as the minimum cost of the heating utility (expressed as annual cost of fossil fuel + total annualized cost of the solar energy – GHG credit for the solar energy) was identified under the various scenarios of GHG

credit. In all these scenarios, the excess process heat provides 0.75/(1.00/0.7)*100% = 52.5%. In the case of no GHG credit, the solution indicates that fossil fuel is the preferred external source of energy. All of the external heating utility was provided by the fossil fuel at an annual cost of $128 k/yr. However, with a modest GHG credit of $5/tonen CO_2 eq., solar energy become more competitive requiring a collector area of 3,943 m2 and incurring a utility cost (including the GHG credit) of $126 k/yr. When the credit is increased to $20/ tonne CO_2 eq., then almost all of the external heat if provided by solar energy. It is worth noting that several European countries are already providing carbon credits higher than $20/tonne CO_2 eq. [49]. Tables 4.3 and 4.4 summarize the optimization results of the monthly distribution of the fossil and solar forms of energy for the two scenarios of GHG credit.

Table 4.3. Percentage Contribution of Fossil versus Solar Energy to the Monthly Heating Requirement of the AR System for the Scenario: $5/tonne CO_2 eq. GHG credit (A_c = 2,477 m^2).

Month	Solar	Fossil
January	22.0	25.5
February	26.8	20.7
March	37.0	10.5
April	47.5	0.0
May	47.5	0.0
June	47.5	0.0
July	47.5	0.0
August	47.5	0.0
September	43.3	4.2
October	33.2	14.3
November	24.6	22.9
December	19.9	27.6

Table 4.4 Percentage Contribution of Fossil versus Solar Energy to the Monthly Heating Requirement of the AR System for the Scenario: \$20/tonne CO_2 eq. GHG credit (A_c = 4,779 m^2).

Month	Solar	Fossil
January	42.4	5.1
February	47.5	0.0
March	47.5	0.0
April	47.5	0.0
May	47.5	0.0
June	47.5	0.0
July	47.5	0.0
August	47.5	0.0
September	47.5	0.0
October	47.5	0.0
November	47.5	0.0
December	38.3	7.2

CASE STUDY II: FORMIC ACID PROCESS

Consider the formic acid process shown by Fig. 4.8 [50-51]. The feed mixture of carbon monoxide and methanol is fed to a carbonylation reactor that operates at 353 K and 4 MPa in the presence of an alkoxide catalyst to produce methyl formate. The reaction products are fed to the methyl formate distillation column where methyl formate is separated as the distillate while methanol and catalyst are collected as bottoms and sent back to the carbonylation reactor. The bottom stream entering the reboiler (C_1) is heated to create the boilup vapor to be returned to the column. A partial condenser is used for the top vapor product (H_1) followed by a refrigerant-using condenser acting on the remaining vapor (H_2) to recover methyl formate from the rest of the stream which is sent to an incinerator as a

purge gas. Methyl formate is heated (C_2) then reacted with water in the hydrolysis reactor to produce formic acid. The reaction products are flashed to recover methanol and methyl formate which are cooled (H_3) and recycled to the hydrolysis reactor.

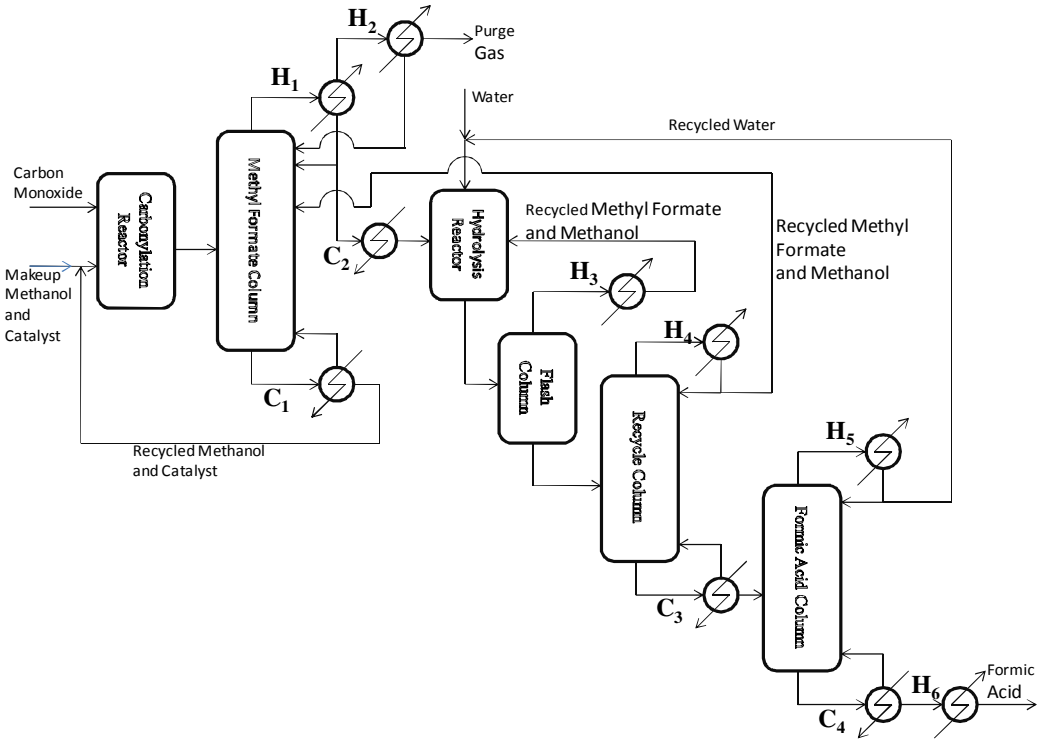

Figure 4.8. A Simplified Flowsheet of the Formic Acid Process Used in Case Study II[50-51].

The bottom product from the flash tank is fed to a distillation column to recover recyclable components (methanol and methyl formate). The column requires cooling and heating duties for the overhead condenser and the reboiler (H_4 and C_3, respectively). The bottom product of the recycle distillation column is fed to the formic acid. The column requires cooling and heating duties for the overhead condenser and the reboiler (H_5 and C_4). The concentrated formic acid (H_6) leaves the separation unit at 423 K and is to be cooled to 308 before storage. The stream data are given in Table 4.5.

Cooling water may be used as an external utility to cool the hot streams down to 308 K below. Also, available for service is an LiBr-water AR system which can be used to cool the hot stream to 288 K. A minimum driving force (ΔT^{min}) value of 10 K is used. The solar collector and site location described in Case Study I are also used in Case Study II.

Table 4.5. Data for the Process Hot and Cold Streams for Case Study I.

Stream	Supply temperature, K	Target temperature, K	Rate of Enthalpy Change MW
H_1	338	333	-5.3
H_2	333	288	-0.3
H_3	330	288	-1.4
H_4	310	308	-2.7
H_5	393	308	-4.3
H_6	423	308	-0.2
C_1	368	370	5.8
C_2	333	393	0.8
C_3	368	383	2.9
C_4	423	430	4.7

The key results of the thermal pinch analysis for the process are illustrated by the GCC shown by Figure 4.9. The process requires 12.90 MW of heating utility and it has refrigeration requirement of 0.80 MW. The analysis also shows that the process can provide 0.78 MW of excess process heating at 358 K that can be used as part of the energy supply to drive the AR system. Similar to Case Study I, hot water is used as the heat transfer medium in the LiBr-Water AR system whose COP is 0.7. Hence, the external heat (solar and/or fossil) needed to drive the AR system is 0.36 MW. The data

for the process location, solar collector, fossil fuel, and GHG credit were given in Case Study I.

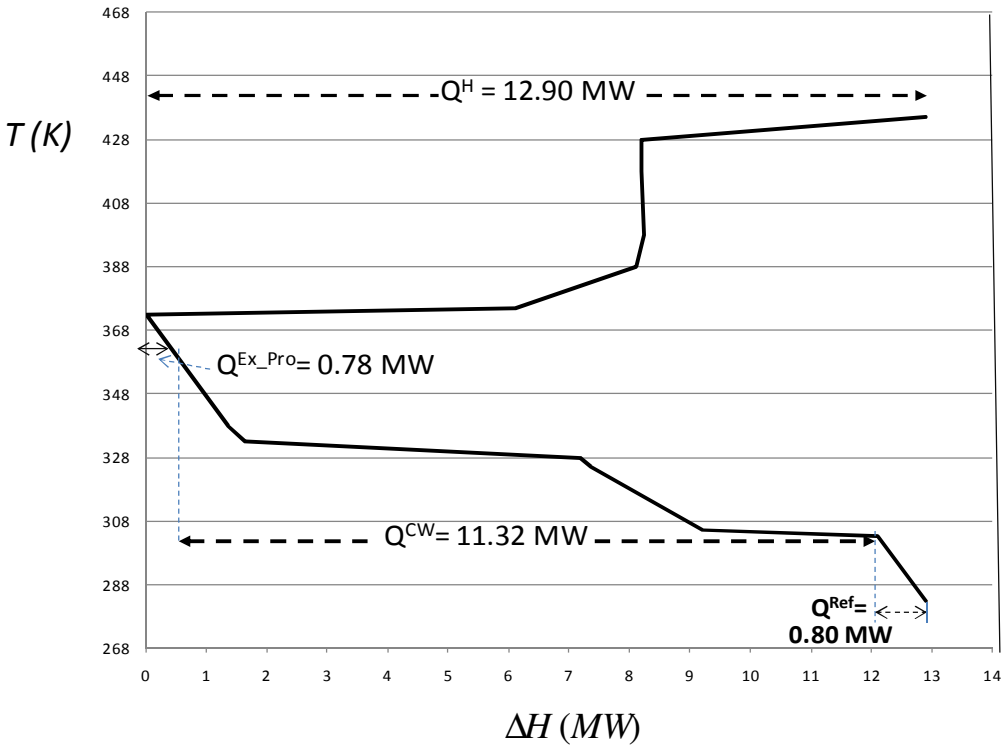

Figure 4.9. The GCC for the Formic Acid Process.

The proposed optimization formulation is applied to the data of the formic acid case study and solved using the software LINGO. The minimum cost of the heating utility (expressed as annual cost of fossil fuel + total annualized cost of the solar energy – GHG credit for the solar energy) was determined under various scenarios of GHG credit. While the excess process heat provided 68.2% of the total energy needed to drive AR, the solar and fossil forms of energy were used to supply the rest of the needed energy. In a similar trend to the pharmaceutical process case study, in the case of no GHG credit, fossil fuels is the preferred external source of energy. Nonetheless, as GHG credit increases, the portion of solar contribution increases reaching almost all the required

external energy when the credit is increased to \$20/ tonne CO_2 eq. These results are summarized in Tables 4.6 and 4.7.

Table 4.6. Percentage Contribution of Fossil versus Solar Energy to the Monthly Heating Requirement of the AR System for Case Study II for the Scenario: \$5/tonne CO_2 eq. GHG credit (Cost = \$53 k/yr, A_c = 1,272 m^2).

Month	Solar	Fossil
January	14.1	17.7
February	17.2	14.5
March	23.7	8.0
April	31.8	0.0
May	31.8	0.0
June	31.8	0.0
July	31.8	0.0
August	30.5	1.3
September	27.8	3.9
October	21.3	10.5
November	15.8	16.0
December	12.8	19.0

Table 4.7. Percentage Contribution of Fossil versus Solar Energy to the Monthly Heating Requirement of the AR System for Case Study II for the Scenario: \$20/tonne CO_2 eq. GHG credit (A_c = 2,348 m^2).

Month	Solar	Fossil
January	26.0	5.8
February	31.8	0.0
March	31.8	0.0
April	31.8	0.0
May	31.8	0.0
June	31.8	0.0
July	31.8	0.0
August	31.8	0.0
September	31.8	0.0
October	31.8	0.0
November	29.2	2.6
December	23.5	8.3

CASE STUDY III: ACRYLIC ACID PROCESS

An industrial plant producing acrylic acid is to be located in Abu Dubai (N 24^o 25`, E 54$^o$ 39`), United Arab Emirates. The process flowsheet [50-54] is shown by Figure 4.10. The plant consists mainly of two parts: the oxidation reactions and the product separation and purification. The oxidation part has two exothermic reactors. A feed mixture of propylene, steam, and air is fed to the first reactor where acrolein is produced. The product stream is fed to the second reactor to be converted to acrylic acid as the main product. A cooler is used between these two reactors to adjust the temperature of the stream leaving the first reactor before entering the second reactor. The temperature inside the reactors is adjusted by using molten salt to cool the reactors down to the design temperature. This salt is used to produce steam. The product separation and

purification include a solvent extraction unit, solvent stripping, and distillation columns to get the desired purity of acrylic acid. The solvent recovery has a distillation column that requires refrigeration at 10°C to condense the evaporated solvent then circulate it to the solvent extraction unit. The process stream data is given at Table 4.8.

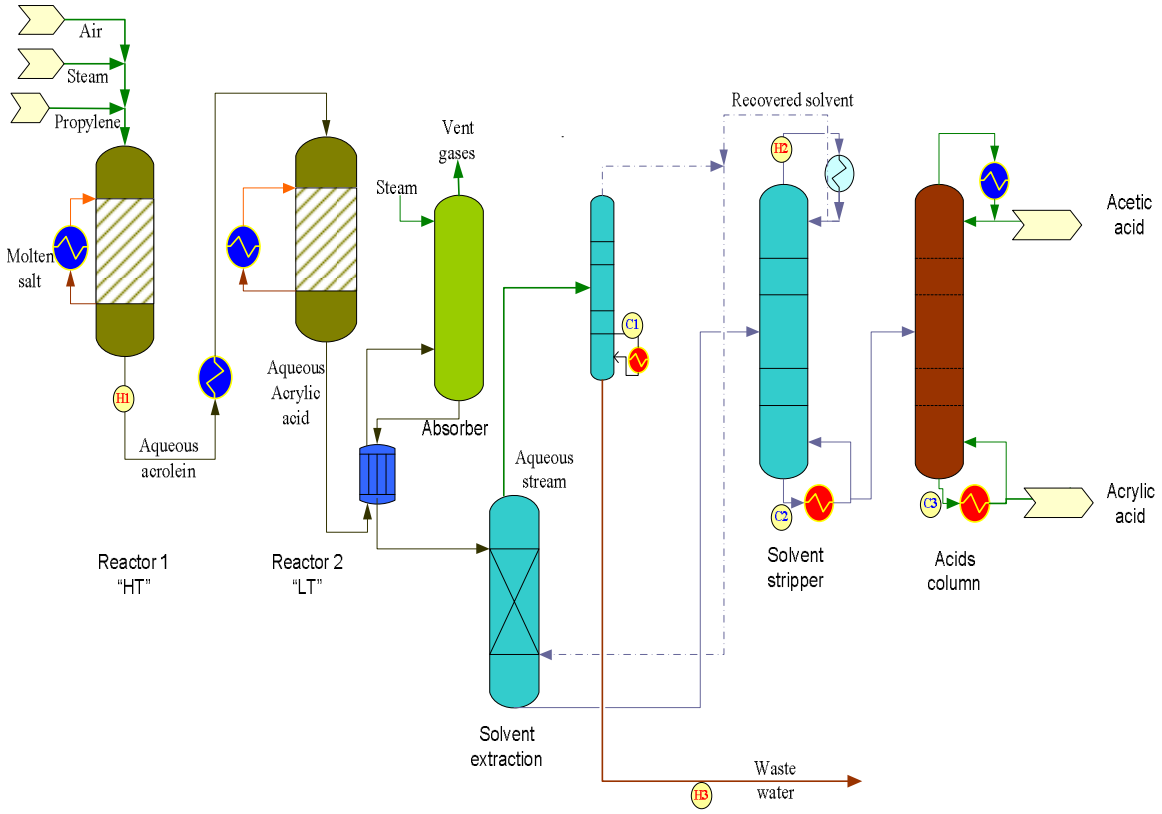

Figure 4.10 Acrylic Acid Production Flow Sheet [51-54].

Table 4.8. Data of the Targeted Process Hot and Cold Streams for the Acrylic Acid Case Study.

Stream#	Supply Temperature (K)	Target Temperature (K)	Rate of Enthalpy Change (kW)
H1	623	563	-75
H2	288	288	-7,500
H3	383	313	-423
C1	443	448	233
C2	443	448	1212
C3	443	448	30

For the solar data, the typical meteorological year is obtained from the Energy Plus web site: http://apps1.eere.energy.gov/buildings/energyplus/cfm/weather_data.cfm. The net hourly useful solar radiation is estimated using parabolic trough solar collector used in the previous two case studies. Figure 4.11 shows the hourly useful solar radiation through the year and Table 4.9 gives the monthly average data for Abu Dhabi.

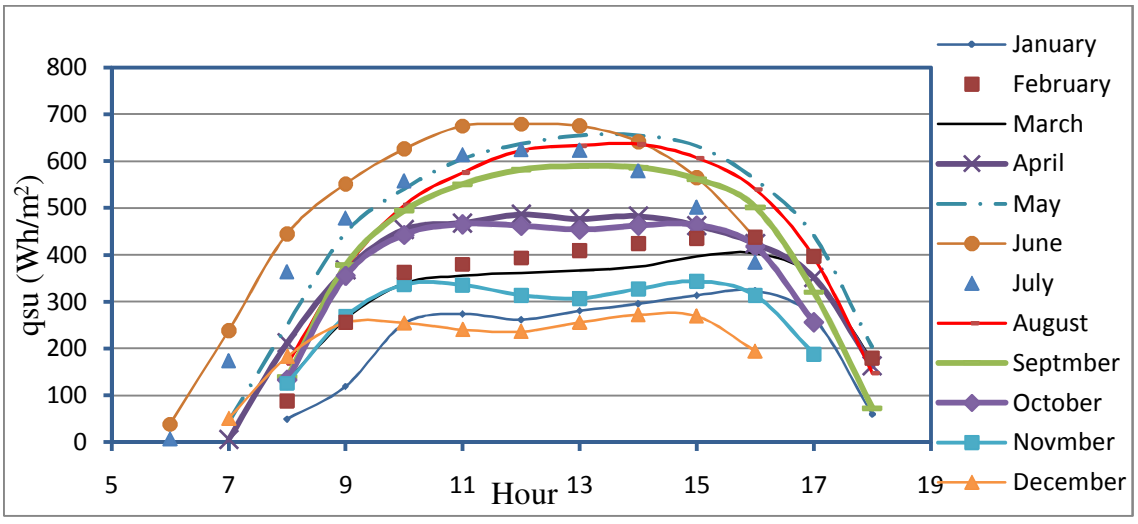

Figure 4.11 Hourly Useful Solar Radiations at Abu Dhabi.

Table 4.9. Monthly Average of Usefully Collected Solar Energy for Abu Dhabi.

Month	qsu(kWh/m2.month)
January	77.28
February	105.34
March	108.93
April	130.62
May	175.77
June	173.01
July	157.33
August	161.20
September	143.19
October	121.18
November	85.71
December	68.54

Process heat integration is performed and the resulting GCC is plotted in Fig. 4.12. The GCC shows that 151 kW of heat can be extracted from the process at temperature (358 K) suitable to run a single effect LiBr-H_2O AR. The cooling-water load is 272 kW and the refrigeration demand for AR is 7,500 kW. After recovering 151 kW from the process and using an AR system with a COP of 0.7, there is still a need of 10,563 kW of heat from the external sources to run the AR.

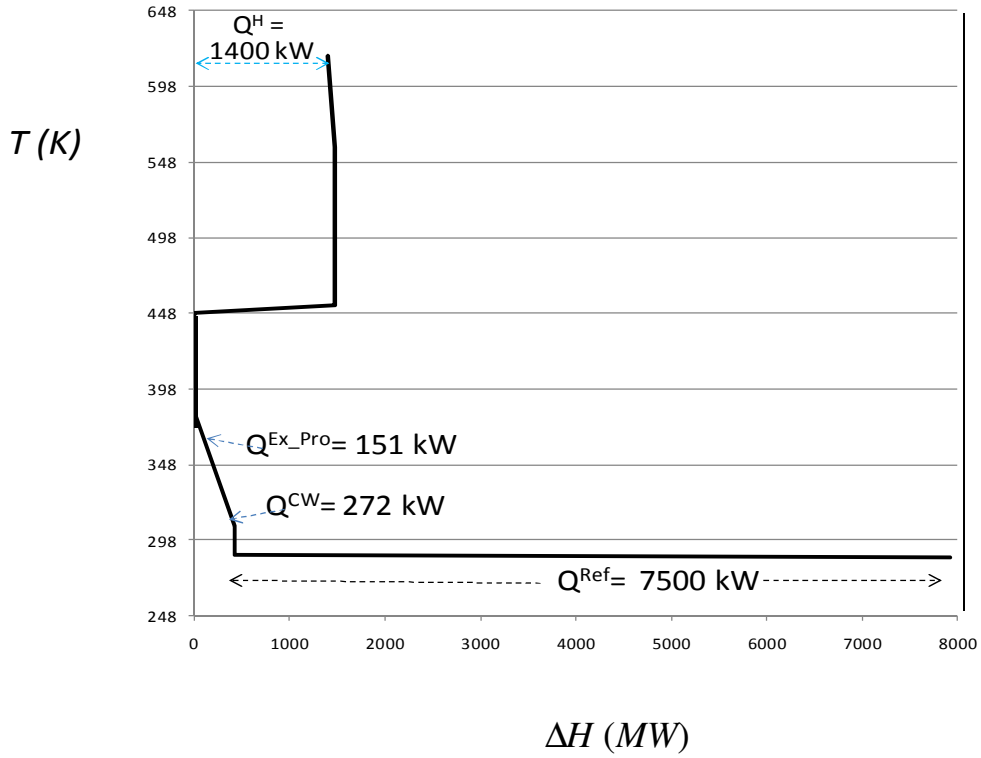

Figure 4.12 The GCC of the Acrylic Acid Production Process.

The optimization formulation is developed for the acrylic acid case study then solved using LINGO optimization program. For the case of no GHG credit, the optimal solution is to use fossil fuel as the only external energy source. The annual cost is \$1.999 MM/yr. However, when the GHG credit is increased to \$5/tonne CO_2 eq., 90% of the annual energy needed to drive the AR is provided by the solar system (A_c = 64,852 m^2). The solar energy becomes more competitive in this case than in the previous two case studies primarily to the economy of scale since the heat duty of this application is significantly larger than the previous two case studies.

IV.2.2. THERMAL COUPLING OF TWO-LEVEL DUAL ABSORPTION REFRIGERATION SYSTEM WITH INTEGRATION TO INDUSTRIAL PROCESS

IV.2.2.1. OBJECTIVE

It is aimed at the development of a systematic procedure for the integration of AR systems into industrial systems. Specifically, the following contributions are methodically addressed:

- Utilization of excess process heat to drive AR
- Delivery of two cooling levels using two AR systems which are heat integrated by extracting the heat from one cycle and using it to drive the other

The result of such a thermally-coupled double-effect AR system that utilizes heat recovered from one cycle to the other and process heat is an enhancement of the coefficient of performance of the system and a reduction in the overall energy consumption.

IV.2.2.2. APPROACH

Heat is used to drive the cycle and two fluids are recirculated: a working fluid (e.g., water or ammonia) and an absorbent (LiBr or water, respectively). First, an absorbent is used to dissolve a low-pressure vaporous working fluid from the evaporator resulting in the release of exothermic heat. The working fluid-absorbent solution is pressurized using a pump. Then, the working fluid is desorbed in a stripper (or generator) where heat is added to the solution. The regenerated absorbent is recirculated back to the absorber. On the other hand, the high-pressure vaporous working fluid is sent to the condenser to condense at a moderate temperature (e.g. ambient). The high-pressure working fluid is

throttled and fed to the evaporator which extracts the refrigeration duty at a low temperature.

Because the pumping energy is relatively small compared to the heat input, the coefficient of performance (COP) for the AR system is defined as:

$$COP = \frac{Q_{\mathrm{Re}\,f}}{Q_{Str}} \tag{4.9}$$

The heat added to the stripper can be delivered via a heat transfer medium. We consider hot-water loops. Recirculating water is passed via heat exchangers to extract heat from hot sources then dispatched to provide the necessary heat for stripping. Figure 4.13 is a schematic representation of common configurations AR cycle using the NH_3/H_2O and the H_2O/LiBr cycles. Each of the two cycles need heat source at a certain temperature level. The single-effect NH_3/H_2O cycle requires heat source at a temperature higher than that needed for the H_2O/LiBr cycle. The two cycles have the same units but the NH_3/H_2O cycle requires an additional rectifier for high-level separation of NH_3 from H_2O.

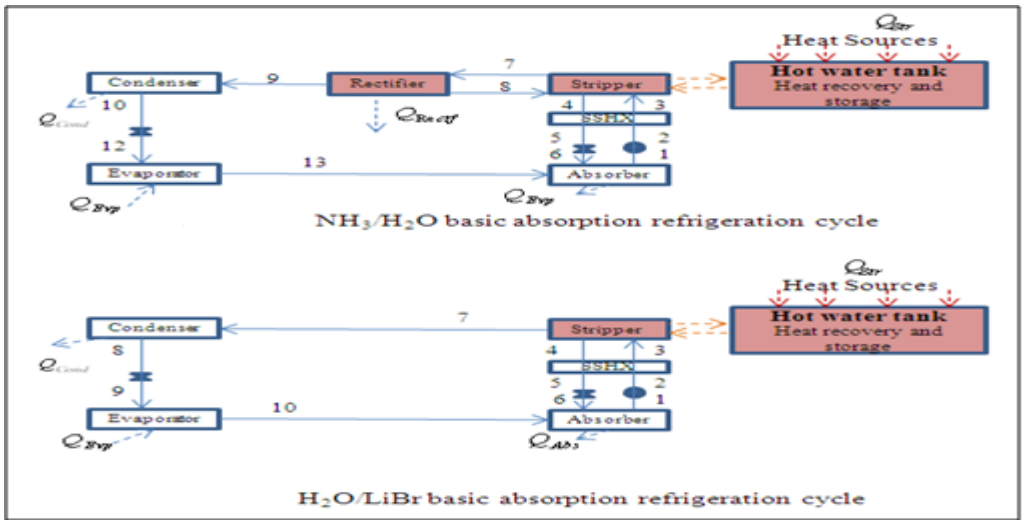

Figure 4.13. AR Systems with Hot Water Loop for Heat Recovery.

Prior to using external sources of heat, it is useful to extract excess process heat. In this context, thermal-pinch analysis [6-10] should be implemented first to transfer heat between process hot and cold streams, to determine minimum heating and cooling utilities, and to determine minimum refrigeration load and excess heat below the pinch to be extracted to drive the AR cycle.

The grand-composite curve (GCC) is developed for the process by plotting temperature (arithmetic average of hot and cold temperatures) versus residual enthalpy as shown by Fig. 4.14.

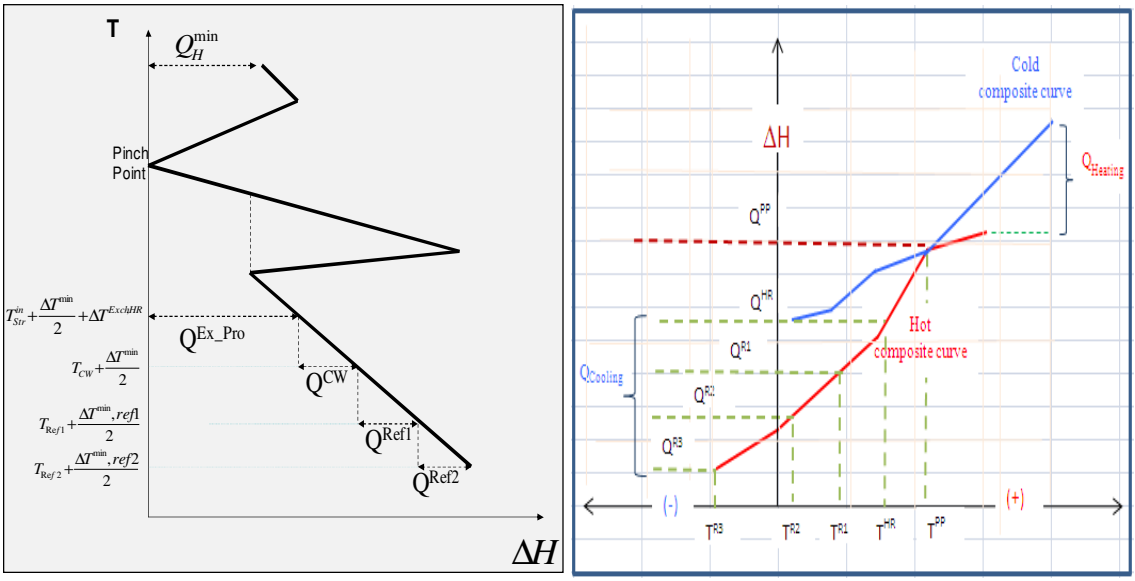

Figure 4.14. Target Identification and Integration of the GCC Representation with the Hot Water Loop.

The pinch point corresponds to the zero-residual point. Additionally, the top and bottom residuals represent the minimum heating and cooling utilities. Next, it is important to use the GCC to derive additional insights specifically for the AR system. Noting that the hot water leaving the top stripper enters the heat recovery network at a temperature (T_{Str}^{out}). This temperature is represented on the GCC by adding half of the minimum approach

temperature between the hot and the cold stream ($T_{Str}^{out} + \Delta T^{\min}/2$); where $\Delta T^{\min}$ refers to the minimum approach temperature between hot and cold streams used in constructing the GCC. Therefore, the excess process heat must be higher than this temperature at least with a minimum heat-transfer driving force, i.e. $T_{Str}^{out} + \Delta T^{\min}/2 + \Delta T^{Exch,HR}$;where $\Delta T^{Exch,HR}$ is the driving force of the heat exchanger recovering heat from the process streams to the AR hot water tank. One can determine the excess heat to be recovered for usage in AR. This is shown by Fig. 4.2 as $Q^{Ex,\Pr o}$. This heat recovery offers two benefits: reduction of the required cooling lead for the process and contribution to the heat needed to drive the AR system. In order to reduce the cooling cost of the process, cooling water is used to remove the maximum feasible load which corresponds to the temperature of the cooling water. Finally, the remaining heat loads are distributed to the two refrigerants depending on their temperatures to determine the minimum refrigeration demands for the process to be provided by the two AR systems (Q^{Ref1} and Q^{Ref2}); where Q^{Ref1} is needed at a temperature below the ambient temperature and Q^{Ref2} is needed at a temperature above the ambient temperature.

The graphical approach identifies the values of Q^{Refi} and Q^{Ex_Pro}. Consequently, the external heat demand for the top cycle and the bottom cycle can also be determined. For a given COP, the total heating rate needed for AR is determined via Eq. 1.

Since the external heat is one of the largest operating cost items of AR, it is desired to reduce such heat usage. In addition to using excess process heat, we also propose the use of heat from the hot stream leaving the stripper (generator) of the top cycle (NH_3/H_2O).to provide heat to the stripper (generator) of the bottom cycle (H_2O/LiBr). In addition to reducing (or eliminating) the amount of external heat needed of the bottom cycle, this thermal coupling also reduces the amount of cooling needed in the rectifier of the top cycle. The proposed system is shown by Fig.4.15.

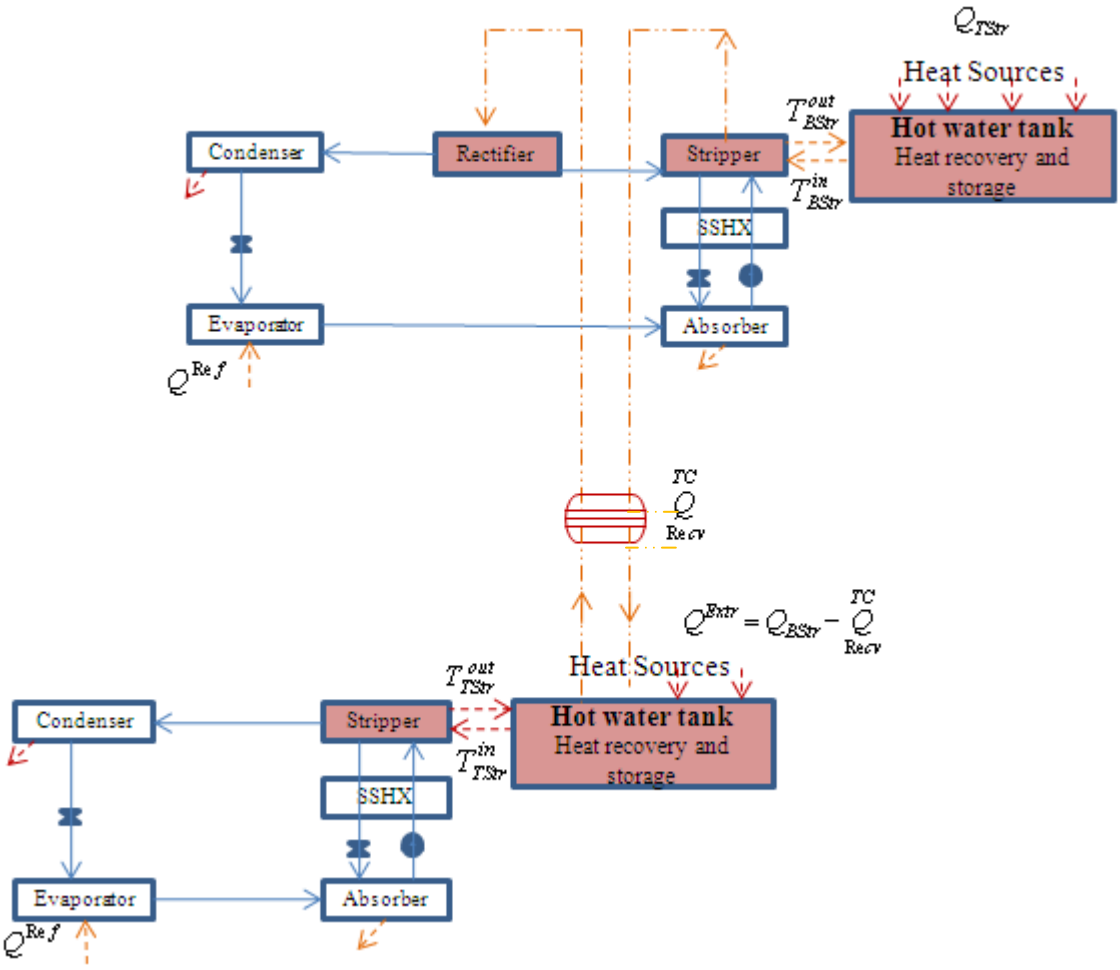

Figure 4.15. The Two Cycles Coupled Thermally by Internal Heat Integration.

The H_2O/LiBr cycle produces cooling at temperatures above water freezing temperature typically around 5°C and the (NH_3/H_2O) cycle produces cooling at lower temperatures typically around -33°C, and can be down to -77°C.

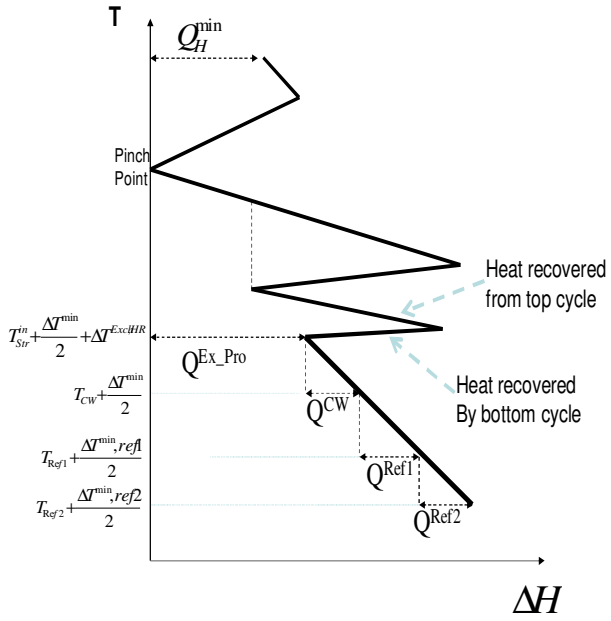

Figure 4.16. The GCC for the Process with Thermal Coupling of the Two AR Cycles.

The heat release by both AR cycles is added to the GCC to determine the extent of thermal coupling between the two cycles as well as the rest of the process. Figure 4.16 is a schematic representation of the GCC for the process and the two AR cycles. The H_2O/LiBr cycle is represented by four streams: two cold streams passing through the generator and the evaporator and two hot streams passing through the absorber and the condenser. On the other hand, the NH_3/H_2O cycle is represented by five streams because of the presence of one hotter stream passing through the rectifier. Table 4.10 summarizes the streams involved in heat integration.

Table 4.10: AR Streams Data to be Integrated Thermally with the Process Streams.

Top cycle: (NH_3/H_2O)			
Stream	Supply Temperature T^s	Target Temperature T^t	Q^*
H_1	T_{Cond}^{in} T_{Rectf}^{DP}	T_{Cond}^{out}	Q_{Cond}
H_2	T_{Rectf}^{in}	T_{Rectf}^{DP}	Q_{Rectf}
H_3	$T_{Abs\|PTX}^{Solution}$	T_{Abs}^{Des}	Q_{Abs}
C_1	T_{str}^{out}	T_{str}^{in}	$Q_{Str} = \frac{Q^{REf1}}{COP}$
C_2	T_{Evp}^{in}	T_{Evp}^{out}	Q_{Evp} Q^{REf1}
Bottom cycle (H_2O/LiBr)			
H_1	T_{Cond}^{in}	T_{Cond}^{out}	Q_{Cond}
H_2	$T_{Abs\|PTX}^{Solution}$	T_{Abs}^{Des}	Q_{Abs}
C_1	T_{str}^{out}	T_{str}^{in}	Q_{Str} $\frac{Q^{REf1}}{COP}$
C_2	T_{Evp}^{in}	T_{Evp}^{out}	$Q_{Evp} = Q^{REf1}$

Considering the H_2O/LiBr cycle shown by Fig. 4.13; the following expressions are used to evaluate the heat duties of the different components:

$$Q_{Cond} = h_8 - h_7 \tag{4.10}$$

$$Q_{Str} = h_7 - h_4 + \frac{m_3}{m_7}(h_4 - h_3) \tag{4.11}$$

$$Q_{Evp} = h_{10} - h_9 \tag{4.12}$$

$$Q_{Absf} = m_{10}h_{10} + m_6 h_6 - m_1 h_1 \tag{4.13}$$

Similar expressions are used for the NH_3/H_2O cycle shown by Fig. 4.13 with one more equation for the rectifier:

$$Q_{\mathrm{Re}ctf} = h_7 - h_9 + \frac{x_9 - x_7}{x_7 - x_8}(h_7 - h_8) \tag{4.14}$$

The enthalpy for any stream is a function of temperature, pressure, and composition, i.e.

$$h_i = f(T_i, P_i, X_i) \tag{4.15}$$

IV.2.2.3. CASE STUDY

The GCC of an industrial food plant determines the need for cooling at two levels. The refrigeration duties (in refrigeration tons) are 17.2 kWat and 148.4 kW at -7^{o}C. The GCC also determines that the plant has excess heat below the pinch with temperature typically 130^{o}C. That can be extracted to drive AR instead of paying electricity in case of vapor-compression refrigerator usage.

The proposed thermally-coupled H_2O/LiBr-NH_3/H_2O is considered for providing the cooling demand at the two required levels with the objective of minimizing or eliminating the need to external heat to drive the H_2O/LiBr cycle.

It is also desired to make sensitivity analysis to investigate the feasibility of using the proposed system at the plant if the plant operates at less-than-maximum capacity (which will require lower refrigeration duties).

Aspen Plus simulation tool is used to simulate the AR system and to estimate its performance. The top cycle has an evaporator operating at -10^{o}C; while the bottom cycle has an evaporator operating at 5^{o}C.

IV.2.2.4. RESULTS AND DISCUSSION

The two AR cycles have been simulated using ASPEN Plus. The simulation used the Peng Robinson equation of state in case of the NH_3-H_2O cycle. The desorber (generator) has been simulated as a three-stage distillation column (using ASPEN's RadFrac module) with no condenser. Optimum feed stages and the numbers of the stages that minimize the reboiler heat duty have been determined by a sensitivity analysis. The strong solution from the absorber is fed to stage number 1. The rectifier is simulated as a flash column; with a design specification to set the NH_3 purity at the vapor stream at 0.9996 by changing the temperature of the flash column. The separated water from the rectifier is circulated again to the desorber column at stage 1. Also the rectifier can be simulated as part of the desorber (RadFrac.) by selecting a RadFrac with partial condenser as shown by Fig.4.17.

Figure 4.18 shows the heating curve for the generator of the top cycle. The other heat-exchange units have been represented by heater blocks; except the solution heat exchanger which has been simulated as HeatX; which is a shell-tube heat exchanger module in ASPEN Plus. Similarly, the H_2O/LiBr cycle has been simulated without using a rectification step.

The simulation used the thermodynamic databases electrolyte NRTL model considering the salt (LiBr) and formation of ions. The entire system has been simulated with thermal coupling by connecting the two cycles by a heat exchanger. Figure 4.19 gives the ASPEN Plus Representation of the thermally-coupled double-effect AR System.

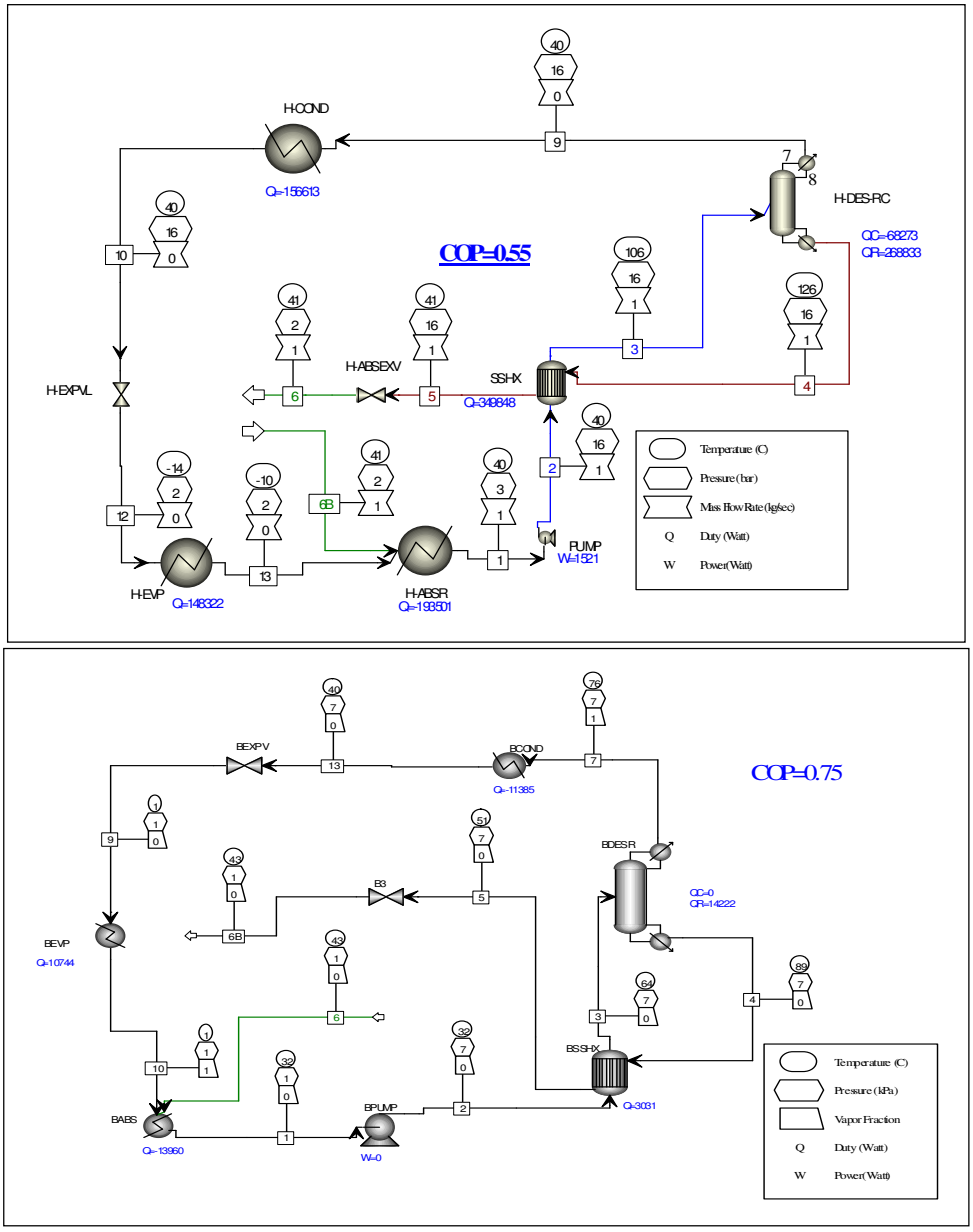

Figure 4.17. The Top Cycle is"NH_3/H_2O" and the Bottom Cycle is "$H_2O/LiBr$" Simulation Flow Sheet.

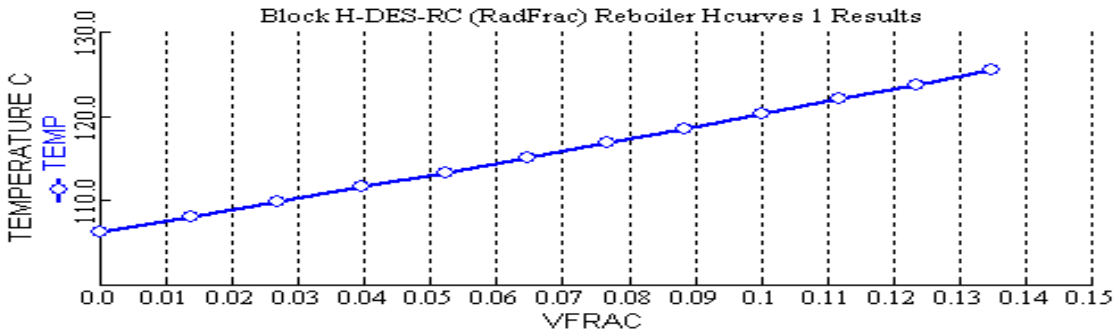

Figure 4.18. Simulation Results of the Temperature versus Vapor Fraction for Generator of the Top Cycle "NH_3/H_2O".

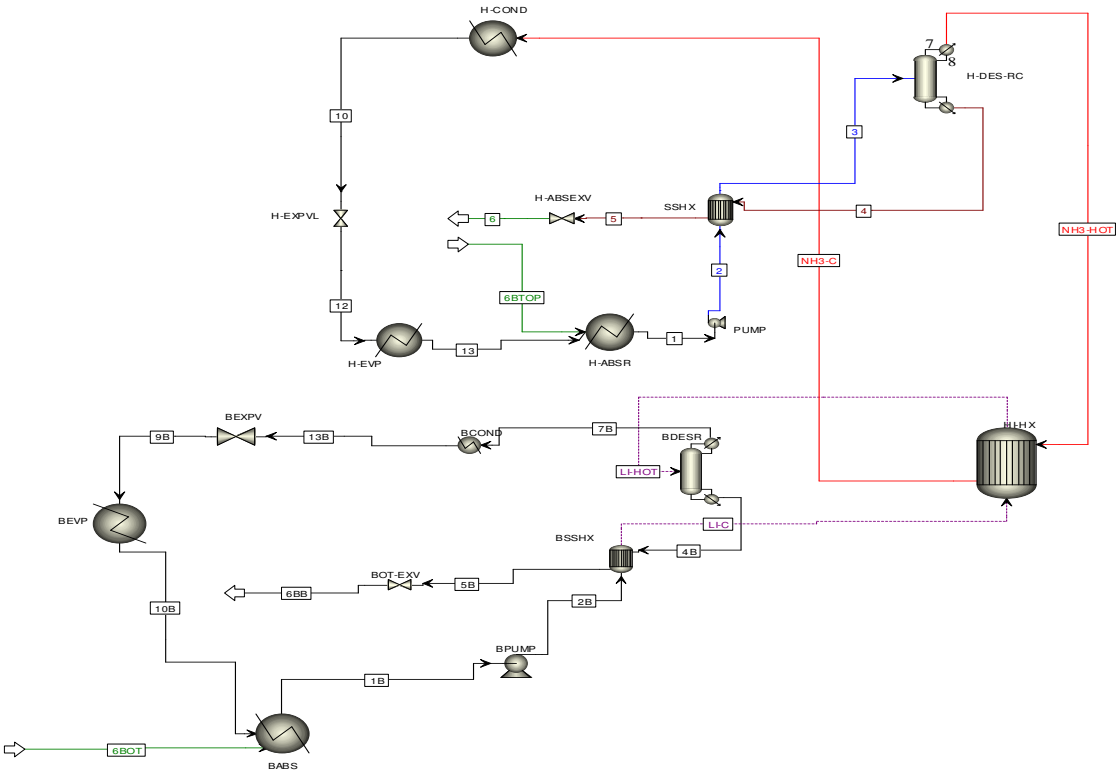

Figure 4.19. Thermally Coupled Dual System.

Process simulation was also used to investigate the potential merits of the thermally-coupled AR systems. Table 4.11 summarizes the conditions of the simulation. The conditions of the absorber, the condenser, and the evaporator have been fixed. Meanwhile, conditions of the other units have been varied and assessed through a sensitivity analysis.

The minimum temperature needed to run the bottom cycle was taken to be 85^{o}C. The effect of the temperature of the heat source driving the top cycle has been studied in the range of (125-165)^{o}C. The following results have been observed:

A. Increasing the heat source of the top cycle improves the NH_3/H_2O cycle COP to certain limit, but increasing the temperature more than 130^{o}C decreases the COP
B. Increasing the temperature of the top cycle heat source provides more recovered heat to the bottom cycle.

Table 4.11. Input Data Used in the Simulation.

Top cycle	T(^{o}C)	P(kPa)	X
Evaporator	-10	240	0.99965
Absorber	31	240	0.3686
Condenser	40	1555	0.99965
Bottom cycle	T(^{o}C)	P(kPa)	X
Evaporator	1.3	0.673	1
Absorber	31	0.673	0.433
Condenser	40	7.4	1
X = refrigerant mass fraction (kg/kg)			

This is explained by increasing the temperature approach between the minimum temperature needed to run the H_2O/LiBr cycle and the available recovered heat. Table 4.12 provides a summary of the simulation results and the merits of thermal coupling of the two AR cycles; and also the results are shown at Fig. 4.20.

The COP of the proposed dual cycle thermally coupled through the desorbers can be better than the individual NH_3/H_2O cycle under certain circumstances. This is mainly at heat temperatures higher than 130°C. Therefore using the dual system is recommended when the heat sources available at temperatures higher than that needed to run the single cycle and lower than that needed to run the two-stage NH_3/H_2O cycle. The result is that this dual system increases the entire COP and produces extra cooling at the second level.

Table 4.12. Summary of Simulation Results.

TOP CYCLE				Recovered Q (kW)	Bottom cycle	NH_3/H_2O COP	Dual system COP	COP% increase
Boiler Exit T °C	Desorber °C	Evaporator Q(kW)	Pump kW		Q kW			
126	125-99	147.3	1.60	6.7	4.7	0.592	0.611	3.2
133	**132-104**	**148.3**	**2.14**	**14.9**	**10.4**	**0.572**	**0.612**	**7.0**
140	**139-109**	**148.4**	**2.05**	**24.6**	**17.2**	**0.552**	**0.617**	**11.8**
153	152-117	147.9	2.75	47.2	33.0	0.508	0.622	22.4
164	163-120	147.7	3.35	66	46	0.456	0.609	33.6

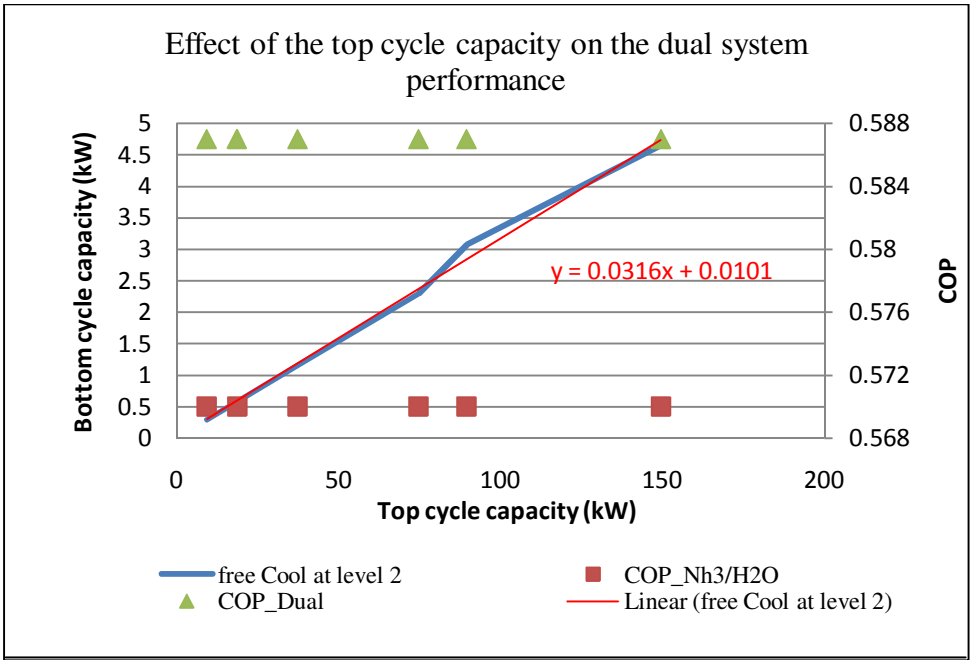

Figure 4.20. Effect of Top Cycle Size on the Bottom Cycle Size.

C. Increasing the heat source of the top cycle improves the NH_3/H_2O cycle COP to certain limit, but increasing the temperature more than 130°C decreases the COP.

D. Increasing the temperature of the top cycle heat source provide more recovered heat to the bottom cycle, this is explained by increasing the temperature approach between the minimum temperature needed to run H_2O/LiBr cycle and the available recovered heat.

Figure 4.21 shows that COP of the dual cycle can be better than the only NH_3/H_2O cycle under certain circumstances. That is mainly at heat temperatures higher than 130°C. Therefore using the dual system is recommended when the heat sources available at temperatures higher than needed to run the single cycle and lower then the needed to run the two stage NH_3/LiBr cycle. As this dual system increases the entire COP and produces extra cooling at the second level. Under the simulation assumed conditions, the optimum COP of the proposed dual system is 0.61 corresponding to 0.515 in case of only using NH_3/H_2O single effect cycle; this takes place when using high pressure of the

top cycle equal 2000 KPa (139^{o}C); which is 19% increase in COP of the entire system, in addition to producing typically 6 TR free at 2 ^{o}C.

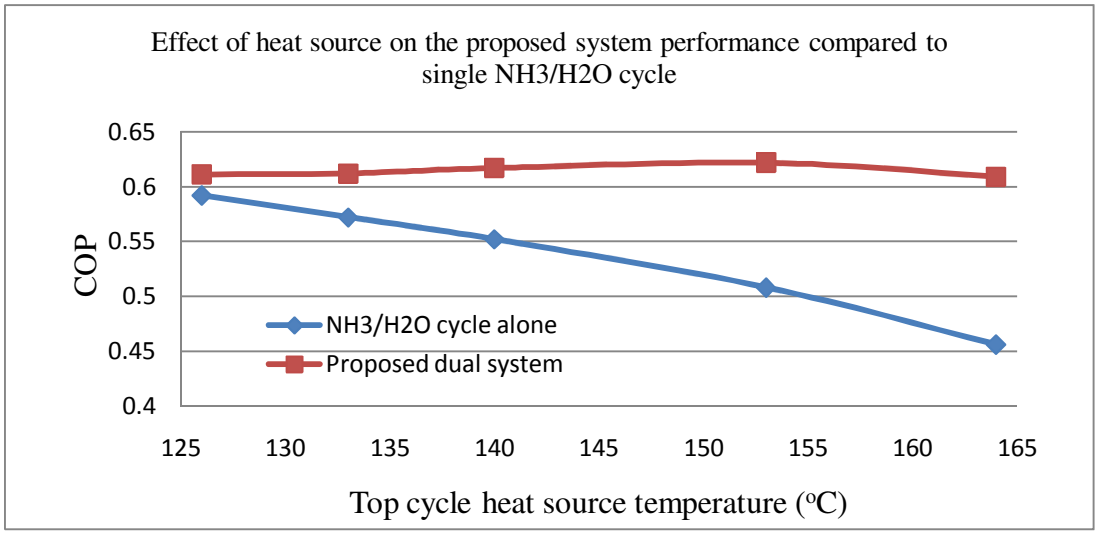

Figure 4.21. Effect of the Top Cycle Heat Source on the Entire Dual System Performance.

CHAPTER V
INTEGRATED DESIGN OF SOLAR-ASSISTED TRIGENERATION SYSTEMS

The growing concern about the depleting fossil-energy sources and the increasing desire to reduce greenhouse gas (GHG) emissions are motivating the process industries to adopt various approaches to conserving energy and moving to more sustainable energy sources. This work is aimed at the development of a systematic procedure for energy conservation through the integrated design of trigeneration systems (combined cooling, heating, and power "CCHP") while incorporating solar energy as a renewable form of energy with low GHG emissions. Absorption refrigeration is used to utilize excess process heat and any needed external energy in the form of fossil and/or solar energy. To account for the fluctuation in collected solar energy, the decision-making horizon is discretized into multiple periods. An extended transshipment representation is developed to embed potential configurations of interest. Power generation is achieved through steam turbines and refrigeration is induced through absorption refrigeration. Next, a nonlinear programming formulation is developed. Heat integration and energy transformation constraints are included. The integrated systems exchange energy through feasible intervals that are tied to the models characterizing the different components of the system. The solution of the optimization formulation determines the optimal levels of power, external heating, external cooling, heat integration, mix of fossil/solar energy forms to be supplied to the process, and the scheduling of the system operation. A case study is solved to show the applicability of the devised approach.

V.1. INTRODUCTION

The dwindling fossil energy sources and the increasing concern about the consequences of greenhouse gas emissions on global climatic changes provide much motivation for the use of renewable energy sources. As such, there is a significant need to incorporate renewable energy sources in industrial processes. There is also much need for integrated energy systems that address the combined cooling, heating, and power needs of the process which is referred to as *trigeneration*. Several advantages accrue as a result of using trigeneration. Thermodynamic and thermo-economic analyses indicate an enhanced performance and increased cost effectiveness when trigeneration systems are properly designed and operated [55-59] report that for cases when the efficiency of a conventional power plant was reported to be about 40%, the use of trigeneration can enhance the plant efficiency by a factor of 2. Trigeneration contributes to enhanced sustainability through the reduction of greenhouse gas (GHG) emissions [60]. It has been shown that 200 kg CO_2/ MWh^{-1} reduction can be achieved when trigeneration is applied instead of a conventional power cycle [61]. Trigeneration can use a variety of sources including waste heat [62] and offers enhanced flexibility [62]. More details on trigeneration can be found in recent literature reviews [63-64].

There are several configurations of trigeneration systems that can be integrated into the process industries. Because of the critical role played by heat transfer in industrial processes, this work focuses on trigeneration systems that employ extraction steam turbines for power generation with the exhaust steam used for heating. For low-temperature cooling, absorption refrigerators (AR) are considered in this work because they are largely driven by heat which may be extracted from process sources or provided from external energy. In addition to using fossil fuels for supplying external energy, this work includes the use of solar energy as a renewable and sustainable form of energy. Since solar energy cannot be collected continuously throughout the day, it is usually supplemented with other forms of energy or with an energy storage system. This poses

an additional level of complexity in designing solar-assisted trigeneration systems. Solar systems are being increasingly considered in industrial facilities for combined heat and power (cogeneration) systems [64] and in absorption refrigeration [65].

The overall objective of this work is to develop a systematic procedure for the optimal design trigeneration systems that are integrated with the process. The system includes extraction turbines, heating, cooling, and absorption refrigeration. Heat integration is to be considered among the process hot and cold streams as well as with the trigeneration components. Fossil and solar forms of energy are used to provide external sources of energy. The developed procedure is aimed at answering the following questions:

- What are the optimum heating and cooling requirements for the process?
- What fractions of energy should be provided by solar energy and fossil fuel?
- How to handle dynamic changes for the solar energy while providing a steady-state performance to meet the process requirements for heating, cooling, and power?
- What are the optimum design and operating variables of the system?
- What is the impact of GHG policies (e.g., carbon credits) on the system design?

To address these challenging tasks, process integration techniques are coupled with an optimization formulation to evolve an effective and methodical approach.

V.2. PROBLEM STATEMENT

Consider a process with several process hot and cold streams. Heat may be exchanged among the hot and cold streams and external utilities may also be needed to provide external heating and cooling at different temperature levels. In addition to heat integration, the process is considering the following options:

- Combined heat and power: Steam may be provided directly to the process or through a power-generation extraction turbine

- Absorption refrigeration: excess process heat or external heating sources may be used to induce refrigeration through an absorption refrigeration cycle
- Solar energy and fossil fuel are considered for usage as external sources of heat (to be used in steam generation and/or absorption refrigeration)

The problem to be addressed involves the design and integration of a cogeneration system and an AR cycle into an industrial facility and the optimal selection of the optimal mix of energy (solar and fossil) sources which vary dynamically throughout the year. The problem is formally stated as follows:

Given a continuous process with:

- A number N_H of process hot streams (to be cooled) and a number N_C of process cold streams (to be heated). Given also are the heat capacity (flowrate x specific heat) of each process hot stream, $FC_{P,u}$; its supply (inlet) temperature, T_u^s; and its target (outlet) temperature, T_u^t, where $u = 1,2,...,N_H$. In addition, the heat capacity, $fc_{P,v}$, supply and target temperatures, t_v^s and t_v^t, are given for each process cold stream, where $v = 1,2,.,N_C$.
- Available for service are the following:
- A set C_UTILIITY = {clc = 1,2, …, N_{CU}}of cooling utilities whose supply and target temperatures (but not flow rates) are known.
- A set FOSSIL_UTILITY = {flf = 1,2, …, N_{FHU}}of fossil-based heating utilities. For each fossil-based heating utility, the temperature (T_f^{Fossil}) and the cost (C_f^{Fossil}) are known.
- Solar energy is a candidate as a source of heat. The useful collected solar energy varies dynamically. The size and cost of the solar energy collection system are unknown and are to be determined through optimization. An economic incentive (e.g., a carbon tax credit) may be available for the use of solar energy to reduce the emission of greenhouse gases GHGs.

- The cogeneration system involves the use of a steam turbine to produce power and heat. The optimal values of power and steam are to be determined.
- A portion of the process refrigeration demand is to be fulfilled using AR. These refrigerators can obtain the needed heat from process excess heat, solar energy, and fossil fuel. Hot water loops are used to pick up the heat from the three energy sources and deliver the heat to the AR System. The rest of the cooling duty of the process is to be provided by other cooling utilities (e.g., cooling water, refrigerants). Figure 5.1 is a schematic representation of the problem.

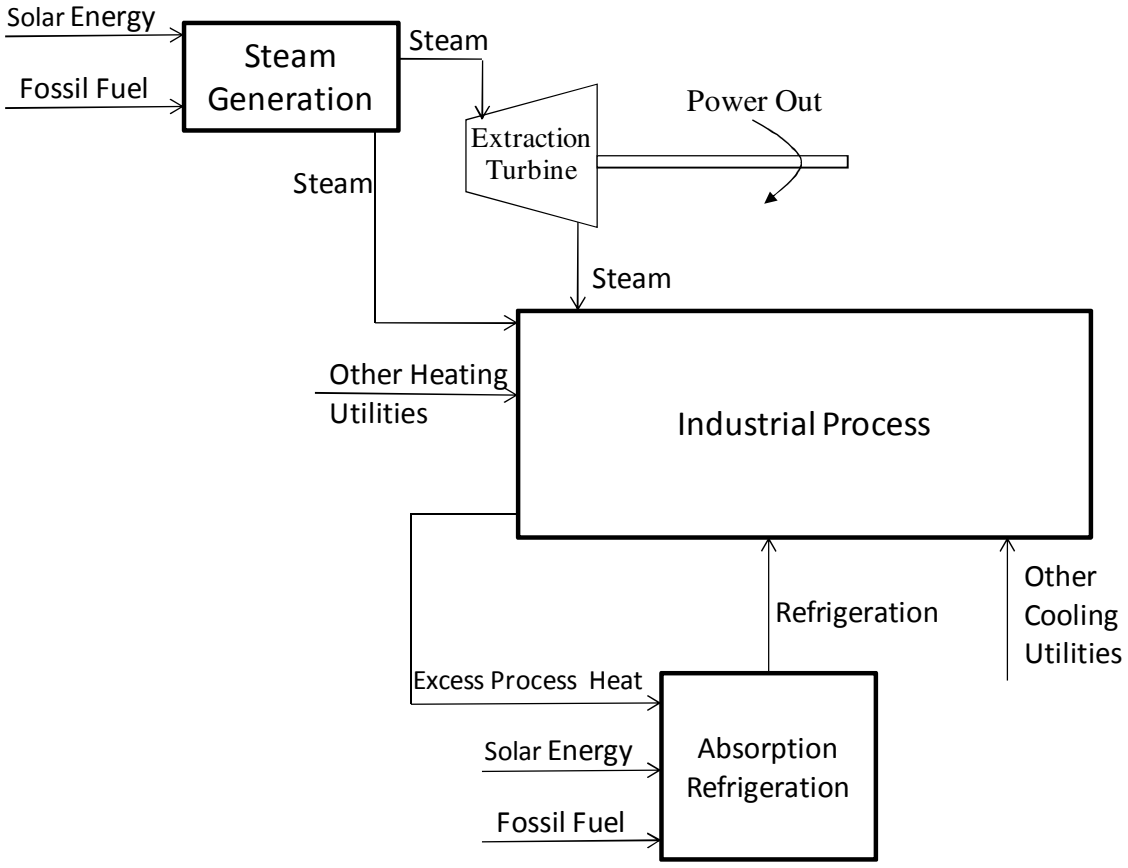

Figure 5.1. Schematic Representation of the Problem Statement.

V.3. APPROACH

The first step in the solution methodology is to develop a structural representation which embeds the potential configurations of interest. An "extended transshipment model" is introduced. It is an extension of the transshipment model developed by [66] for the synthesis of heat-exchange networks. The transshipment model starts by developing a temperature-interval diagram (TID) by representing each stream as a vertical arrow between supply and target temperatures. Horizontal lines are drawn at the locations of the supply and target temperatures. The distance between each two consecutive horizontal lines is referred to as a temperature interval. Within the same interval, heat may be transferred from hot to cold streams. Furthermore, heat may be transferred down where it can exchange heat with a cold stream at a lower interval.

We now revise the transshipment model to the multi-period extended transshipment model by introducing the following modifications and assumptions:

- The decision-making time horizon (e.g., a year) is discretized into N_p periods leading to a set of operating periods: PERIODS = $\{p|p= 1,2, \ldots,N_p\}$. Within each time period, the values of energy usage are averaged and the analysis within that period is carried out for the averaged energy values of each energy type. In selecting the number and duration of the periods, it is important to reconcile the accuracy of fluctuations (e.g., in solar energy) versus the computation efforts.
- For absorption refrigeration, a heat recovery system along with a hot-water storage and dispatch network are used. This arrangement enables the collection of heat from different sources and the inter-period heat integration (i.e., storing heat in one period and dispatching it in another period)
- For steam generation for cogeneration, it is only allowed to have intra-period integration (i.e., no energy is stored, integrated, or exchanged over more than one period)

- For each period, the transshipment model is now extended by introducing cogeneration and absorption refrigeration as follows:
- Solar energy and fossil fuel are considered for steam generation. The relative contribution of each type of energy may vary from one period to another. The generated steam is allowed to go through an extraction turbine which produces power and lets down steam for further usage as a heating medium. The power generated from the turbine during period p is calculated through the turbine performance model, ψ_p, as follows:

$$POWER_p = \psi_p(H_p^{Steam\_Cogen}, H_p^{Steam\_Exit\_Turbine}) \qquad \forall p$$

where $POWER_p$ is the electric power produced during period p from the steam turbine receiving steam enthalpy $H_p^{Steam\_Cogen}$ and discharging steam enthalpy $H_p^{Steam\_Exit\_Turbine}$ during period p. Steam is also allowed to bypass the power generation system and to be used directly for heating. The outlet steam splits (from the turbines or from the steam-generation system) are assigned to different temperature intervals depending on their temperatures and the steam headers to which they are allocation. The flow rates of the steam splits are to be determined through optimization.

- The AR system is driven largely by heat. There are two fluids employed in AR: a working fluid (e.g., ammonia or water) and an absorbent (e.g., water or LiBr, respectively). When a low-pressure vapor from the evaporator is absorbed in the absorbent, heat is released. The absorption mixture of the working fluid and absorbed is pumped and fed to a stripper (generator) where heat is added to the solution and the working fluid is released as a high-pressure vapor. The absorbent is returned to the absorber while the high-pressure vapor is fed to the condenser to condense at a moderate temperature. The high-pressure working fluid is throttled and fed to an evaporator which extracts the refrigeration duty at a low temperature. An effective method for delivering heat to the stripper is through the use of hot-water loops. Recirculating water is passed via heat

exchangers to pick up heat from the three considered sources of energy (excess process heat, fossil, and solar). The heat needed to drive the AR is delivered to the stripper through the hot water then returned back to the heat recovery system. Heat recovered beyond that needed to immediately drive the AR system is stored in well-insulated tanks for later usage. Such a heat storage and dispatch system is quite useful in handling the dynamic fluctuation in the collected solar energy.

Therefore, the transshipment model is modified by including the following:

- Steam allocation to the corresponding temperature intervals from the exit of the steam turbines or directly from the steam-generation system.
- Extraction of heat from the temperature intervals to the hot-water loop storage and dispatch network. Such extraction is limited to intervals that lie above the minimum acceptable temperature for heating the water loop to obtain T_{str}^{in}. The amount of heat (Q_{Str}) is to be determined via optimization.
- Extraction of the AR refrigeration duty (Q_{Ref}) at the refrigeration temperature $T_{Ref.}$ At this temperature, an interval (u = Ref) is created specifically for the withdrawal of Q_{Ref}. The value of Q_{Ref} is an optimization variable.
- Addition of heat from the absorber of the AR cycle. An interval is created at the temperature T_{Abs} and the heat to be removed from the absorber (Q_{Abs}) is added to this interval. When the pumping energy is neglected compared to the heat duties of the AR cycle, then Q_{Abs} can be related to Q_{Ref} and QStr through heat balance and the COP.

V.4. MATHEMATICAL FORMULATION

Let us first start with developing the heat balances over the temperature intervals. The exchangeable load of the u^{th} hot stream (assuming that it is losing sensible heat but it can

be readily modified to account for latent heat) which passes through the z^{th} interval is defined as

$$HH_{u,z,p} = F_{u,p}\ C_{p,u,p}\ (T_{z-1,p} - T_{z,p}) \tag{5.1}$$

where $T_{z-1,p}$ and $T_{z,p}$ are the hot-scale temperatures at the top and the bottom lines defining the zth interval for period p. On the other hand, the exchangeable capacity of the vth cold stream (gaining sensible heat) which passes through the zth interval is computed through

$$HC_{v,z,p} = f_{v,p}\ c_{p,v,p}\ (t_{z-1,p} - t_{z,p}) \tag{5.2}$$

where $t_{z-1,p}$ and $t_{z,p}$ are the cold-scale temperatures at the top and the bottom lines defining the zth interval for period p.

By summing up the heating loads and cooling capacities, we get:

$$HH_{z,p}^{Total} = \sum_{\substack{u\ passes\ through\ interval\ z \\ where\ u=1,\ 2,\ .....,\ N_H}} HH_{u,z,p} \tag{5.3}$$

and

$$HC_{z,p}^{Total} = \sum_{\substack{v\ passes\ through\ interval\ z \\ and\ v=1,2,....,N_C}} HC_{v,z,p} \tag{5.4}$$

Next, we move to incorporating heating and cooling utilities (excluding steam and AR). For temperature interval z, the heat load of the u^{th} heating utility is given by:

$$HHU_{u,z,p} = FU_{u,p}\ C_{p,u,p}\ (T_{z-1,p} - T_{z,p}) \tag{5.5}$$

where $u = N_H + 1, N_H + 2, ..., N_H + N_{HU}$

where $FU_{u,p}$ is the flowrate of the u^{th} heating utility during period p. The sum of all heating loads of the heating utilities in interval is expressed as:

$$HHU_{z,p}^{Total} = \sum_{\substack{u\ passes\ through\ interval\ z \\ where u = N_H+1,\ N_H+2,\ .....,\ N_H+N_{HU}}} HUU_{u,z,p} \tag{5.6}$$

The total heating load of the u[th] utility in the network during period p may be evaluated by summing up the individual heat loads over intervals:

$$QH_{u,p} = \sum_{z} HHU_{u,z,p} \tag{5.7}$$

Similarly, during the p[th] period, the cooling capacities of the v[th] cooling utility in the zth interval is calculated as follows:

$$HCU_{v,z,p} = fU_{v,p}\ c_{p,v,p}\ (t_{z-1,p} - t_{z,p}), \qquad v = N_C+1,\ N_C+2,\ ...,\ N_C+N_{CU} \tag{5.8}$$

where $fU_{v,p}$ is the flowrate of the v[th] cooling utility during period p.

The sum of all cooling capacities of the cooling utilities during period p is expressed as:

$$HCU_{z,p}^{Total} = \sum_{\substack{v\ passes\ through\ interval\ z \\ where v = N_C+1,\ N_C+2,\ .....,\ N_C+N_{CU}}} HCU_{v,z,p} \tag{5.9}$$

The total cooling capacity of the u[th] utility in the network over period p may be evaluated by summing up the individual cooling loads over intervals:

$$QC_{v,p} = \sum_{z} HCU_{v,z,p} \tag{5.10}$$

During period p, the heat added by steam allocated directly from the steam-generation system is given by:

$$H_{p}^{Steam\_Direct} = \sum_{z} H_{z,p}^{Steam\_Direct} \tag{5.11}$$

Similarly, during period p, the heat added by steam allocated from the exit of the turbines is given by:

$$H_p^{Steam\_Exit\_Turbine} = \sum_z H_{z,p}^{Steam\_Exit\_Turbine} \tag{5.12}$$

For the zth temperature interval lying above the minimum acceptable temperature to heat the stripper via the hot-water loop, the amount of heat extracted from the process excess heat to the hot-water loop is designated by $Q_{z,p}^{Str,process}$. Hence, for such intervals, one can write the following heat-balance equation for period p as follows:

$$HH_{z,p}^{Total} - HC_{z,p}^{Total} + HHU_{z,p}^{Total} - HHC_{z,p}^{Total} + H_{z,p}^{Steam\_Direct} + H_{z,p}^{Steam\_Exit\_Turbine} - Q_{z,p}^{Str,process} = r_{z-1,p} - r_{z,p}$$

$$z = 1,2,\ldots n_{Tstr} \tag{5.13}$$

where $r_{z-1,p}$ and $r_{z,p}$ are the residual heats entering and leaving interval z during period p.

For the temperature interval corresponding to the absorber temperature, the heat balance is written as follows:

$$HH_{z,p}^{Total} - HC_{z,p}^{Total} + HHU_{z,p}^{Total} - HHC_{z,p}^{Total} + H_{z,p}^{Steam\_Direct} + H_{z,p}^{Steam\_Exit\_Turbine} - Q_{z,p}^{Str,process} + Q_p^{Abs} = r_{z-1,p} - r_{z,p}$$

$$\text{z = Abs} \tag{5.14}$$

For the temperature interval where the AR refrigeration duty is withdrawn, the heat balance may be expressed as:

$$HH_{z,p}^{Total} - HC_{z,p}^{Total} + HHU_{z,p}^{Total} - HHC_{z,p}^{Total} + H_{z,p}^{Steam\_Direct} + H_{z,p}^{Steam\_Exit\_Turbine} - Q_p^{Abs} = r_{z-1,p} - r_{z,p}$$

$$\text{Z = Ref} \tag{5.15}$$

The following additional constraints are also needed:

$$r_{0,p} = r_{n_{\text{int}},p} = 0 \tag{5.16}$$

This guarantees that all heat duties are in balance within the network.

$$r_{z,p} \geq 0 \qquad z = 1,2,\ldots n_{\text{int}} - 1 \qquad (5.17)$$

This insures that heat flows downwards. Furthermore, non-negativity constraints are written for the flows and heat duties of the utilities.

Figure 5.2 is a schematic representation of the proposed extended transshipment model for the trigeneration system.

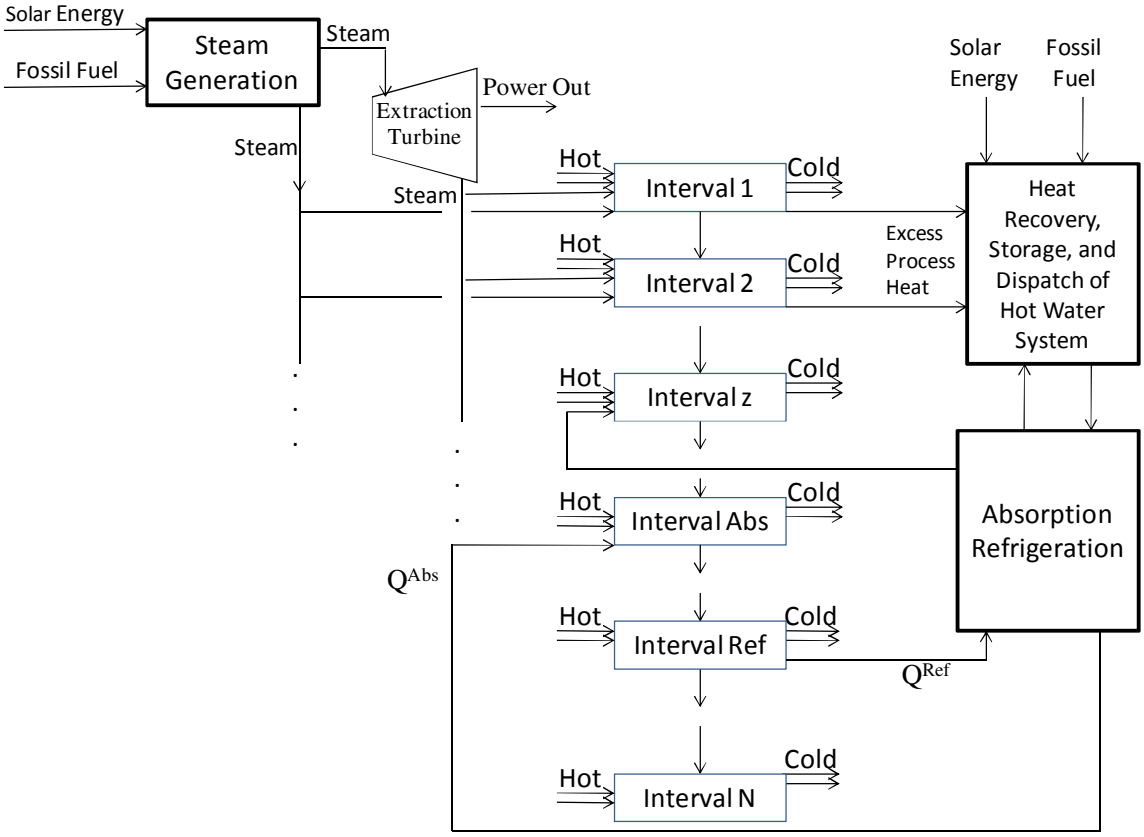

Figure 5.2. The Extended Transshipment Model for Trigeneration.

The contributions of fossil fuel and solar energy are calculated for cogeneration, direct steam heating, and absorption refrigeration through the following expressions:

$$Q_p^{Solar\_Cogen} + Q_p^{Fossil\_Cogen} = H_p^{Steam\_Cogen} \tag{5.18}$$

With the turbine modeling equation that relates the power to the inlet and outlet steam conditions, i.e.,

$$POWER_p = \psi_p(H_p^{Steam\_Cogen}, H_p^{Steam\_Exit\_Turbine}) \qquad \forall p \tag{5.19}$$

$$Q_p^{Solar\_Steam\_Direct} + Q_p^{Fossil\_Steam\_Direct} = H_p^{Steam\_Direct} \tag{5.20}$$

Where

$$H_p^{Steam\_Direct} = \sum_{z_p} H_{z,p}^{Steam\_Direct} \tag{5.21}$$

Similarly, for the AR system,

$$Q_p^{Solar\_AR} + Q_p^{Fossil\_AR} = Q_p^{External\_AR} \tag{5.22}$$

where $Q_p^{External\_AR}$ is the external heat added to the stripper of the AR cycle through fossil fuel and solar energy. The heat added to the hot-water loop heating the stripper may come from excess process heat and/or external sources (fossil and solar), i.e.

$$Q_p^{Str} = Q_p^{Str\_Process} + Q_p^{External\_AR} \tag{5.23}$$

where the excess process heat is collected from the intervals above the minimum acceptable temperature for the hot-water loop, i.e.

$$Q_p^{Str\_Process} = \sum_{z=1}^{n_{Tstr}} Q_{z,p}^{Str\_Process} \tag{5.24}$$

Because the pumping energy in the AR cycle is relatively small compared to the heat input, the coefficient of performance (COP) for the AR system is defined as:

$$COP_p = \frac{Q_p^{Ref}}{Q_p^{Str}} \tag{5.25}$$

The COP is assumed to be known for the selected type of AR. Hence, the COP provides the linkage between the heat added to the stripper and the refrigeration duty of the AR system. The evaluation of the dynamic performance of solar systems and its dependence on location and collector characteristics has been described by another researcher [67]. The following is a brief description of relating the collected energy to the surface area of the collector. The solar energy collected by the s^{th} collector in period p is given by:

$$Q_{s,p}^{Solar} = Q_{s,p}^{Useful\_Solar} * A_s \qquad \forall s\ ,\ \forall p \tag{5.26}$$

$Q_{s,p}^{Useful\_Solar}$ is the useful power collected (and delivered in a thermal form) per unit area of the s^{th} solar collector in period t and A_s is the area of the s^{th} solar collector.

Therefore,

$$Q_{s,p}^{Solar\_Cogen} = Q_{s,p}^{Useful\_Solar} * A_{s,p}^{Cogen} \tag{5.27}$$

$$Q_{s,p}^{Solar\_Direct\_Steam} = Q_{s,p}^{Useful\_Solar} * A_{s,p}^{Direct\_Steam} \tag{5.28}$$

$$Q_{s,p}^{Solar\_AR} = Q_{s,p}^{Useful\_Solar} * A_{s,p}^{AR} \tag{5.29}$$

The design value of the surface area of the collector is the largest over all the periods, i.e.,

$$A_{s,p}^{Cogen} \le A_s^{Cogen} \qquad \forall p \tag{5.30}$$

$$A_{s,p}^{Direct\_Steam} \le A_s^{Direct\_Steam} \qquad \forall p \tag{5.31}$$

$$A_{s,p}^{AR} \le A_s^{AR} \qquad \forall p \tag{5.32}$$

The annualized fixed cost of the s^{th} solar power plant is given as a function (α_s) of the size:

$$AFC_s^{Cogen} = \alpha_s(A_s^{Cogen}) \tag{5.33}$$

$$AFC_s^{Direct\_Steam} = \alpha_s(A_s^{Direct\_Steam}) \tag{5.34}$$

$$AFC_s^{AR} = \alpha_s(A_s^{AR}) \tag{5.35}$$

It is worth noting that the cogeneration terms in the previous equations refer to the simultaneous production or power and useful thermal energy [11]. The solar collectors and fossil-fuel systems may be designed to provide energy for the cogeneration and AR systems separately or jointly. The foregoing equations describe the more general case of installing separate units for each. When the same energy systems are used simultaneously for cogeneration and AR, the problem representation and formulation become simpler with a single term describing the performance and cost of the energy systems [37].

The objective of the optimization formulation is to minimize the total annualized cost of the system which may be expressed as:

$$\begin{aligned}\text{Minimize: } & \sum_p C_p^{Fuel}(Q_p^{Fossil\_Cogen} + Q_p^{Fossil\_Steam\_Direct} + Q_p^{Fossil\_AR}) \\ & + AFC_s^{Solar\_Cogen} + AFC_s^{Solar\_Steam\_Direct} + AFC_s^{Solar\_AR} \\ & + \\ & \sum_p (C_{p,s}^{Solar\_Cogen} Q_p^{Solar\_Cogen} + C_{p,s}^{Solar\_Steam\_Direct} Q_p^{Solar\_Steam\_Direct} + C_{p,s}^{Solar\_AR} Q_p^{Solar\_AR}) \\ & + AFC^{AR} + AFC^{Cogen} + \sum_p \sum_{u=N_H+1}^{N_H+N_{HU}} CH_{u,p} * QH_{u,p} + \sum_p \sum_{v=N_C+1}^{N_C+N_{CU}} CC_{v,p} * QC_{v,p}\end{aligned} \tag{5.36}$$

where C_p^{Fuel}, $C_{p,s}^{Solar\_Cogen}$, $C_{p,s}^{Solar\_Steam\_Direct}$, $C_{p,s}^{Solar\_AR}$ are the unit operating costs of the fossil fuel, the solar system used for cogeneration, the solar system used for direct steam generation, and the solar system used for heating the stripper in the AR cycle, respectively, in period p. The AFC is the annualized fixed cost. Also, $CH_{u,p}$ designates the cost of the u^{th} heating utility and $CC_{v,p}$ designates the cost of the v^{th} cooling utility in period p. When credits are given for the reduction of greenhouse gas emissions resulting

from the use of solar systems, a credit terms (carbon credit per tonne of CO_2-equivalent*annual reduction in tonnes of CO_2-equivalent emissions). This formulation is a nonlinear program that can be solved using commercially available software (e.g., LINGO).

V.5. CASE STUDY: SOLAR - ASSISTED TRIGENERATION IN A PHMARMCEUTICAL PLANT

Consider the pharmaceutical processing facility shown in Fig. 5.3 adapted from El-Halwagi [65]. The plant is located at the city of Daggett in San Bernardino County in California with the following coordinates {N 34° 52'} {W 116° 46'}. The data for the process hot and cold streams are given in Table 5.1. A steam turbine is used in cogenerating heat and power. The combined power and thermal efficiencies of cogeneration are 70% (distributed as 38% for power and 32% for heating using the outlet steam at 545 K). Exchanges to the power grid are allowed. Therefore, when the cogeneration system produces more than the demand for the plant, the additional power is exported to the grid. Conversely, when the power generated from cogeneration is less than the process demand, external power is imported from the grid. Cooling water may be used as an external utility to cool the hot streams down to 314 K below which an LiBr-water AR system is used to provide chilling water at 283 K. A minimum driving force (ΔT^{min}) value of 10 K is used. Hot water is used as the heat transfer medium in the LiBr-Water AR system whose COP is 0.7.

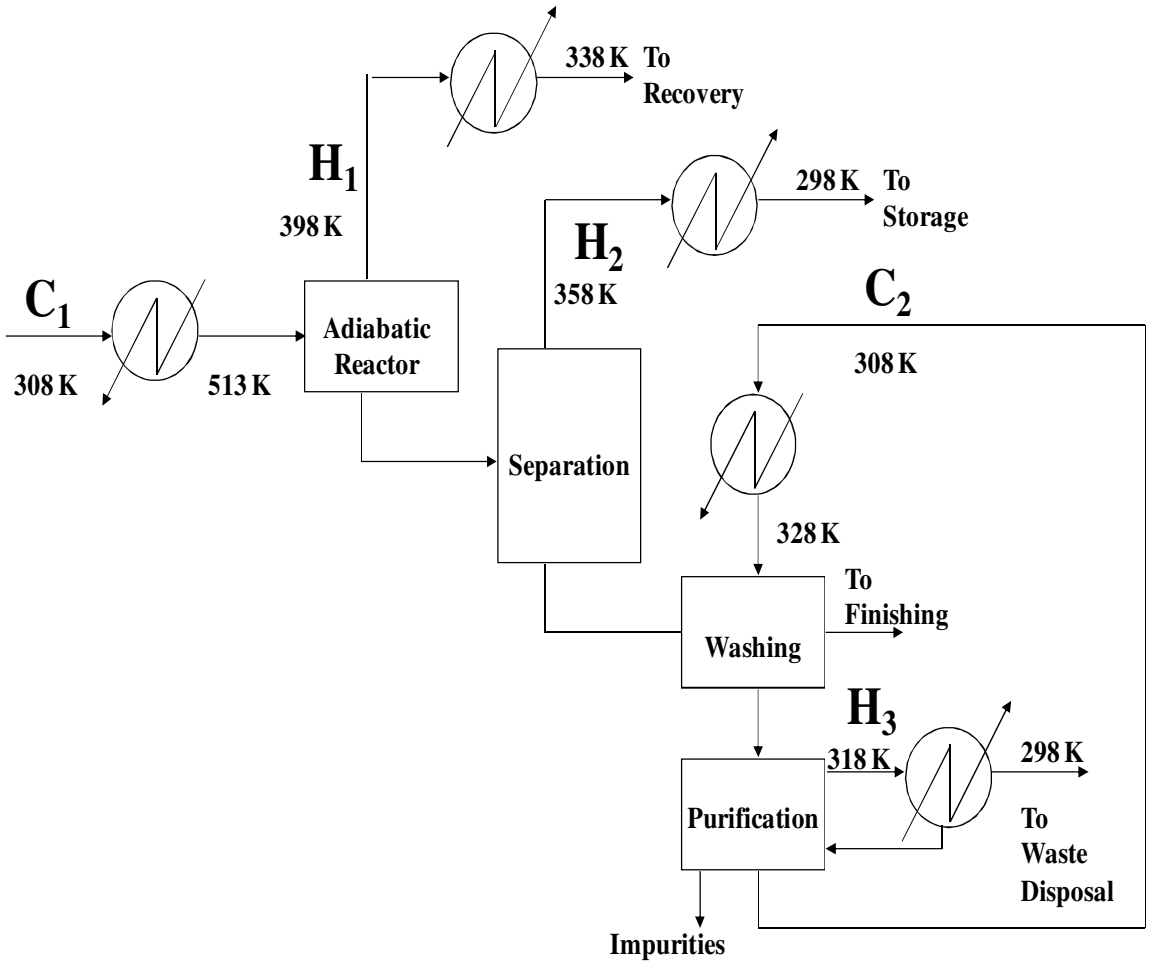

Figure 5.3. A Simplified Flow Sheet of the Pharmaceutical Process of Case Study I.

Table 5.1. Data for the Process Hot and Cold Streams for Case Study I.

Stream	Supply temperature, K	Target temperature, K	Rate of Enthalpy Change kW
H_1	398	338	-186
H_2	358	298	-90
H_3	318	298	-70
C_1	308	513	328
C_2	308	328	58

Solar energy is collected using parabolic trough collectors. The procedure monthly average collected energy data are calculated according to the procedure reported by [68] and are reported in Table 5.2. The total annualized cost ($/yr) of the solar system is given by:

$$TAC_{Solar} = 20A_s + 1{,}085A_s^{0.6} + 0.012Q_{Solar}^{Annual} \quad (5.37)$$

A_s is the area of the solar collector (m^2) and Q_{Solar}^{Annual} is the annual energy collected by the solar system (kWhr/yr). The cost of the fossil fuel is $\$6.0/10^9$ J. The use of solar energy earns the company a GHG credit of $0.008/kWh when the avoided CO_2 is worth $1/ton CO_2 equivalent [69]. For the case study, a sensitivity analysis is carried out for GHG credits ranging from no credit up to $20/ ton CO_2 equivalent.

Table 5.2. Monthly Average of Usefully Collected Solar Energy.

Month	Useful Collected Energy Per Unit Area of Solar Collector ($kWh/m^2.month$)
January	94.24
February	103.88
March	158.72
April	205.50
May	213.28
June	228.90
July	221.34
August	203.98
September	179.70
October	142.29
November	102.30
December	85.25

Using the aforementioned formulation and solving the resulting optimization problem using LINGO 11, we get a trigeneration system which produces 0.24 MW of power, 0.20 MW of heating, and 0.08 MW of refrigeration. The optimization program was solved for different values of carbon credit. In the case of no carbon credit, all of the external energy is supplied by the fossil fuel for an annual cost of $128 k/yr. However, when the carbon credit is $5/tonne CO_2 eq., solar energy becomes more competitive requiring a collector area of 3,943 m^2 and incurring a utility cost (including the GHG credit) of $126 k/yr. When the credit is increased to $20/ tonne CO_2 eq., then almost all of the external heat if provided by solar energy. Figure 5.4 shows the percentage of external energy provided by the solar collectors for two scenarios of carbon credit.

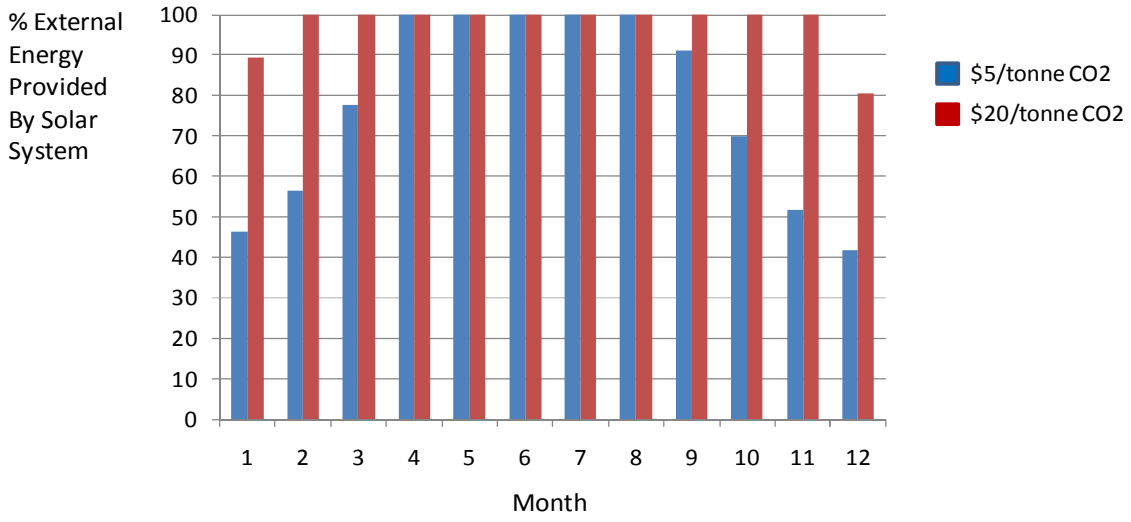

Figure 5.4. Percentage External Energy Supplied by the Solar Collectors for Two Levels of Carbon Credits.

CHAPTER VI
CONCLUSIONS AND RECOMMENDATIONS

A set of systematic procedures have been introduced for the design and integration of energy systems that employ solar energy directly or used in conjunction with fossil fuel and/or biofuel. The work has also addressed the following design problems involving:

- Solar and fossil for power generation
- Solar, bio, and fossil for cogeneration
- Solar energy, and fossil fuels integration with process extra heat to run absorption refrigeration and produce cool
- AR systems using solar energy, excess process heat, and fossil fuels
- Thermal coupling of dual AR systems
- Solar-assisted trigeneration systems in industrial processes

The developed procedures include a combination of gathering and generation of certain required data, modeling the various components, analyzing different scenarios and configurations, optimizing system performance, and estimating the system economics. Several case studies have been solved to illustrate the applicability of the developed procedures and to evaluate the results. Although the power, heating, and cooling generated by the solar-fossil or solar-bio-fossil hybrid systems may be more expensive than that commercially generated by fossil fuels, there are significant environmental and sustainability merits for using the solar system. For instance, the operation of a solar system is virtually free of greenhouse gas emissions. As such, if there are carbon credits, the cost gap between the solar/biofuels and the fossil energies can be readily diminished. The case studies show that a credit of \$5 to 20/tonne CO_2 equivalent can render the solar-assisted systems commercially viable.

The following future work is recommended:

- Integration of molecular design approaches with the developed procedures for the synthesis and screening of refrigerants
- Design under uncertainty: the design procedures can be modified to account for uncertainties in solar energy and process performance
- Incorporation of safety metrics in the objective functions of the design procedures
- Incorporation of commercial solar-design software in the developed procedures

REFERENCES

1. El-Halwagi, MM. *Process Integration*, *Process Systems Engineering*, Vol. 7. Elsevier: New York, 2006.
2. Kreith F, Goswami YD. *Handbook of Energy Efficiency and Renewable Energy*. CRC Press: Boca Raton, FL, 2007.
3. Zakhidov RA, Anarbaev AI. Application of Solar Heat Sources at Thermal Electric Power Plants. *Applied Solar Energy* 2010; **46**: 66–70.
4. Stoecker WF. *Industrial Refrigeration Handbook*. McGraw-Hill: New York, 1998.
5. Smith R. *Chemical Process: Design and Integration*. John Wiley& Sons Ltd: West Sussex, UK, 2005.
6. Kemp I. *Pinch Analysis and Energy Integration: A User Guide on Process Integration for the Efficient Use of Energy*. Elsevier: New York, 2006.
7. Herold KE, Radermacher R, Klein SA. *Absorption Chillers and Heat Pumps*. CRC Press, Inc: Boca Raton, FL, 1996.
8. Duffie JA, Beckman WA. *Solar Engineering of Thermal Process*. John Wiley & Sons: New York, 2006.
9. Meniel AB, Meinel MP. *Applied Solar Energy: An Introduction*. Addison-Wesley Publishing Company: Reading, MA, 1976.
10. Sukhatme SP, Nayak NK. *Solar Energy: Principles of Thermal Collection and Storage*. Tata McGraw-Hill Publishing Company Limited: New Delhi, India, 2008.
11. Potential for Renewable Energy in the San Diego Region August 2005. Access on 17th. October 2010. http://www.renewablesg.org/docs/Web/AppendixE.pdf.
12. Vogel W, Kalb H. *Large-Scale Solar Thermal Power: Technologies, Costs and Development.* John Wiley& Sons: New York, 2010.
13. Weiss W. Rommel M. Process Heat Collectors State of the Art within Task 33/IV. IEA SHC-Task 33 and SolarPACES-Task IV: Solar Heat for Industrial. AEE INTEC: Gleisdorf, Feldgasse 19, Austria, 2008.

14. Compact Linear Fresnel Reflector: Simple. Compact. Durable. Reliable. Access on 17th. October 2010. http://www.ausra.com/technology/
15. Canada S, Cohen G, Cable R, Brosseau D, Price H. *Parabolic Trough Organic Rankine Cycle Power Plant.* NREL/CP-550-37077: National Renewable Energy Laboratory, Golden, CO 80401-3393, January 2005.
16. Srikhirin P, Aphornratana S, Chungpaibulpatana S. A Review of Absorption Refrigeration Technologies. *Renewable and Sustainable Energy Reviews* 2001; **5**: 343-372.
17. Australia Government: The Treasury, Chapter 5: Mitigation Scenarios -International results. Access on 17th. October 2010. http://www.treasury.gov.au/lowpollutionfuture/report/html/05_Chapter5.asp
18. Adams DC. Agriculture and Greenhouse Gas Cap-and-Trade. AAEA Agricultural & Applied Economics Association. PI3- June 2009. Access on 17th October 2010. http://www.aaea.org/publications/policy-issues/PI3.pdf
19. Cape and Trade: A New Tax in Energy. Access on 17th October 2010, http://www.alec.org/AM/Template.cfm?Section=Cap_and_Trade
20. Herrmann U, Kelly B, and Price H. Two-tank Molten Salt Storage for Parabolic Trough Solar Power Plants. Energy 2004; **29**: 883-893.
21. Hassani V, Price H. Modular Trough Power Plants: Proceedings of Solar Forum 2001. Solar Energy: The Power to Choose, Washington, DC, APRIL 21-25, 2001.
22. DC Badran O, Eck M. The Application of Parabolic Trough Technology under Jordanian Climate. Renewable Energy 2006; **31**: 791-802.
23. Eck M, Zarza E. Direct Steam Process with Direct Steam Generating Parabolic Troughs. *Solar Energy* 2006; 80: 1424-1433.
24. Cohen GE, Kearney DW, Price HW. Performance History and Future Costs of Parabolic Trough Solar Electric Systems. *Journal of Physics* 1999; **9**: 169-179.
25. Al-Azri N, Al-Thubaiti M, El-Halwagi MM. An Algorithmic Approach to the Optimization of Process Cogeneration. *Journal of Clean Technology and Environmental Policy* 2009; **11**:329-338.

26. El-Halwagi MM, Harell D, Spriggs HD. Targeting Cogeneration and Waste Utilization through Process Integration. *Applied Energy* 2009; **86**: 880-887.
27. Cohen GE, Kearney DW, Price HW. Performance History and Future Costs of Parabolic Trough Solar Electric Systems, *Proceedings of the 9th SolarPACES International Symposium on Solar Thermal Concentrating Technologies*, Font-Romeu, France, June 22 – 26, 1998; Pr3-169-Pr3-179.
28. Myint L, El-Halwagi MM. Process Analysis and Optimization of Biodiesel Production from Soybean Oil. *Journal of Clean Technology and Environmental Policy* 2009; **11**: 263- 276.
29. Ziegler F, Riesch P. Absorption Cycles: A Review with Regard to Energetic Efficiency. *Heat Recovery Systems & CHP* 1993; **13**: 147-159.
30. Klein SA, Reindl DT. Solar Refrigeration. *ASHRAE Journal* 2005; 9: S26-S30.
31. Kim DS, Ferreira CAI. Solar Refrigeration Options: A State-of-the-Art Review. *International Journal of Refrigeration* 2008; **31**: 3-15.
32. Zhai XQ, Wang RZ. A Review of Absorption and Adsorption Solar Cooling Systems in China. *Renewable and Sustainable Energy Reviews* 2009; **13**:1523-1531.
33. Hwang Y, Radermacher R, Al Alili A, Kubo I. Review of Solar Cooling Technologies. *HVAC&R Research* 2008; **14**: 507-528.
34. Assilzadeh F, Kalogirou SA, Ali Y, Sopian K. Simulation and Optimization of a LiBr Solar Absorption Cooling System with Evacuated Tube Collectors. *Renewable Energy* 2005; **30**: 1143-1159.
35. Masloumi M, Naghashzadegan M, Javaherdeh K. Simulation of Lithium Bromide – Water Absorption Cooling System with Parabolic Trough Collector. *Energy Conversion and Management* 2008; **49**: 2820-2832.
36. Vargas JVC, Ordonez JC, Dilay E, Parise JAR. Modeling, Simulation, and Optimization of a Solar Collector Driven Water Heating and Absorption Cooling Plant. *Solar Energy* 2009; **83**: 1232-1344.

37. Desideri U, Proietti S, Sdringola P. Solar Powered Cooling Systems: Technical and Economic Analysis and Air-Conditioning Applications. *Applied Energy* 2009; **86**: 1376-1383.
38. Abu Ein SQ, Fayyad SM, Momani W, Al-Bousoul M. Performance Analysis of Solar Powered Absorption Refrigeration System. *Heat Mass Transfer* 2009; **46**:137-145.
39. Hovsapian R,Vargas JVC, Ordonez JC, Krothapalli A, Parise JAR, Bernadsen AJC. Thermodynamic Optimization of a Solar System for Cogeneration of Water Heating and Absorption Cooling. *International Journal of Energy Research* 2008; **32**: 1210-1227.
40. Fathi R, Guemimi C, Ouaskit S. An Irreversible Thermodynamic Model for Solar Absorption Refrigerator. *Renewable Energy* 2004; **29**: 1349-1365.
41. Dhole V, Linnhoff B. Total Site Targets for Fuel, Co-generation, Emissions and Cooling, *Computers and Chemical Engineering* 1993; **17:** s101-s109.
42. Linnhoff B, Townsend DW, Boland D, Hewitt GF, Thomas BEA, Guy AR. Marsland RH. *A User Guide on Process Integration for the Efficient Use of Efficient Use of Energy*. IChemE: London, UK, 1982.
43. Lecuona A, Ventas M, Venegas A, Salgado R. Optimum Hot Water Temperatura for Solar Cooling. *Solar Energy* 2009;**83**: 1806-1814.
44. Tora EA, *Optimal Design and Integration of Solar Systems and Fossil Fuels for Process Cogeneration*. M.S.2008, Texas A&M University, College Station.
45. Gorsek A, Glavi P. Process Integration of a Steam Turbine. *Applied Thermal Engineering* 2003; **23**: 1227-34.
46. Elder JE, Lonzetta CM, Hall TA, Sornson JD, Klughers PD, Kaminski A, Ebert DA. *Single Reactor for Preparing Acrylic Acid from Propylene Having Improved Catalyst*. US Patent 6384274B1, 2002.
47. Tora EA, El-Halwagi MM. Optimal Design and Integration of Solar Systems and Fossil Fuels for Sustainable and Stable Power Outlet. *Clean Technologies and Environmental Policy* 2009; **4**: 401-407.

48. Reutemann W, Kieczka H. *Formic Acid in Ullmann Encyclopedia of Industrial Chemistry*. Wiley-VCH: Weinheim, 2005.
49. Foster R, Ghassemi M, Cota A. *Solar Energy: Renewable Energy and the Environment.* CRC Press; Boca Raton, FL, 2009.
50. Karim K, Bhat SY, Zaheer SI. *Catalysts for Low Conversion of Propylene*, US Patent 006143928A, 2000.
51. Elder JE, Lonzetta CM, Hall TA, Sornson JD, Klughers PD, Kaminski A, Ebert DA. *Single Reactor for Preparing Acrylic Acid from Propylene Having Improved Catalyst*. US Patent 6384274B1, 2002.
52. Mark HF, Othmer DF, Overberger CG, Seaborg GT. *Encyclopedia of Chemical Technology*. Vol. 1, pp 341. John Wiley & Sons: New York, 1963.
53. Gebreslassie BH. Economic Performance Optimization of an Absorption Cooling System under Uncertainty. *Applied Thermal Engineering* 2009; **29**: 3491-3500.
54. Stoecker WF. *Industrial Refrigeration Handbook*. McGraw-Hill: New York, 1998.
55. Herold KE, Radermacher R, Klein SA. *Absorption Chillers and Heat Pumps*. CRC Press, Inc: Boca Raton, FL, 1996.
56. Alefeld G, Radermacher R. *Energy Conversion System*. CRC Press: New York, 1993.
57. Wu S, Eames IW. Innovations in Vapor-Absorption Cycles. *Applied Energy* 2000; **24**:251-166.
58. Al-Sulaiman F, Hamdullahpur F, Dincer I. Tri-generation: A Comprehensive Review Based on Prime Movers. *International Journal of Energy Research* 2010; DOI: 10.1002/er.1687.
59. Trigeneration Technologies. Access on October 17th 2010. http://www.trigeneration.com/
60. Horlock JH. *Technical and Economic Impact of Co-generation*. Seminar: Steam Plant Committee of the Power Industries. Mechanical Engineering Publications for the Institution of Mechanical Engineers: London, 1986.

61. Lai SM, Hui CW. Feasibility and Flexibility for a Trigeneration System. *Energy* 2009; **34**: 1693–1704.
62. Buck R, Friedmann S. Solar-assisted Small Solar Tower Trigeneration. *Journal of Solar Energy Engineering* 2007; **129**: 349-354.
63. Heller P, Pfänder M, Denk T, Tellez F, Valverde A, Fernandez J, Ring A. Test and Evaluation of a Solar Powered Gas Turbine System. *Solar Energy* 2006; **80**: 1225–1230.
64. Cohen GE. *Solar Electrical Generating Systems for Nevada*: *Eldorado Solar Electric Generating System*. National Solar Energy Conference: Portland, 2004.
65. El-Halwagi MM. *Polution Prevention through Process Integration*. Academic Press: San Deigo,1997.
66. Kearney D. Solar Electric Generating Stations (SEGS). *IEEE Power Engineering Review*. 1989; **9**(8):4-8.
67. LI B, MA S. Analysis on Prospects of Solar Trough Thermal Power in China, *International Conference on Power Engineering*, Hangzhou, China, October 23-27, 2007.
68. Duran MA, Grossmann IE. Simultaneous Optimization and Heat Integration of Chemical Processes, *AIChE Journal* 1986; **32**: 123-138.
69. Lecuona A, Ventas R, Venegas M, Zacarı A,Salgado R. Optimum Hot Water Temperature for Absorption Solar Cooling. *Solar Energy* 2009; **83**:1806–1814.

VITA

Eman Abdel-Hakim Aly Mohamed Tora was born and raised in Elminia City, Egypt. She received a Bachelor of Science in chemical engineering from Elminia University in 2000. She worked at the Egyptian National Research Center in 2001 as a research assistant. She joined the graduate program at the Department of Chemical Engineering in Cairo University in 2001 and completed her Master of Science degree in July 2005. The Egyptian Government gave her a scholarship to study for her Ph.D. in the USA. She joined Texas A&M University in August 2006. Eman completed her Master of Science degree in August 2008, and completed her Ph.D. in December of 2010. While at Texas A&M University, she was involved with process systems related to solar energy integration into industrial processes. Her research addressed integrating and optimizing solar energy, biofuels, process low quality/waste heat and fossil fuels into industrial processes to provide power, heat, and cool. She has also participated in other projects including development of new biofuels pathway, educational modules for Qatar University, Qatar natural gas thermodynamic database, and new generation of Fischer Tropsch reactors.

Her permanent contact details are:
Eman Abdel-Hakim Aly Mohamed Tora
Chemical Engineering Department - National Research Center
Cairo- Egypt
011-2-012-690-2346
emantora@gmail.com
eman.tora@yahoo.com